

**Functional characterization of a lipid transporter gene,
LEM3 (ligand-effect modulator 3) in human
pathogenic fungus *Candida albicans***

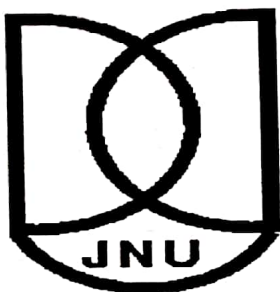
**Thesis submitted to Jawaharlal Nehru University
for the partial fulfillment of the award of**

DOCTOR OF PHILOSOPHY

PRANJALI AGARWAL



**Yeast Molecular Genetics Laboratory
School of Life Sciences
Jawaharlal Nehru University
New Delhi-110067
INDIA
2019**



School of Life Sciences
Jawaharlal Nehru University
New Delhi-110067
India

CERTIFICATE

This is to certify that this thesis entitled “**Functional characterization of a lipid transporter gene, *LEM3* (ligand-effect modulator 3) in human pathogenic fungus *Candida albicans***” submitted to the Jawaharlal Nehru University, New Delhi, by Ms. **Pranjali Agarwal** is based on the studies carried out in School of Life Sciences, Jawaharlal Nehru University, New Delhi. This work is original and has not been submitted so far, in part or in full, for any degree or diploma in this or any other university or institute.

Pranjali Agarwal

Pranjali Agarwal

(Candidate)

Dr. Sneh Lata Panwar

Dr. Sneh Lata Panwar

(Supervisor)

K. Natarajan

Prof. K. Natarajan
(Dean)

31/12/15



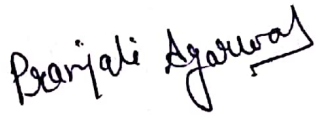
School of Life Sciences
Jawaharlal Nehru University
New Delhi-110067
India

CERTIFICATE OF ORIGINALITY

The research work embodied in the thesis entitled “**Functional characterization of a lipid transporter gene, *LEM3* (ligand-effect modulator 3) in human pathogenic fungus *Candida albicans***” has been carried out by me at the School of Life Sciences, Jawaharlal Nehru University, New Delhi under the supervision of Dr. Sneh Lata Panwar.

The thesis has been subjected to plagiarism check by ‘Turnitin’.

This work is original and has not been submitted so far in part or full, for award of any degree or diploma of any university.



Pranjali Agarwal

(Candidate)



Dr. Sneh Lata Panwar

(Supervisor)

Dedicated to..

Maa Papa

&

Mumma

Acknowledgement

*First and foremost, I would like to express my sincere gratitude to my supervisor **Dr. Sneh Lata Panwar** for her patient guidance, dedicated help, wholehearted encouragement, insightful and constructive suggestions and continuous support throughout my Ph.D. I appreciate the way she generously gave her time and energy to guide me throughout the process with her immense knowledge and expertise in the field of study. It was instrumental in defining the path of my Thesis, in widening it from various perspectives and making it productive and interesting. I wholeheartedly thank Ma'am for her confidence and positive outlook towards my research, the opportunity she gave me to grow as a scholar and also her enormous support in my personal life as it inspired me immensely and gave me enough confidence to complete it successfully. Without Ma'am's guidance and constant feedback, this Ph.D. would not have been achievable. I feel blessed to have the best mentor like her.*

*I am thankful to the Dean, School of Life Sciences, Jawaharlal Nehru University **Prof. K Natarajan** and previous HOD's, **Prof. S. K. Goswami, Prof. B. C Tripathi** for providing excellent facilities in the School of Life Sciences, Jawaharlal Nehru University. I would also like to acknowledge our corroborators for conducting experiments for us and for their constant support during the work.*

*I also extend my thanks to all members of Central Instrumentation Facility (CIF), SLS, JNU including **Surya Prakash, S. K. Mishra, Sarika Gupta, Tripti Panwar, Amar Chand, Jogendra and Rajendra Meena** for their help at in making my work run smoothly. I would also like to thank the administrative staff of SLS **Poddar sir, Sunita ma'am, Shyni ma'am, Poonam ma'am, Kirti ma'am** and **K. D. sir** for their help in official work during these years.*

I acknowledge DST for providing the funding for the work.

I want to thank the laboratory staff members Vijay bhaiya, Rajeev ji and storekeeper Ram Kripal ji for providing the necessary technical support and always being around to extend their help.

*Lab 106 is the place where we come as a stranger and become a part of family and this family extended and further we accept new members whole heartedly. I also joined this lab as a stranger and now I am a member of this family. This family includes **Edwina, Archita, Sumit, Shivani, Farha, Pranjali, Darakshan, Prerna and Pritam.***

***Edwina ma'am**, thank you so much for your trainings in the lab. I will always grateful for the knowledge and skills that I have gained working with you. **Archita ma'am** was the first with whom I interacted on the first day in lab. I also got the chance to do lots of experiment with her. Thank you ma'am for all the teachings and learnings during lab experiment and for yours advice on personal front also. **Sumit sir**, you can troubleshoot any problem related to experiments. It was a great experience to learn cloning with you. Whenever I am stuck in any experiment I always come to you for solution. Yours cooking skill is awesome, I enjoyed a lot ghr ka khana. Thank you sir for all the learnings.*

***Shabnam, Shivani, Farha, Darakshan, Prerna and Pritam** really it was a great time with all of you. We spend cheerful time together either in lab work or tea time or outing time.*

*Thank you **Shabnam** for always helping me in experiments whenever I need any suggestions. Yours directions help me a lot to prepare a better version of draft. **Shivani** , it's really a nice experience with you. "Our brosome is awesome". You always there when I needed you either at personal or professional front. "Thank you Bro". **Farha**, you always help me from the starting in this lab. You are very kind hearted person. I am thankful for all your help and guidance during the entire process of the thesis.*

***Darakshan**, we joined the lab together and from that day it's a great experience with you. I have a strong bonding with you. You always understand me and motivate me. Thank you so much for all your help during lab work and thesis writing. You always share your food with me and also suggests new places to go for tasty food. Thanks for bring that "coffee mug jisme chai lane ka socha tha" but success nhi ho paya lock down ki vajah se.*

***Prerna** you are very calm and nice person. I share a deep bond with you. You are a very good listener who is always there for me and try to solve my issues. You was always with me whenever I need you. Thank you for all your help during experiments as well as writing time of thesis. You always motivate me and dilute the stressed things ye bolke "ho jayega maam sb".*

***Pritam** you are a kind and helpful person. I am thankful to you for your help during no dues process.*

*I am thankful to my seniors from Tripathy's sir lab. Thank you **Deepika ma'am** for all your help, guidance and motivation. It was always a good time to talk and discuss with you. Thank you **Barnali ma'am**, **Garima**, **Ragini**, and **Sabir sir** for help and discussion.*

All the guards, security staff, cleaning staff of SLS especially guard at the SLS entrance have always been so cooperative and helpful. Smiling faces at the entrance of the gate gave me positive energy at the start of the day.

*I am very thankful to you **Anu**. It was never possible to complete this thesis without your help and support. My stay with you was so wonderful, it's always like another home and seriously I am going to miss it. You are so loving and caring. I will always remember the great time we had. You always gave me green tea or black tea that help me to wake up and speed up the work. I can never forget when you bring dinner and blanket at the center on that so chilled night just because of I was feeling low. Seriously this very crucial writing time was so easy as I was with*

*you. You always give me “some mantra” that boost up the work. You was always more stressed than me. Thank you **Shikha** for your motivation, you always said ho jayega di don't worry.*

*Thank you **Keka** for helping me during very initial process of submission.*

***Manoj** you always support me, help me and motivate me ye bolkr “tension mt le PA sb ho jayega”. It was always a good time with you either that was our research work in IVRI or our momoz party. I always remember that was you who push me to go JNU for pursuing PhD. Whenever I stuck somewhere I know you have the solution. Thank you so much for helping me on very short notice in thesis writing.*

***Paulo, Supuu, Ranu, Payal, Harry, Shabnam Di** you guys are awesome. It was always a great time with all of you in JNU during the initial year of PhD. We enjoyed many hostel nights and outings, our tea time at room and “Litti chokha” party was awesome. I badly miss that great time we had.*

*Lastly, I would like to thank my family for all their love and encouragement. **Maa**, your unconditional love and belief always strengthen me and motivate me to do well in my life. You always care and love me and also get worried for me (maa ho na aap). You are very simple and loving person. You always think about us before yourself. You are the one who made us, nurture us. Thanks is a word that is not enough to express my gratitude for my **Papa**. A strong personality and very hard working person, who always motivate me, support me, understand me. What I am today and what I will be tomorrow is just because of yours belief. I am so lucky as I got you and Maa as a parents who always try to do their best to fulfill our wishes in all odd situations also. It was never possible to begin this journey without yours love, belief and support. I always wish a healthy life for both of you.*

***Mumma** you are an iron lady who always guide me well to do good in life and to be stronger in life. It was never possible to complete this without your help and support and especially during the most crucial time of this thesis. I am blessed that you also understand the value of my studies and support me.*

***Gaurav**, my husband and my ultimate support system, I am so lucky to have you in my life. You always understand and care for me in every possible way. It would have been impossible to complete this thesis without your support and motivation. You were always there to listen to me and solve my problems. You understood the fact that it is food that makes me happy in stressed times. You always try to find out solutions to my problems.*

***Priya Di**, you are a blessing for me. You are my bestie and I can say that you are the one who understands me. You always motivate me since childhood. Whenever I feel low I just talk to you and you gave me the solution. Thank you so much for listening to all my problem and stress patiently and giving me the solution. Thank you **Jiju** for your care and support.*

*Thank you **Ankit** for supporting me always. I know you are always there whenever I needed you. I am always blessed to have you as my brother. We always share a strong bond of friendship which is quite different from the traditional bond of brother-sister. Thank you **Neha** for being with me and motivating me during this journey. Thank you **Mannu Bhaiya** for your help and support during thesis writing. **Amit Bhaiya**, thank you for your inspiring words. It always motivate me to give my best.*

To acknowledge in mere words is never enough to thank the people who played significant role directly or indirectly to shape my Ph.D. My sincere thanks and sense of gratitude are extended to all of them. I would like to thanks the Almighty GOD who has provided me this wonderful opportunity to acknowledge those who are a precious part of my life. I pray to Him to enlighten

me towards the path of a meaningful and successful life as a good human being. Finally, I would like to thank everybody who was important to the successful realization of this thesis, as well as express my apology that if I have inadvertently missed anyone.

Pranjali Agarwal

TABLE OF CONTENT

1.0 INTRODUCTION.....	1
1.1 CANDIDA: AN OVERVIEW	1
1.1.1 Candida albicans.....	1
1.1.2 Virulence factors of <i>C. albicans</i>	2
1.1.2.1 Morphogenesis.....	2
1.1.2.2 Adhesins.....	4
1.1.2.3 Invasion.....	5
1.1.2.4 Biofilm formation	6
1.1.3 Diseases caused by <i>C. albicans</i>	8
1.1.3.1 Mucosal infections.....	8
1.1.3.2 Candidemia and disseminated/invasive candidiasis	9
1.1.4 Treatment of candidiasis.....	10
1.1.4.1 Classification of antifungal drugs and mechanism	10
1.1.5 Challenges in candidiasis treatment	12
1.2 Plasma membrane asymmetry: an important determinant for cell physiology.....	13
1.2.1. Composition of plasma membrane	14
1.2.2. Generation of transmembrane lipid asymmetry	16
1.2.3 Maintenance of plasma membrane lipid asymmetry by lipid transporters.....	18
1.2.3.1. Active inward translocation: the aminophospholipid translocase (Flippases).....	19
1.2.3.2. Active outward translocation: involvement of ABC transporters.....	20
1.2.3.3. Bi-directional movement: the scramblase.....	21
1.3 P-type ATPase superfamily	22
1.3.1 Physiological significance of P4-ATPase.....	23
1.3.1.1 P4-ATPases in phospholipid asymmetry	23
1.3.1.2 P4-ATPases as lipid scavengers.....	24
1.3.1.3 Role of P4-ATPases in vesicle formation.....	24
1.3.1.4 P4-ATPases as membrane scaffolds	26
1.3.1.5 P4-ATPases exhibit different substrate specificities.....	27
1.3.2 Significance of P4-ATPases beta subunit.....	27
1.4 P4-ATPases and their beta subunits in yeast.....	29
1.4.1 Saccharomyces cerevisiae	29
1.4.2 Aspergillus nidulans	31

1.4.3 <i>Cryptococcus neoformans</i>	32
1.4.4 <i>Candida albicans</i>	34
1.5 AIM OF PRESENT WORK	35
2.0 MATERIALS AND METHODS	39
2.1. Materials	39
2.1.1 Strains, chemicals and growth conditions	39
2.2 Methods.....	43
2.2.1 PCR Amplification	43
2.2.2 DNA purification by gel extraction	46
2.2.3 Preparation of competent cells	46
2.2.4 Transformation of competent <i>E. coli</i>	47
2.2.5 Gel electrophoresis	48
2.2.5.1 Agarose gel electrophoresis	48
2.2.5.2 RNA gel electrophoresis	48
2.2.6 Yeast transformation by Electroporation.....	49
2.2.7 Yeast genomic DNA isolation.....	50
2.2.8 Bacterial plasmid DNA isolation (Mini-preparation).....	50
2.2.9 Strain construction.....	52
2.2.9.1. Deletion cassette construction.....	52
2.2.9.2. C-Myc tagging of <i>LEM3</i>	52
2.2.9.3. Overexpression strain construction.....	53
2.2.10 Southern Blot Analysis.....	53
2.2.11 Microscopy	54
2.2.12 Antifungal susceptibility tests	54
2.2.12.1 Spot analysis	54
2.2.12.2 Minimum inhibitory concentration (MIC) assay	54
2.2.13. Internalization of phospholipids into yeast cells	55
2.2.13.1 Flippase activity.....	55
2.2.14 Flow cytometry assays.....	55
2.2.15 Efflux of rhodamine 6G.....	56
2.2.16 Gene expression analysis.....	56
2.2.16.1 RNA isolation and cDNA synthesis	56
2.2.16.2 Real-time PCR (qRT-PCR).....	57
2.2.17 Steady state phospholipid analysis	57

2.2.18 Protein extracts and immunoblot analysis	57
2.2.19 Virulence testing assays.....	58
2.2.19.1 Morphogenesis assays.....	58
2.2.19.2 <i>In vitro</i> biofilm formation	59
2.2.19.3 <i>In vivo</i> virulence testing in mice model	59
3.0 RESULTS	60
3.1 Evolutionary relationship of <i>CaLem3</i> to other fungal orthologs.....	60
3.2. <i>LEM3</i> influences miltefosine susceptibility in <i>C. albicans</i>	64
3.2.1. Absence of <i>LEM3</i> impacts intracellular accumulation of M-C6-NBD-PC while cellular phospholipid levels remain unchanged.....	66
3.2.2. Reduced internalization of NBD-PC is attributed to decreased PC-specific flippase activity	69
3.3 Increased azole susceptibility of <i>lem3Δ/Δ</i> cells is due to decreased activity of <i>CDR1</i> efflux pump.....	70
3.4 <i>LEM3</i> influences pathogenicity in <i>C. albicans</i>	74
3.5 Lem3 activity is regulated by Rta3, a 7-transmembrane receptor protein of <i>C. albicans</i>	79
4.0 DISCUSSION	84
5.0 REFERENCES.....	89
6.0 APPENDICES.....	114

LIST OF FIGURES

1.0 GENERAL INTRODUCTION

Figure 1.1. Polymorphic forms of <i>Candida albicans</i>	3
Figure 1.2. Pathogenicity mechanism of <i>Candida albicans</i>	6
Figure 1.3. Sign and symptoms of candidiasis	8
Figure 1.4. Classification of antifungal agents	11
Figure 1.5. Mode of action of antifungal drugs	11
Figure 1.6. (A) Schematic representations of three types of membrane lipid. (B) A membrane bilayer and liposome	15
Figure 1.7. Diagrammatic representation of precise trafficking and proper Regulation of lipid transporter crucial for asymmetric distribution of phospholipids	17
Figure 1.8. Lipid transporters and membrane lipid asymmetry.	20
Figure 1.9. Cellular functions involving P4-ATPases.	26
Figure 1.10. Membrane topology of P4-ATPases and their subunits.	28
Figure 1.11. Diagrammatic representation of intracellular location and function of lipid transporters in <i>S. cerevisiae</i> .	31

3.0 RESULTS

Figure 3.1: Predicted topology of Lem3.	60
Figure 3.2: A prediction for the transmembrane domain organization of Lem3 as deduced from Transmembrane Helices Hidden Markov Models (THHMM).	61
Figure 3.3: Sequence alignment of <i>C. albicans</i> Lem3 with its orthologs by CLUSTAL OMEGA.	62
Figure 3.4: Phylogenetic analysis.	63
Figure 3.5: Disruption of <i>LEM3</i> .	65
Figure 3.6: Spot assay of <i>lem3</i> Δ/Δ for miltefosine susceptibility.	66
Figure 3.7: Internalization of NBD-PC in <i>lem3</i> Δ/Δ cells.	68
Figure 3.8: Steady state phospholipid analysis.	68
Figure 3.9: Flippase Activity.	70

Figure 3.10: Spot assay of <i>lem3Δ/Δ</i> for fluconazole susceptibility.	71
Figure 3.11: Reduced <i>CDR1</i> pump activity in <i>lem3Δ/Δ</i> .	72
Figure 3.12: Disruption of <i>LEM3</i> in azole-resistant clinical isolate GU5.	73
Figure 3.13: Minimum inhibitory concentration (MIC) assay.	74
Figure 3.14: Spot assay of <i>lem3Δ/Δ</i> in clinical isolate for fluconazole susceptibility.	74
Figure 3.15: Bud-to-hyphae switch is compromised in absence of <i>LEM3</i> in liquid Spider medium.	76
Figure 3.16: Bud-to-hyphae switch is compromised in absence of <i>LEM3</i> on solid spider media.	76
Figure 3.17: In vivo virulence analysis of <i>lem3Δ/Δ</i> strain in mice model of systemic infection.	77
Figure 3.18: Cellular morphology is not affected in <i>lem3Δ/Δ</i> .	78
Figure 3.19: In vitro biofilm formation in <i>lem3Δ/Δ</i> .	78
Figure 3.20: Spot assay for miltefosine susceptibility.	80
Figure 3.21: Intracellular accumulation of M-C6-NBD-PC in <i>lem3Δ/Δrta3Δ/Δ</i> cells.	81
Figure 3.22: Spot assay for fluconazole susceptibility.	82
Figure 3.23: Bud-to-hyphae switch is compromised in absence of <i>LEM3</i> .	82
4.0 DISCUSSION	
Figure 4.1. A model depicting roles of <i>LEM3</i> and its interaction with the membrane localized 7- transmembrane receptor protein Rta3 in <i>C. albicans</i> .	88

LIST OF TABLES

Table 1: Strains used in this study	39
Table 2: Culture media compositions	40
Table 3: Drugs/dyes used in the study	42
Table 4: Oligonucleotide used in this study	44
Table 5: Plasmids used in this study	51
Table 6: Similarity of <i>CaLem3</i> with others fungal and human orthologs	63
Table 7: Minimum inhibitory concentration (MIC ₈₀) of <i>lem3Δ/Δ</i> in GU5 background with Fluconazole	74

ABBREVIATIONS

TM	Transmembrane
PC	Phosphatidylcholine
PS	Phosphatidylserine
PE	Phosphatidylethanolamine
NBD	7-Nitrobenz-2-oxa-1,3-diazol-4-yl
TMD	Transmembrane domain
ABC	ATP binding cassette
MDR	Multidrug resistance
MFS	Major facilitator superfamily
AIDS	Acquired immunodeficiency syndrome
SDS	Sodium dodecyl sulphate
SDC	Synthetic dextrose complete
SC	Synthetic complete
YEPD	Yeast extract peptone dextrose media
DMSO	Dimethyl sulphoxide
min	Minute
kb	Kilo base pairs
kDa	Kilo Dalton
ATP	Adenosine 5'-triphosphate
PCR	Polymerase chain reaction

qPCR	Quantitative real time polymerase chain reaction
CGD	Candida genome database
°C	Degree centigrade
μg	Microgram
μm	Micrometer
μM	Micromolar
μl	Microliter
ng	Nanogram
mM	Millimolar
ml	Milliliter
mg	Milligram
DAPI	4',6-Diamidino-2-phenylindole dihydrochloride
PBS	Phosphate Buffer Saline
EDTA	Ethylene-Diamine-Tetra-Acetic acid
DMSO	Dimethyl Sulfoxide
ORF	Open Reading Frame
rpm	Round Per Minute
WT	Wild Type
FACS	Fluorescence-Activated Cell Sorting

1.0 INTRODUCTION

1.1 CANDIDA: AN OVERVIEW

1.1.1 *Candida albicans*

Around 8.7 million eukaryotic species has been estimated on Earth till date and approximately 7% (611,000 species) belongs to the fungal kingdom(Mora et al., 2011) amongst which only around 600 species are pathogenic to humans (Brown et al., 2012). On the basis of severity of infections pathogenic fungal group is further divided into three subgroups. Dermatophytes and *Malassezia* species cause relatively mild infections of the skin, while *Sporotrix schenkii* is known for severe

cutaneous infections. Fungi such as *Cryptococcus neoformans*, *Aspergillus fumigatus*, *Candida albicans* and *Histoplasma capsulatum* can cause life-threatening systemic infections.

Incidence of invasive candidiasis varies from 1 to 12 per thousand admissions in different hospitals across India. As inferred from studies carried in a tertiary care hospital in northern India, an eleven fold increase in cases of candidemia is observed in second half of the 1980's, which further increased to eighteen fold rise during late 1990's (Chakrabarti et al., 1996; 2002).

SCIENTIFIC CLASSIFICATION

Kingdom:	Fungi
Phylum:	Ascomycota
Subphylum:	Saccharomycotina
Class:	Saccharomycetes
Order:	Saccharomycetales
Family:	Saccharomycetaceae
Genus:	<i>Candida</i>
Species:	<i>albicans</i>

In the United States *Candida* species are accountable for hospital-acquired systemic infections with crude mortality rate up to 50% (Pfaller and Diekema; 2007, 2010).

C. albicans, is one of the most prevalent fungal species of human microbiota significantly contributing to candidiasis. It colonizes asymptotically in many areas of healthy individuals, particularly in the genitourinary and gastrointestinal tracts. However, any alterations in host immunity, resident microbiota, and other factors may lead to its overgrowth which can cause superficial mucosal infections to hematogenously disseminated candidiasis. The *C. albicans* strain SC5314 is used for molecular and genetic analysis worldwide and its complete genome is sequenced (Fonzi., 1993). Its genome size is 14.3 Mb containing about 6107 protein-coding genes. It is interesting that out of these protein coding genes, 774 are specific to *C. albicans* and homologues of these genes are not available in *Saccharomyces cerevisiae* or *Schizosaccharomyces pombe* (Inglis et al., 2012). According to the gene annotation data of CGD, only 22.97% of genes have been characterized experimentally, whereas 77.03% of the genes remain uncharacterized in *C. albicans* (Inglis et al., 2012).

1.1.2 Virulence factors of *C. albicans*

1.1.2.1 Morphogenesis

C. albicans have the ability to grow in a variety of morphological forms thus, termed as a polymorphic fungus. Different growth forms include (i) elongated ellipsoid cells with constrictions at the septa called as pseudohyphae, (ii) ovoid-shaped budding yeast and (iii) parallel-walled true hyphae (Berman and Sudbery, 2002) (Figure 1.1). Moreover, other morphological forms include white and opaque cells (formed during switching), and thick-walled spore-like structures, chlamydo spores (Sudbery et al., 2004). Interestingly, during infection yeast and true hyphae are the two form observed frequently while chlamydo spores are not been reported in patient samples. (Staib and Morschhäuser 2007; Soll, 2009). Both, yeast and hyphal

growth forms are important for causing infection in human host and transition between these two morphological forms is termed as dimorphism (Jacobsen et al., 2012). Yeast form is involved in dissemination whereas hyphal form is important for invasion. Mutants defective in hyphae formation displayed diminished virulence under in vitro conditions (Lo et al., 1997).



Figure 1.1. Polymorphic forms of *Candida albicans*.

Candida morphology is affected by a wide variety of environmental factors ranging from pH to nutritional diversity. Hyphal growth is induced at high pH (> 7) while low pH (< 6) induce yeast form (Odds, 1988). In addition, hyphal formation is promoted by a number of conditions namely, presence of serum or N-acetylglucosamine, starvation, CO₂ and physiological temperature (Sudbery, 2011). A series of molecular cascades transmit signals from the media to the transcriptional machinery thereby affecting the expression of a large number of genes, consequently changing the cell morphology. Morphogenesis is regulated via various signaling pathways for instance the cAMP-dependent pathway, matrix sensing pathway, pH-sensing pathway and MAP kinase signaling pathway (Kabir et al., 2012). Transcription factor Efg1, regulated via cAMP pathway is crucial for morphological regulation in *C. albicans* (Stoldt et al., 1997). Morphogenetic processes like yeast-hyphae transition, chlamydospore generation and cell shape determination during white-opaque switching is regulated by Efg1 and mutations in this

pathway severely affects the hyphal development in this pathogenic fungus (Doedt et al., 2004; Sonneborn et al., 1999; Srikantha et al. 2000).

1.1.2.2 Adhesins

Adherence is a crucial feature of *C. albicans* for its colonization and attachment to human host, other microorganisms and abiotic sources (Figure 1.2). This adherence process is induced and controlled by several cell signaling cascades. Some non-specific factors like hydrophobicity and electrostatic forces mediate initial attachment while further specific adhesins present on the surface of fungal cells are responsible for recognition of ligands such as proteins, fibronectin and fibrinogen (Li et al., 2003). In *C. albicans* a group of adhesin proteins known as agglutinin like sequence (ALS) protein family are well studied. This ALS family consists of eight members (Als1–7 and Als9), out of which hypha associated adhesion, Als3 is particularly important for adhesion (Zordan and Cormack 2012; Phan et al., 2007; Murciano et al., 2012). Expression of Als3 gets upregulated during in vivo vaginal infection and infection of oral epithelial in vitro (Wächtler et al., 2011; Zakikhany et al., 2007; Cheng et al., 2005). These ALS genes encode glycosylphosphatidylinositol (GPI)-linked cell surface glycoproteins. These proteins are predicted to have three major components: N-terminal domain similar to immunoglobulin-like fold (Ig), a central domain consisting of a variable number of tandem repeats (TR) of a 36-residue threonine-rich sequence, and C-terminal serine/threonine-rich stalk region, of variable length which is highly glycosylated. N-terminal domain contains motifs responsible for mediating substrate specific adherence (Gaur and Klotz 1997; Sheppard et al., 2004).

Hwp1 a hypha-associated GPI-linked protein is another important adhesin serving as a substrate for mammalian transglutaminases (Staab et al., 1999; Sundstrom et al., 2002). This reaction may facilitate the covalent attachment of *C. albicans* hyphae to the host cells. Deletion of *HWPI*

leads to diminished virulence in a mouse model of systemic candidiasis and reduced adherence to buccal epithelial cells (Staab et al., 1999; Sundstrom et al., 2002). Another group of proteins important for adhesion are GPI-linked proteins (Eap1, Ecm33 and Iff4), non-covalent wall-associated proteins (Phr1, a β -1,3 glucanosyl transferase and Mp65, a putative β -glucanase), integrin-like surface protein Int1 and cell-surface associated proteases (Sap9 and Sap10) (Zhu and Filler 2010; Naglik et al., 2011).

1.1.2.3 Invasion

C. albicans can deploy two different mechanisms to enter into host cells i.e., active penetration and induced endocytosis (Zakikhany et al., 2007; Naglik et al., 2011; Zhu and Filler 2010; Dalle et al., 2010). Invasins are a specialized set of proteins found on the fungal cell surface, mediating binding to the host ligands which promotes engulfment of the fungal cell into the host cell. E-cadherin present on epithelial cells (Phan et al., 2007) and N-cadherin on endothelial cells (Phan et al., 2005) are best examples of ligand proteins. Induced endocytosis is a passive process that does not require activity of viable fungus. This is supported by the observation that even killed hyphae are also endocytosed (Dalle et al., 2010; Park et al., 2005). Als3 a known adhesin and Ssa1, a member of the heat shock protein 70 (Hsp70) family are the two invasins present in this pathogen that induce endocytosis by a clathrin-dependent mechanism in the host. Besides these, macropinocytosis is also been reported to be involved in induced endocytosis in *C. albicans* (Phan et al., 2007; Dalle et al., 2010). Deletion studies on *ALS3* and *SSA1* have shown a reduced epithelial adherence and invasion to host with a compromised virulence in a murine model of oropharyngeal candidiasis (Naglik et al., 2011; Sun et al., 2010).

In contrast to induced endocytosis, active penetration requires viable *C. albicans* hyphae (Wächtler et al., 2011; Dalle et al., 2010). Factors that mediate this second route of invasion into

host cells is still not much clear, however physical forces and fungal adhesion are likely to be critical for this process. Secreted aspartic proteases (Saps) are another group of protein, that contribute to active penetration (Naglik et al., 2011; Dalle et al., 2010).

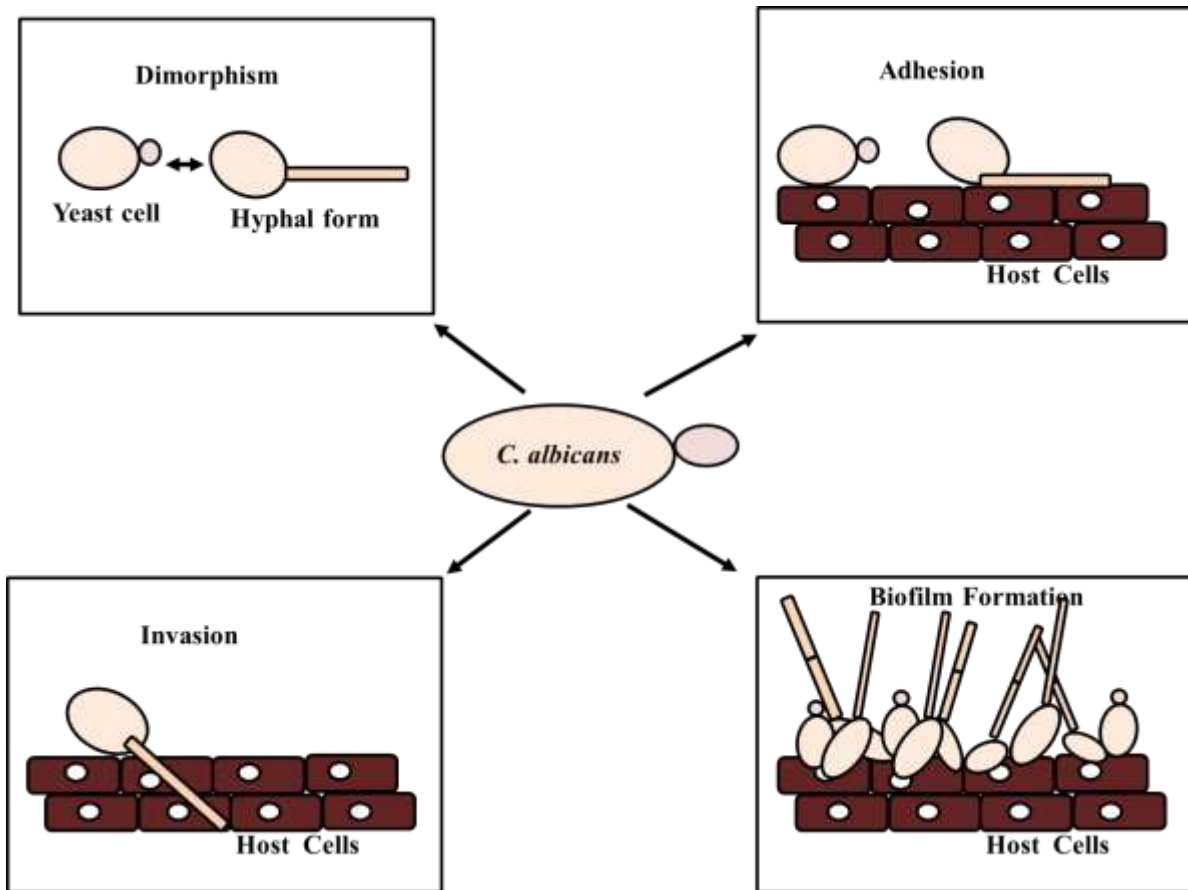


Figure 1.2. Pathogenicity mechanism of *Candida albicans*.

1.1.2.4 Biofilm formation

Another crucial virulence factor of this pathogenic fungus is to form biofilms on abiotic (catheters, dentures) as well as biotic (mucosal cell surfaces) surfaces (Figure 1.2) (Fanning and Mitchell, 2012). Biofilm formation is a series of events occurring in sequential manner as (i) adherence of yeast cells to the substrate, (ii) proliferation of yeast cells, (iii) hyphal cells formation, (iv) formation of extracellular matrix material and (v) dispersion of yeast cells (Finkel

and Mitchell, 2011). Biofilms maintain pathogenicity of *C. albicans* by an increased resistance to antifungal treatment, evading host immune mechanisms and withstanding competitive pressure from other organisms (Ozkan et al., 2005). Various factors are responsible for increased resistance of biofilm matrix including complex architecture, metabolic plasticity and increased expression of drug efflux pumps in biofilm cells (Fanning and Mitchell, 2012). Several proteins have significant role in biofilm formation. Hsp90, a heat shock protein is a key regulator of dispersion in *C. albicans* biofilms which is also required for antifungal drug resistance of biofilms (Robbins et al., 2011). In addition, many transcription factors Bcr1, Efg1 and Tec1 are also known to regulate biofilm formation (Fanning and Mitchell, 2012). Some novel factors regulating biofilm include Brg, Rob1 and Ndt80. Deletion of any of these regulators (*BCR1*, *EFG1*, *TEC1*, *BRG1*, *ROB1* and *NDT80*) are known to lead a defect in biofilm formation in vivo rat infection models (Nobile et al., 2012). It is also known that biofilm shows resistance to killing by neutrophils and compromised in producing reactive oxygen species (ROS) (Xie et al. 2012). β -glucans of extracellular matrix are suggested to play a role in protecting the pathogenic fungus from the attack of neutrophils (Xie et al. 2012). Production of extracellular matrix is further controlled by various factors such as Zap1 (zinc-responsive transcription factor) negatively regulates the expression of β -1,3 glucan, a major component of matrix, while Gca1 and Gca2 (Glucoamylases), Bgl2 and Phr1 (glucan transferases) and the Xog1 (exo-glucanase) are positive the regulators of β -1,3 glucan production (Nobile et al., 2009; Taff et al., 2012). Zap1 also regulate expression of *GCA1* and *GCA2* but the enzymes Bgl2, Phr1 and Xog1 function independently of this key negative regulator (Taff et al., 2012). Upon deletion of *BGL2*, *PHR1* or *XOG1* biofilms show increased susceptibility to antifungals like fluconazole (Taff et al., 2012).

1.1.3 Diseases caused by *C. albicans*

1.1.3.1 Mucosal infections

Under favorable circumstances it can cause infections of mucosal membranes, referred as thrush which is characterized as white spots that can be taken off to reveal the inflammation area in the underlying membrane (Odds, 1988). This infection is also known as pseudomembranous candidiasis, which usually affect gastrointestinal, oral-pharangeal, vaginal, esophageal mucosae. Once in their life time up to 75% of women suffered by Vulvo Vaginal Candidiasis (VVC) (Sobel 1997). In some women, repeated infection has been reported a condition known as Recurrent Vulvo Vaginal Candidiasis (RVVC). Diabetes, use of oral contraceptives and reproductive hormones, antibiotic treatment are some factors that can lead to VVC. The innate immunity plays a crucial role in the defense mechanism against mucosal infections and overaggressive inflammatory response triggers VVC symptoms (Fidel Jr, 2007). Signs and symptoms of candidiasis alter according to infected area (Figure 1.3).

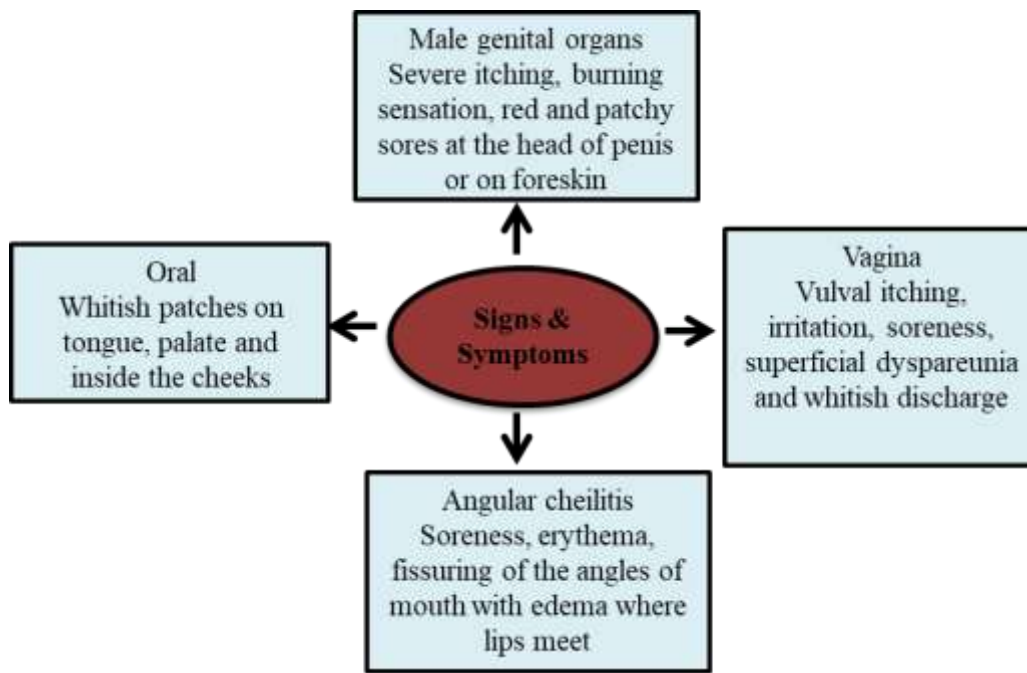


Figure 1.3. Sign and symptoms of candidiasis.

First line of defense is cell mediated immunity for this kind of mucosal infections but apparently azole antifungals like fluconazole, albaconazole also used for the treatment of VVC. Oral-pharyngeal candidiasis (OPC) is another type of infection that normally occurs in AIDS patients and further its appearance is considered to be marker of the development of AIDS in HIV-positive individuals (Klein et al. 1984). Cell-mediated mechanisms are crucial to defense against *C. albicans* in oropharyngeal and esophagus mucosa, in contrast to the vaginal mucosa.

1.1.3.2 Candidemia and disseminated/invasive candidiasis

C. albicans blood stream infections are termed as candidemia. In normal healthy individuals action of neutrophils provides protection against such type of infections. Neutrophils number declines in patients who suffered with certain blood cancers or following immunosuppressant therapy and this condition provide chance to this opportunistic pathogen to cause candidemia. Other risk factors are breaching of gastrointestinal (GI) tract after surgery that allow *C. albicans* spreading and biofilm formation on catheters in intensive care units. Condition in which *C. albicans* further colonizes the internal organs is known as disseminated candidiasis. Both these types of candidiasis are extremely serious medical conditions. Candidemia symptoms are quite similar to bacterial septicemia. Generally, candidemia does not get diagnosed at an early stage of infection and antifungals treatment fails to control the infection. Therefore after bone marrow transplants or abdominal surgery, often antifungal treatments are administered prophylactically. Mortality rate of about 40% have been noted from different surveys (Michael A Pfaller et al., 1998; Kibbler et al., 2003).

1.1.4 Treatment of candidiasis

1.1.4.1 Classification of antifungal drugs and mechanism

Both fungal cells and human cells are eukaryotic, therefore use of antifungal compounds may result in considerable side effects in patients (Sardi et al., 2013; Paramythiotou et al., 2014). Antifungal drugs include azoles (fluconazole, ketoconazole, itraconazole clotrimazole and ,miconazole) that inhibit ergosterol biosynthesis; echinocandins (caspofungins) and polyenes (nystatin and amphotericin B); allylamines; thiocarbamates; morpholines; 5- fluorocytosine, a deoxyribonucleic acid (DNA) analog; (Pappas et al., 2009; Spampinato and Leonardi, 2013). Azoles target the cells by inhibiting ergosterol biosynthesis, consequently membrane composition is perturbed. It inhibits the conversion of lanosterol into ergosterol by targeting the enzyme lanosterol 14- α -demethylase (Sanguinetti et al., 2015). Amphotericin B and other polyenes disrupts the membrane structure by binding to ergosterol and, promotes extravasation of intracellular constituents and, consequently, cell death (Peman et al., 2009; Mesa-Arango et al., 2012). Flucytosine (5-FC) inhibits the thymidylate-synthetase enzyme interfering with DNA. Classification of antifungal agents utilized for the candidiasis treatment is given in schematic below (Figure 1.4).

Echinocandins is a class of drug that targets fungal cell wall, so it has comparatively less side effects as animal cells lack cell wall. Echinocandins inhibit glucan synthesis by preventing β -D glucan synthase. Such kind of antifungals include caspofungin, micafungin and anidulafungin (Grossman et al., 2014; Koehler et al., 2014; Paramythiotou et al. 2014). Echinocandins have an advantage as it can be used in cases of azole-antifungal resistance (Spampinato and Leonardi 2013; Grossman et al., 2014; Maubon et al., 2014; Paramythiotou et al., 2014). Allylamines (naftifine and terbinafine) and thiocarbamates target ergosterol synthesis by inhibiting the enzyme squalene-epoxidase. Mode of action of antifungal drugs shown below (Figure 1.5).

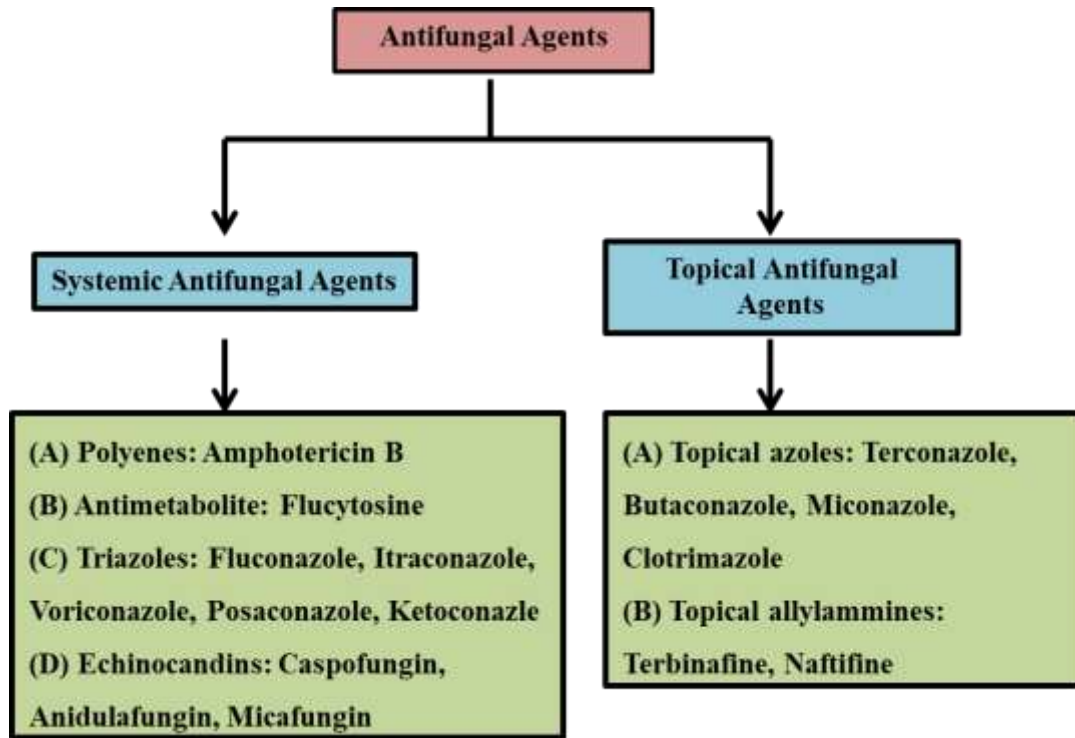


Figure 1.4. Classification of antifungal agents (Hani et al. 2015).

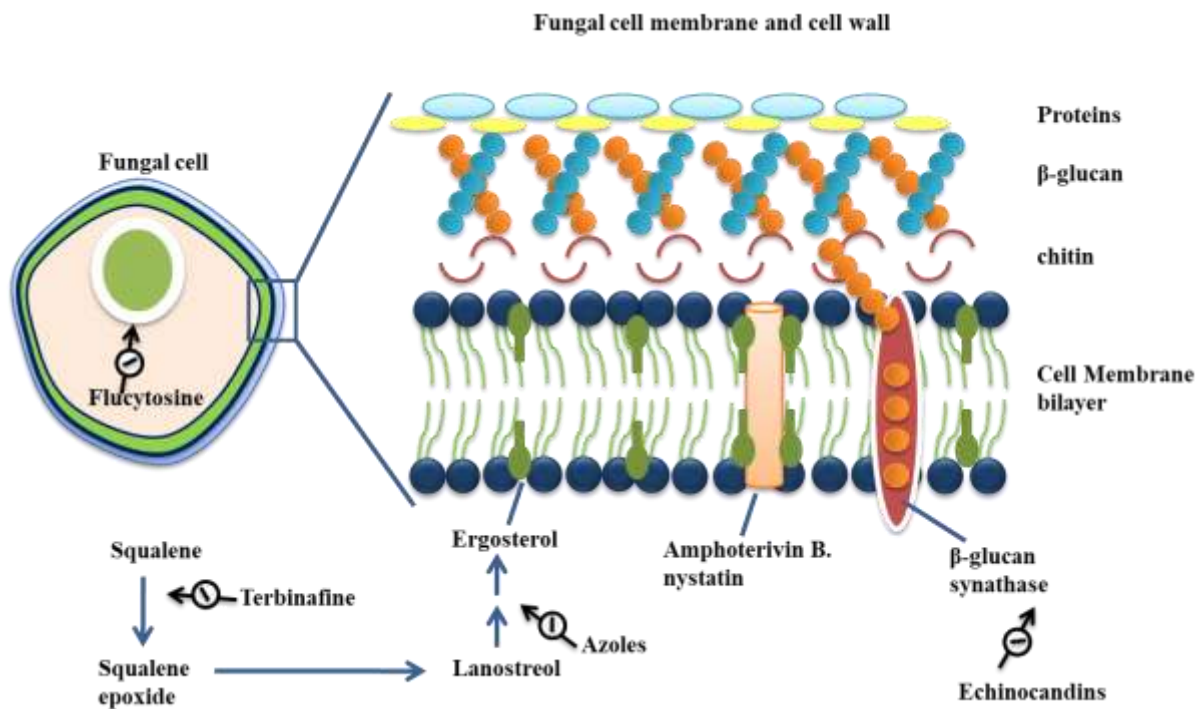


Figure 1.5. Mode of action of antifungal drugs.

1.1.5 Challenges in candidiasis treatment

Antifungal drugs are used to treat dangerous fungal infections, but these pathogenic fungi sometimes can evade from the effect of the drugs by developing resistance against them. The major challenge in treating these pathogenic species of *Candida* is the emergence of drug resistance in them. This resistance is alarming particularly for patients with invasive fungal infections affecting heart, eyes, brain, blood or some other parts of the body. Bloodstream infections caused by resistant *Candida* species causes critical health problems, including disability and even death. More information is needed about the risk antifungal resistance poses to human health and how many people are sickened by drug-resistant fungal infections each year.

About 7% of all *Candida* bloodstream isolates showed resistant against fluconazole. Although *C. albicans* is the major contributor of *Candida* infections but development of drug resistance is a more common phenomenon in other species of *Candida* such as *C. glabrata* and *C. parapsilosis* (Toda et al., 2019). Over the past 20 years the percentage of fluconazole resistant *Candida* isolates has remained moderately constant (Toda et al., 2019; Hajjeh et al., 2004; Kao et al., 1999; Alexander et al., 2013). However, resistance towards echinocandin seems to be emerging, particularly in the isolates of *C. glabrata*. Infections caused by multidrug-resistant strains (resistant to both fluconazole and echinocandin) poses great challenge for its treatment, as Amphotericin B, a drug primarily used in such treatments can be toxic for patients who are already very sick. Growing evidence suggests that patients having drug-resistant candidemia have less survival chances than patients who have candidemia that can be treated by antifungal medications (Alexander et al., 2013; Baddley et al., 2008).

Another challenge in the treatment of *C. albicans* infections is due to its ability to form biofilm as these structured communities are resistant to treatment by antifungals. *C. albicans* form

biofilm mostly on joint prostheses, mechanical heart valves, contact lenses, pacemakers Urinary and central venous catheters, and dentures (Cauda, 2009; Donlan and Costerton, 2002; Kojic and Darouiche, 2004; Seddiki et al., 2013). Owing to the highly resistant nature of these biofilms high doses of antifungals are required along with the removal of the infected medical device to treat infections (Andes et al., 2012; Cornely et al., 2012; Lepak and Andes, 2011; Lortholary et al., 2012; Mermel et al., 2009). Removal of devices such as artificial heart valves and joints is highly expensive as well as risky in some cases. Moreover, administration of high doses of antifungal agents can lead to complications involving liver and kidney damage. Most of the time these treatments are not feasible as in some cases critically ill patients are not able to tolerate them.

We can control emergence of antifungal resistance by,

- i) Developing a better understanding as to why and how antifungal resistance emerges.
- ii) Increasing awareness among public health communities about these infections.
- iii) Uncovering novel drug targets

Recent researches have shown that membrane lipids asymmetry plays a crucial role in fungal virulence so a better understanding of lipid asymmetry and lipid transporters can pave way for the development of new lipid-mediated therapeutic strategies (Rella et al., 2016).

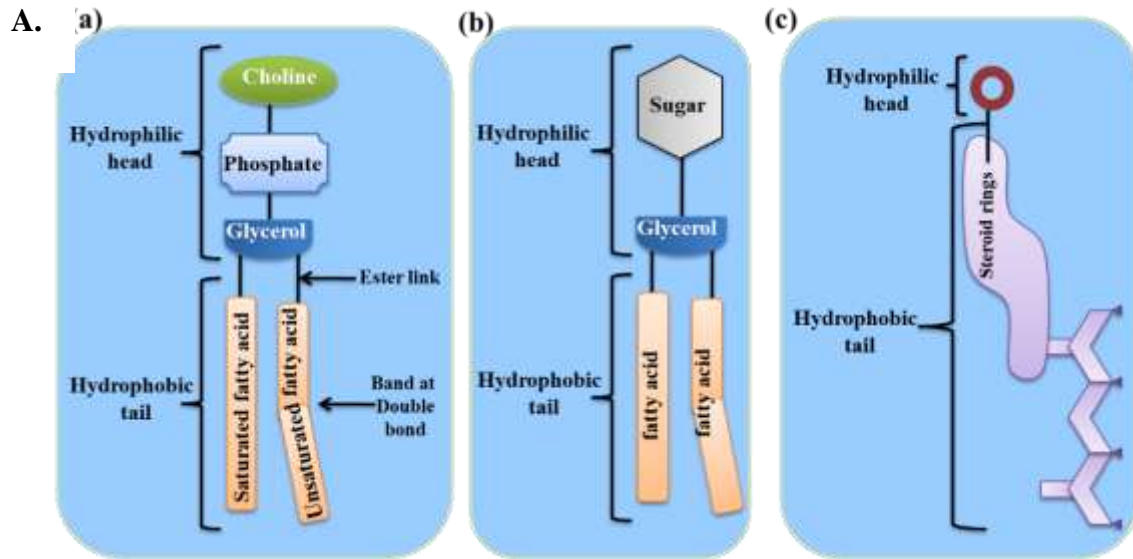
1.2 Plasma membrane asymmetry: an important determinant for cell physiology

Cell membranes are the complex structure of living cells composed of lipids and proteins separating the cell interior from the outside environment. Membranes are the simple bilayer structure. Several lipidomics studies have confirmed a vast variety of lipid species found to be involved in its constitution (Van Meer et al., 2008; Sampaio et al., 2011; Klose et al., 2013).

These lipids asymmetrically distribute between the two leaflets of biological membrane (Engelman, 2005; Lingwood and Simons, 2010). Asymmetrical distribution of lipids is crucial for many cellular processes, e.g., signal transduction, membrane fusion, protein trafficking and aggregation. Any alteration in the expression levels of lipid species is related to and many diseases in human including: cancers, diabetes, Alzheimer's disease, HIV entry, and atherosclerosis (van Meer, 2005; Holthuis and Menon, 2014).

1.2.1. Composition of plasma membrane

Both monolayers of plasma membrane possess different kinds of lipids, carbohydrates and peripheral proteins in different proportion. Moreover, there is a precise orientation of each transmembrane proteins in the membrane. That is why; the unequal distribution of these molecules in both monolayers of plasma membrane is termed as membrane asymmetry which is very critical for the cell. The transbilayer distribution of lipids across biological membranes has been found to be asymmetric (Bretscher, 1972). Like, the outer leaflet of the plasma membrane or the topologically equivalent luminal leaflet of intracellular organelles is mainly enriched with the choline-containing lipids, phosphatidylcholine (PC) and sphingomyelin (SM). On the other hand, the inner leaflet or cytoplasmic leaflet primarily contains the amine-containing glycerophospholipids, phosphatidylethanolamine (PE) and phosphatidylserine (PS). Different type of membrane lipids and their distribution in lipid bilayer shown below (Figure 1.6).



B.

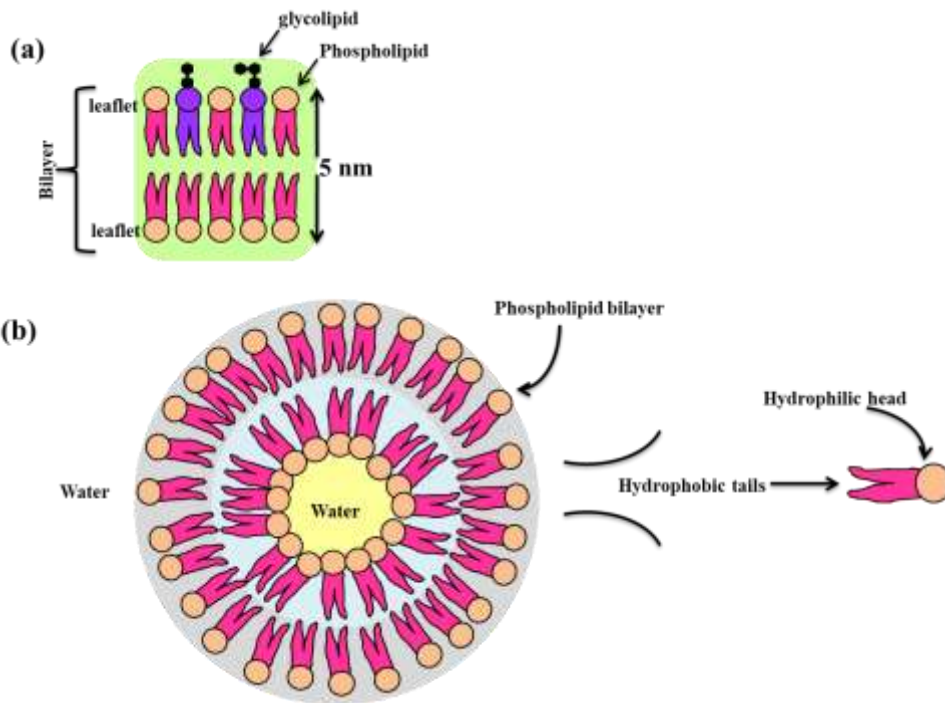


Figure 1.6. (A) Schematic representations of three types of membrane lipid. (a) Phosphatidylcholine, a glycerophospholipid. (b) Glycolipid. (c) A sterol.

(B) A membrane bilayer and liposome. Spontaneous formation of bilayers by membrane lipids. The hydrophilic heads will always face the aqueous environment in bilayers (a) and liposomes (b). The hydrophobic tails will face inward away from the water.

Some minor phospholipids, for example phosphatidic acid (PA), phosphatidylinositol (PI), phosphatidylinositol-4-monophosphate (PIP), and phosphatidylinositol-4,5-bisphosphate (PIP₂), are also found on the inner leaflet of the membrane. In erythrocyte membrane lipid asymmetry is well-characterized, the external leaflet of which has 75–80% of the PC and SM, 20% of the PE, PA, PI, and PIP₂, and no or very less PS or PIP (Bütikofer et al., 1990; Gascard et al., 1991; Bretscher, 1972). While the external leaflet of the plasma membrane is also enriched with glycosylsphingolipids and some other significant membrane component (Kolter et al., 2002).

1.2.2. Generation of transmembrane lipid asymmetry

The biosynthesis of lipid is asymmetric. The enzymes for the synthesis of lipid are mainly present on the one side of the membrane wherein biosynthesis takes place. The synthesis of major glycerophospholipids for example PS, PE, PC, and PI occurs via de novo process towards the inner or cytoplasmic side of the endoplasmic reticulum (ER) (Bell et al., 1981). All newly synthesized lipids except PC is formed towards the side of the membrane where they have to finally enrich in the plasma membrane. These newly synthesized lipids should remain majorly towards cytoplasmic leaflet of the membrane because of the thermodynamic barrier to spontaneous transbilayer movements, so that there should be no perturbation in the membrane dynamics. Since, newly synthesized phospholipids are asymmetrically placed on to the one leaflet of the plasma membrane which is responsible for the instability of membrane which results into membrane bending and consequently membrane shape changes (Daleke and Huestis, 1985; Farge and Devaux, 1992). While, there are some evidence which suggests that membranes of ER and Golgi are less asymmetric than the plasma membrane (Zachowski, 1993). Various lipid transporters are involved in the redistribution of ER phospholipids across the membrane (Hrafnsdóttir and Menon, 2000; Gummadi and Menon, 2002).

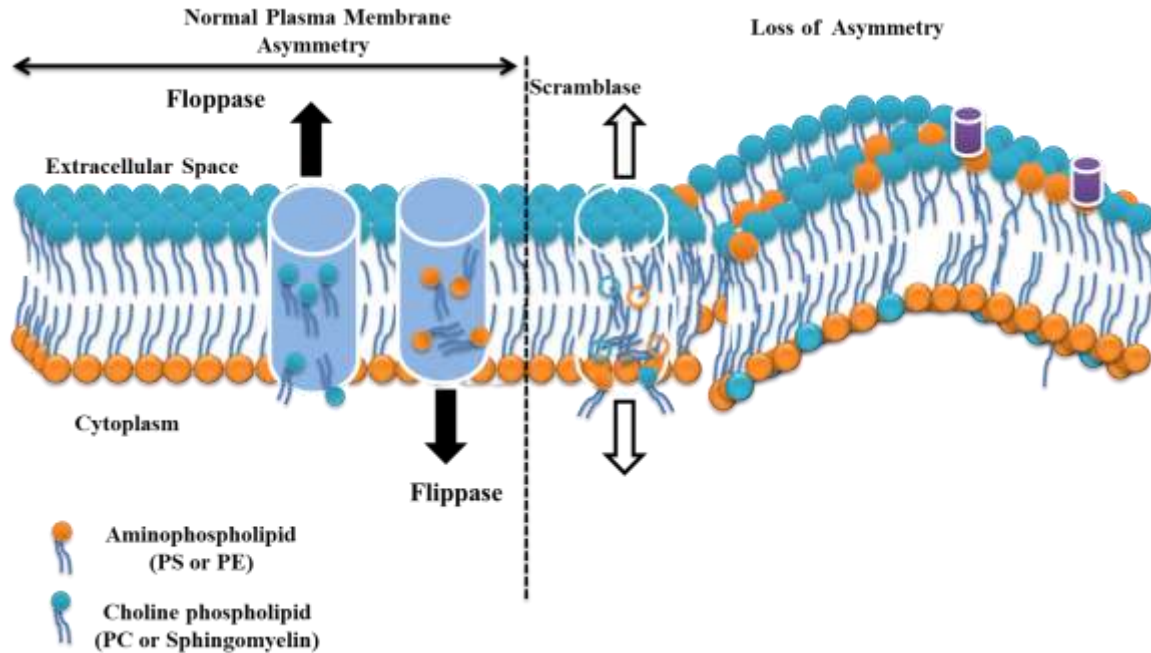


Figure 1.7. Diagrammatic representation of precise trafficking and proper regulation of lipid transporter crucial for asymmetric distribution of phospholipids.

Sphingolipids are predominantly found towards the outer leaflet of the plasma membrane. Unlike the synthesis of PC, sphingolipid biosynthesis takes place on the side of the membrane where these lipids finally have to reside. Exceptionally, the synthesis of glucosylceramide (Glc-Cer) occurs on the cytoplasmic side of the Golgi, while sphingolipids are synthesized on the luminal surface of the ER or Golgi, including SM, galactosylceramide, and complex sugar-linked sphingolipids (Kolter et al., 2002; Holthuis et al. 2001).

The phenomenon of accumulation of particular glycerophospholipids on specific side of the plasma membrane is the result of membrane trafficking from the ER to the plasma membrane that the transbilayer randomizing process be inhibited or that an asymmetry-generating process be activated. To maintain membrane asymmetry for the proper function or to avoid membrane perturbation, it requires an input of energy which helps to generate, or to establish a transbilayer lipid gradient. Both ATP-dependent lipid transporters have been found which is responsible for the selective inward and outward movement of lipids across the plasma membrane. Thus, the

precise trafficking and proper regulation of lipid transporter is found to be important for the asymmetric distribution of phospholipids (Figure 1.7). But the presence of ATP-independent nonselective lipid transporters in the ER in combination with the trafficking of substrate-specific ATP-dependent transporters to the plasma membrane may be responsible for a highly asymmetric plasma membrane in comparison to the more symmetric membranes of ER and Golgi. Although, these lipid randomizing and asymmetry generating lipid transporters found in multiple membranes, but be differentially regulated.

1.2.3 Maintenance of plasma membrane lipid asymmetry by lipid transporters

Lipid asymmetry across lipid bilayer is maintained by diffusion across transbilayer, membrane protein mediated transport and lipid-protein interactions. The rapid diffusion of phospholipids across plasma membrane is prevented by thermodynamic barrier across membrane. Half time for lipid flip flop could vary from several hours to days (McConnell and Kornberg, 1971) depending upon the lipid or membrane nature. It has been shown that flip flop rate in human erythrocyte are described by length of acyl chain and unsaturation of the lipids (Fujii and Tamura, 1983; Middelkoop et al., 1986). As flip time is comparatively shorter than the cell lifespan it is very unlikely that these phenomena could solely account for asymmetry across plasma membrane. It is likely that maintenance and dissipation of transbilayer lipid asymmetry is contributed by different protein catalyzing the lipid transport across plasma membrane. The activity across transbilayer is different type depending upon specificity to substrate, energy requirement and transport direction . The two main transport activities that have been described for ATP-dependent transport of lipids are (Figure 1.8):

(i) First is well characterized “flippase” or aminophospholipid translocase transporting PS from outer monolayer to inner cytoplasmic surface of plasma membrane.

(ii) Second class of ATP-dependent activity is catalyzed by different class of protein called as “floppases,” transporting lipids into opposite direction from inner leaflet to outer leaflet. Most characterized floppase activity catalyse transport of short-chain fluorescent lipids and selective efflux of PC or cholesterol from inner-to-outer monolayer.

(iii) Third type of ATP-independent and relatively nonspecific transport activity includes activity of scramblase. This scramblase is a Ca^{2+} activated transporter on plasma membrane which also works as an ER glycerophospholipid-specific transporter, and an ER mono-hexosyl-lipid transporter.

It is clear that all of the described transport activities have specificities for lipid transporters located on the plasma membrane. In addition, these transporters have a unique specificity or nonspecificity defining determination of lipid organization (Boon and Smith, 2002, 20; Pomorski et al., 2001). In the coming section the literature available on the transporters is summarized.

1.2.3.1. Active inward translocation: the aminophospholipid translocase (Flippases)

Devaux and coworkers were first to report aminophospholipid flippase activity. They measured ATP-dependent uptake of spin-labeled lipid analogs in human erythrocytes (Seigneuret and Devaux, 1984). The activity of this transporter is also studied by using fluorescent fatty acids labeled phospholipids, particularly 7-nitrobenz-2-oxa-1,3-diazol-4-yl (NBD) derivatives (Connor and Schroit, 1987; Sleight and Pagano, 1985; Colleau et al., 1991). These bulky fatty acid substituents may even alter transporter-lipid interactions, thus raising a question whether these measured movement with these fatty acids will exactly refer the endogenous lipids behavior. Though, these fluorescent probes are powerful tools their use require a conscious interpretation (Devaux et al., 2002; Maier et al., 2002) and verification that their final movement reflect the exact movement of the endogenous lipids. Besides spin-labelled and fluorescent lipids other

species used for measuring flippase activity are native and radiolabeled short (Daleke and Huestis, 1985; 1989; Anzai et al., 1993) and long (Tilley et al., 1986) chain fatty acid-containing species. Perhaps, use of these lipids is quite difficult and more restricted, though their behavior might reflect the behavior of endogenous lipids more accurately.

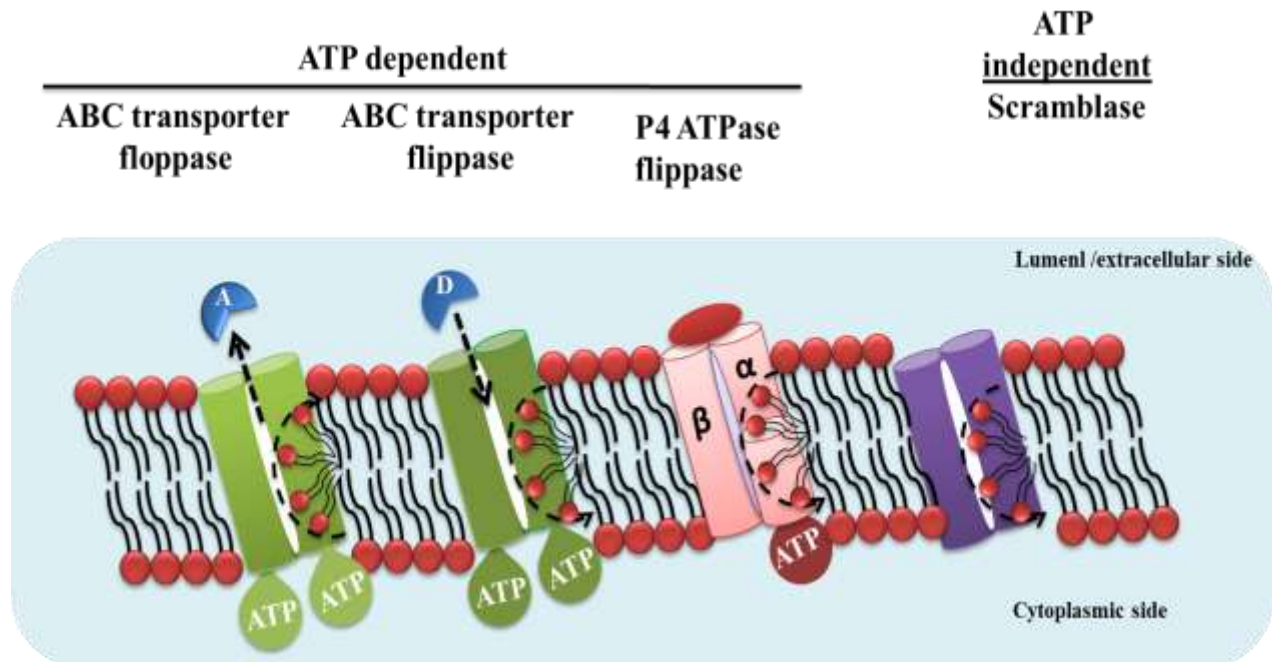


Figure 1.8. Lipid transporters and membrane lipid asymmetry. A) ATP-dependent transporters of the P4 ATPase and ABC transporter families can maintain an asymmetric phospholipid distribution by moving specific lipids towards (flippase) or away from the cytosolic leaflet (floppase)
 B) ATP-independent scramblases, which can translocate lipids bidirectionally across the membrane.

1.2.3.2. Active outward translocation: involvement of ABC transporters

Another class of ATP-dependent lipid transporters are floppases which are localized exofacially. Early studies in red blood cells revealed a nonspecific outward flux pathway for NBD- and spin-labeled lipids (Connor et al., 1992; Bitbol and Devaux, 1988). Members of the ABC transporter superfamily are also capable of transporting lipids (Borst et al., 2000; Borst and Elferink, 2002). These transporters export amphipathic compounds in an ATP dependent manner. This group include the multidrug resistance proteins, initially discovered in drug-resilient tumor cells, transporting the cytotoxic xenobiotics outside. In yeast and *C. albicans* these multidrug

resistance proteins (*CDR1*, *CDR2*, *CDR3*) are known to function as lipid transporters (Prasad and Panwar, 2002; Krishnamurthy and Prasad, 1999). ABC transporters are also present in prokaryotic organisms. One such example of these proteins is MsbA which transports lipids to the outer membrane (Zhou et al., 1998). ABC proteins being common xenobiotic transporters are generally nonspecific in nature. However, some members of this class display specificity for their respective substrate. ABCA1, ABCB1, ABCB4, and ABCC1 are some of the most well characterized lipid floppases. It is noteworthy to mention that ABCR, an ABC protein is a flippase rather than a floppase. ABCR is present in retinal rod cell outer segment disc membranes and transports *N*-retinylidene-PE from the disc lumen to the cytofacial side of the membrane (Weng et al., 1999).

1.2.3.3. Bi-directional movement: the scramblase

Phospholipid asymmetry of the plasma membrane sometimes loses due to Calcium-influx. The bidirectional scrambling process involves almost all classes of phospholipid, which moves at comparable rates ($t_{1/2} = 10$ to 20 minutes), while SM moves at a slower rate (Williamson et al. 1995; Smeets et al. 1994). One study indicates that, at least in platelets, PS and PE are externalized at a priority basis (Basse et al. 1993). Inhibition of the aminophospholipid translocase alone does not directly responsible for the exposure of PS. Protein-modifying reagents sometimes inhibit phospholipid scrambling (Williamson et al., 1995) which is ATP-independent and a calcium-dependent flippase, called scramblase, has been found involved. Scott syndrome, a rare and very severe bleeding disorder occur due to lack of the scramblase; this disorder is associated with an impairment of calcium triggered lipid redistribution in platelets (Beyers et al. 1992).

P-type ATPases are flippase that comprise a well-studied family of proteins involved in the active transport of charged substrates across biological membranes. So, upcoming section is focused on P-type ATPases.

1.3 P-type ATPase superfamily

This family consist of evolutionarily conserved membrane located pumps. These described as P type because during their catalytic cycle they form a phosphorylated intermediate (Palmgren and Nissen, 2011). Further this group divide into five subgroup on the bases of sequence similarity and their distinct transport specificities (Palmgren and Axelsen, 1998):

(i) P1-ATPases perform the transportation of heavy metals and in this manner purifying the cytoplasm, further they also accomplished transport of heavy metals in distinctive cellular compartments.

(ii) Another subgroup P2-ATPases perform the function of sustaining the electrochemical gradients across the membrane. In case of animal cells these pump regulate K^+ and Na^+ while in human H^+/K -ATPase mainly responsible for regulation of acidification of stomach contents and also regulate level of Ca^{2+} in the sarcoplasmic reticulum.

(iii) P3-ATPases which is localized in plasma membrane works by expelling the H^+ from the cell in order to maintain pH gradient across the biological membrane.

(iv) Apart from above mentioned all three P-type ATPases which are present in all the branches of life, P4-ATPases which represents the largest subfamily of P-type ATPase, are only found in eukaryotic organisms.

(v) P5-ATPases (pumps with no assigned function)

In humans, P4-ATPases are encoded by 14 genes, while Drs2, Dnf1, Dnf2, Dnf3, and Neol1 present in yeast. *ATP8B1* an example of human P4 ATPase expressed in various epithelial tissues (Eppens et al., 2001). Alteration in this gene lead to Byler disease and benign recurrent

intrahepatic cholestasis (Bull et al., 1998). Further recent findings have been shown the importance of P4-ATPase and alteration in it resulting in various immunological and neurological disorders, diet induced obesity, liver disease, and type 2 diabetes (Coleman et al., 2013; van der Mark et al., 2013). How these different phenotypes are linked to a altered flippase activity is remains to be decoded. P4-ATPases modulates there activity in heterodimeric form, by working in complex with beta subunits *LEM3* (ligand-effect modulator)/*CDC50* (cell division cycle) family to transport phospholipids between outer and inner cellular membranes. This ATP driven, unidirectional transport of phospholipids play a crucial role to maintain membrane asymmetry, inducing membrane curvature and scavenging of exogenous lipids.

1.3.1 Physiological significance of P4-ATPase

1.3.1.1 P4-ATPases in phospholipid asymmetry

Research in different life form like parasites, yeast and higher eukaryotes unravel the location of these P4-ATPases i.e. plasma membrane and intracellular compartments of the endocytic pathways and late secretory pathways. This suggests that P4-ATPases operates at diverse cellular regions to determine and conserve phospholipid asymmetry (Figure 1.9a). The mechanism by which these P4-ATPases relate their PC translocase activity to asymmetry of membrane is still unexplored. The irregular transbilayer lipids distribution specifies the two membrane leaflets of organelles that have distinctive properties that is essential for biological functions. Besides this membrane asymmetry is also crucial for protein sorting (Hachiro et al., 2013). For example loss of Dnf1 and Dnf2 lead to exposure of cytosolic aminophospholipids at the outer membrane of cell in yeast (Chen et al., 2006; Pomorski et al., 2003). Similarly, alteration in Drs2 and Dnf3 is responsible for the disrupted asymmetry in post-Golgi secretory vesicles (Alder-Baerens et al., 2006; Natarajan et al., 2004). In this manner P4 ATPases regulate phospholipid asymmetrical distribution in late golgi compartments as well as in plasma membrane.

1.3.1.2 P4-ATPases as lipid scavengers

Among all the known P4-ATPases some are identified as the flippases of plasma membrane with comparably broad specificity towards phospholipid. It is, therefore, intriguing to figure out the functions of these P4-ATPases apart from their role in managing the lipid asymmetry in the membrane. For example in *S. cerevisiae* cells takes up extracellular lysophospholipids and used them as a substrates for regeneration of phospholipids (Riekhof et al., 2007). After being transported into the cells *ALE1*-encoded lysophospholipid acyltransferase, acylate lysophosphatidylethanolamine (lyso-PE) and lysophosphatidylcholine (lyso-PC) by utilizing lysophosphatidic acid as a substrate to PE and PC, respectively (Jain et al., 2007; Tamaki et al., 2007). Absence of both Dnf1 and Dnf2 and their subunit Lem3 curb the uptake of radiolabeled lyso-PC or lyso-PE and hinder lyso-PC or lyso-PE-dependent growth, respectively, these further supported the role of these pumps as nutrient scavenger (Figure 1.9b) (Riekhof and Voelker 2006; Riekhof et al. 2007).

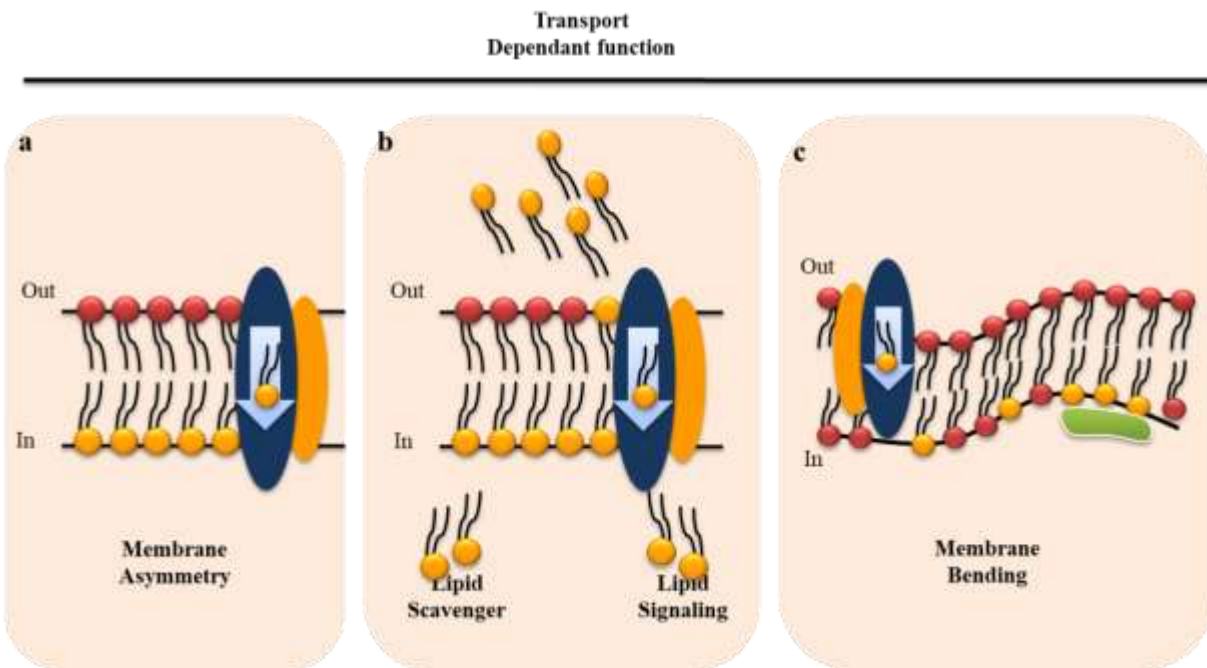
1.3.1.3 Role of P4-ATPases in vesicle formation

Studies in different life forms like mammals, yeast and plants have discovered the role of P4-ATPases in vesicular trafficking. Two models have been proposed to explain contribution of P4-ATPases in vesicle formation (Figure 1.9c).

(i) One model is that P4-ATPases creates a phospholipid imbalance between the two leaflets by directly catalyzing an inward-directed phospholipid translocation across the lipid transbilayer. In turn, this causes bulging of the membrane leading to budding and vesicle formation, which is later stabilized by assembly of coat proteins (e.g., clathrin or COPII proteins). Further this has been found, there is striking change in the shape of red blood cells caused by insertion of exogenous phospholipids to the cytosolic leaflet by a lipid flippase (Daleke and Huestis, 1985;

Seigneuret and Devaux, 1984). Likewise, flipping of lipid can accelerates endocytosis (Farge et al., 1999) and influence the formation of endocytic-like vesicles (Muller et al., 1994).

(ii) According to second model in order to create permissive environment for vesicle budding ATP-driven lipid translocation by P4-ATPases is required. An increase in concentration of aminophospholipids in the inner leaflet promote the activity of peripherally associated proteins which play a crucial role in vesicle budding, such as small ADP ribosylation factor (Arf) GTP-binding proteins, clathrin, coat protein complex II, amphiphysin, and endophilins.



Transport independent function

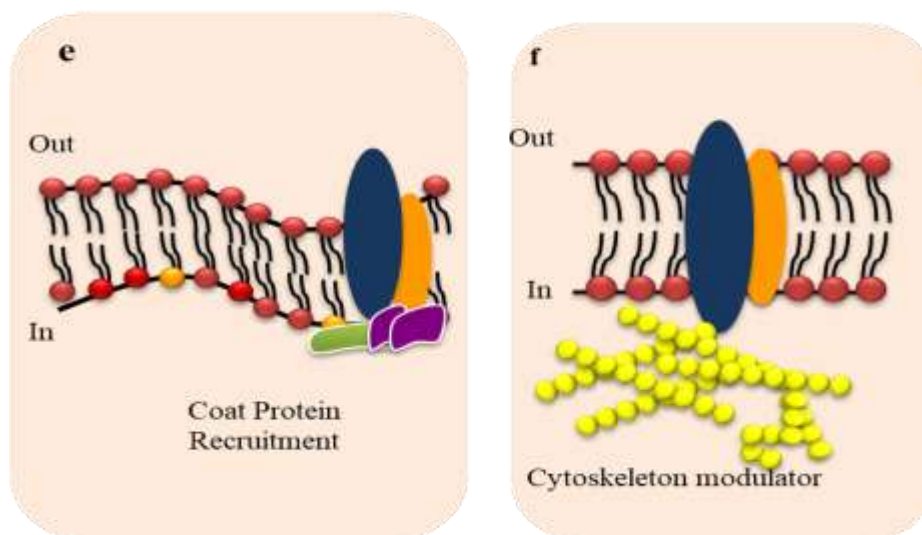


Figure 1.9. Cellular functions involving P4-ATPases. (a) Active transport of lipids from the exoplasmic to the cytosolic membrane leaflet can maintain lipid asymmetry, (b) scavenge lipids, and (c) drive membrane budding by generating a lipid imbalance across the bilayer and/or a membrane environment permissive for vesicle budding. (d) Enzyme-independent functions of P4-ATPases include recruitment of proteins involved in coat assembly, (e) cellular signaling, and cytoskeleton regulation.

The substrate specificity of various members of P4-ATPase family differ with each other which is discussed in more detail in next section. Likewise, loss of *MgATP2*, P4-ATPase in the rice plant pathogenic fungus *Magnaporthe grisea* results in abnormal Golgi-like cisternae (Gilbert et al., 2006). In higher eukaryotes defects in trafficking are often associated with irregular P4-ATPase function. P4-ATPases are crucial during vesicle formation in several parts of the intracellular trafficking pathways.

1.3.1.4 P4-ATPases as membrane scaffolds

P4-ATPases also plays role in some transport-independent functions (Figure 1.9d). During membrane budding some cytosolic proteins like guanine nucleotide exchange factors and small GTPases are required and yeast P4-ATPases, Drs2 and Neo1, interacts with these cytosolic proteins, (Barbosa et al., 2010; Chantalat et al., 2004; S. Chen et al., 2006; Furuta et al., 2007; Tsai et al., 2013; Wicky et al., 2004). Furthermore, proteomic based strategy identified proteins

associated with Drs2 to be involved in phosphoinositide metabolism (Puts et al., 2009). Phosphoinositides are crucial signaling molecules in membrane that play an important role in establishing organelle identity by effector proteins.

Function of both Drs2 and Dnf1 depends on their interaction with Sla1 (Liu et al., 2007), that is part of adaptor complex/ endocytic coat with clathrin. Linking the cytoskeleton to specialized areas of the plasma membrane may thus be a feature shared among several members of the P-type ATPase superfamily. Thus, intracellular P4-ATPases that seem to act without a beta subunit, e.g., Neo1 in yeast or *ATP9B* in mammals (Takatsu et al., 2011), could serve a lipid transport-independent function as scaffold switches to recruit structural components or effectors.

1.3.1.5 P4-ATPases exhibit different substrate specificities

Initial knowledge on P4-ATPases point their involvement in flipping of aminophospholipids only. Studies on different life form like fungi, animals, and plants discovered that the substrate specificities of P4-ATPase differ with each other and besides di-acyl aminophospholipids they also transport lipid substrates (Figure 1.9e). For example in *S. cerevisiae*, loss of Dnf1 and Dnf2 the P4-ATPases abrogate internalization of fluorescent labelled PC, PS and PE, across the plasma membrane (Pomorski et al., 2003). Furthermore, Dnf1 and Dnf2 also govern the translocation of the lyso-PC and lyso-PE across the biological membrane (Riekhof and Voelker, 2006; Riekhof et al., 2007).

1.3.2 Significance of P4-ATPases beta subunit

Association of the beta subunit from the Cdc50 family with the catalytic subunit of P4-ATPases is requisite for the proper function and localization of the enzyme. It consists of large heavily glycosylated exoplasmic loop with a two transmembrane domains (Figure 1.10) (Poulsen et al., 2008; Puts et al., 2009). It also act as a chaperons and this association is crucial for exit of P4-

ATPase from endoplasmic reticulum, these also control catalytic properties of flippase complex as it's essential for translocation of lipid (Bryde et al., 2010; Furuta et al., 2007; Lopez-Marqués et al., 2010). Instead of this some P4 ATPases for example, yeast *Neo1* and mammalian *ATPA9* and *ATP9B* have no requirement of *CDC50* proteins for exit from ER.

P4-ATPases beta subunit are significant for accurate localization of this complex to the membrane, for example *Dnf1* and *Dnf2* and their common beta subunit, *Lem3* localize at plasma membrane, *Drs2* and subunit *Cdc50* are localized to the trans Golgi network. But in contrast in multicellular organisms this specific association is not mandatory for localization. For example in plant three different beta subunits found which can associate any of P4 ATPase *ALA1*, *ALA2*, and *ALA3* for their exit from ER , as well as association with different subunit lead to different final subcellular localization (Lopez-Marqués et al., 2010; López-Marqués et al., 2012). Similarly in human also different P4- ATPases can interact any of three identified human *Cdc50* homologs (Bryde et al., 2010).

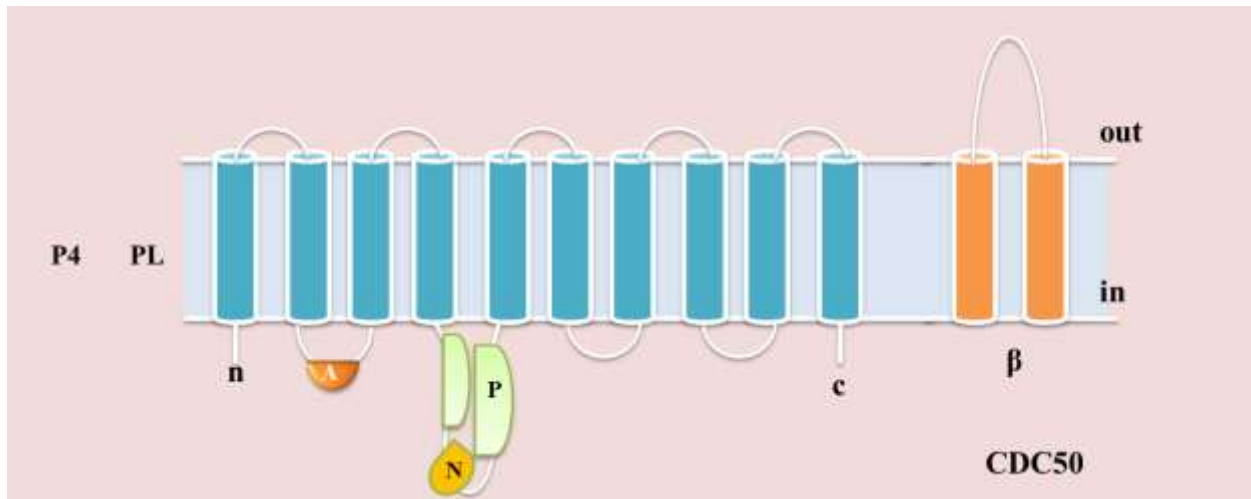


Figure 1.10. Membrane topology of P4-ATPases and their subunits. Ptype ATPases consist of an actuator (A), a phosphorylation (P), a nucleotide-binding domain (N), The CDC50 subunits of P4-ATPases consist of two membrane-spanning domains with a large extracellular loop.

Cdc50 family interactions with P4 ATPases may be different in multicellular organisms than yeast.

As in yeast expression of P4 ATPases and their respective beta subunits occur at the same time in the same cell and may be this will be essential for their appropriate function. However in multicellular organisms to avoid undesired interactions, expression of each protein can be controlled by temporal and spatial expression. In this manner, it will be more applicable for cell to regulate a number of interchangeable beta subunits interaction with various P4-ATPases and their individual physiological functions.

Further interaction of Cdc50 proteins with P4-ATPase also contribute to transport specificity (Coleman et al., 2009; Puts et al., 2009; Zhou and Graham, 2009). It has been found in yeast trans golgi P4-ATPases translocating different phospholipids, interact with different Cdc50 homologs (Alder-Baerens et al., 2006), as Dnf1 and Dnf2, plasma membrane P4-ATPases both interact with Lem3 (Furuta et al., 2007; Saito et al., 2004) and show same substrate specificity (Pomorski et al., 2003), Dnf3 interacts with Crf1 (Furuta et al. 2007), Drs2 with Cdc50 (Saito et al., 2004).

1.4 P4-ATPases and their beta subunits in yeast

Role of P4 ATPases in lipid asymmetry is an unexplored area in eukaryotes, still there is some research has been done in different organisms. The following section highlight the major components of P4 ATPases and their role in pathogenic and non-pathogenic fungi.

1.4.1 *Saccharomyces cerevisiae*

S. cerevisiae is often used as a model system for better understanding of different cellular pathways in eukaryotes. P4-ATPases are well characterized in this nonpathogenic fungus. This yeast expresses five P4-ATPases, Dnf1 and Dnf2 at the plasma membrane, Neo1 in the endosomal membranes, Drs2 and Dnf3 mostly in the trans-Golgi network (Chen et al., 1999;

Hua et al., 2002; Wicky et al., 2004; Pomorski et al., 2003). These P4-ATPases except Neo1 required beta subunit for their function as well localization for example Drs2 and Dnf3 interact with Cdc50 and Crf1 respectively, while Dnf1 and Dnf2 both interact with Lem3 (Saito et al., 2004; Noji et al., 2006; Furuta et al., 2007). Neo1 transport PE and PS across plasma membrane but lipid substrate for this P4 ATPase is still not known (Takar et al., 2016). Dnf1, Dnf2, and Dnf3 act as PE and PC flippases (Pomorski et al., 2003; Alder-Baerens et al., 2006), while Drs2 transport PS and PE across biological membrane (Alder-Baerens et al., 2006; Zhou and Graham, 2009; Natarajan et al., 2004). On association with Lem3, Dnf1 and Dnf2 also transport lysophosphatidylcholine, alkylphospholipids, monohexosyl glycosphingolipids and lysophosphatidylethanolamine (Riekhof and Voelker, 2006; Riekhof et al., 2007; Roland et al., 2019). Alterations in Dnf1, Dnf2 and Drs2 lead to cold-sensitive defect in endocytosis (Gall et al., 2002; Pomorski et al., 2003). ATP-driven phospholipid translocation is required for membrane budding and endocytosis. It has been also reported that loss of Drs2 results in a decrease in clathrin-coated vesicle budding from the trans Golgi network (Natarajan et al., 2004; Gall et al., 2002). The Golgi-localized P4-ATPase Dnf3 and the endosome associated P4-ATPase Neo1p are required for plasma membrane and endosomal / vacuolar system and protein trafficking between the Golgi complex (Hua et al., 2002; Wicky, Schwarz, and Singer-Krüger, 2004; Hua and Graham, 2003). Further shown digramatic representation of intracellular location and function of lipid transporters in *S. cerevisiae* (Figure 1.11).

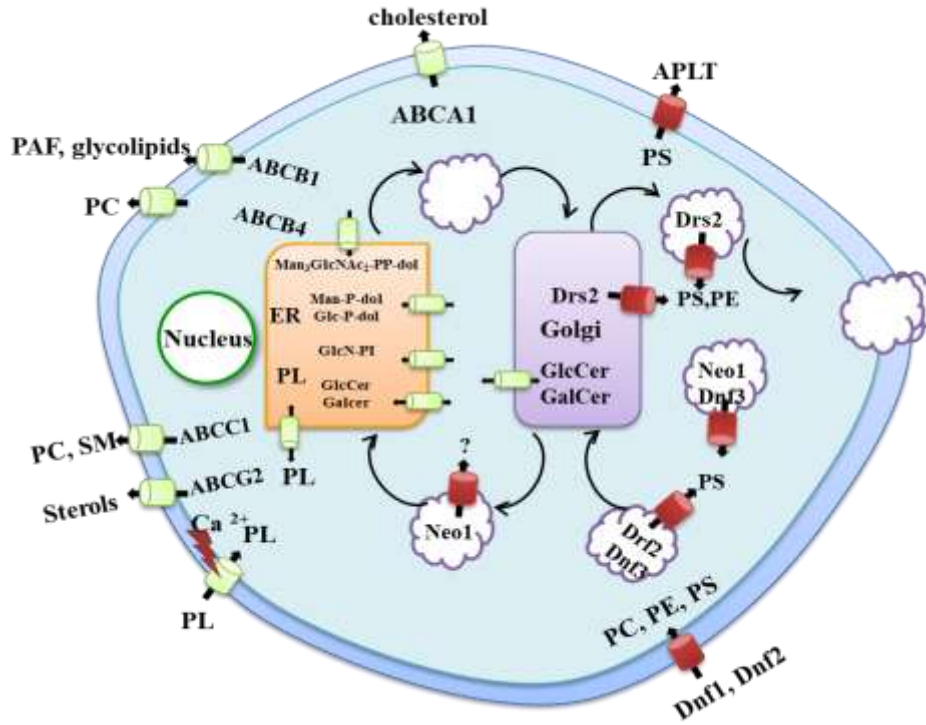


Figure 1.11. Digramatic representation of intracellular location and function of lipid transporters in *S. cerevisiae*. “Flippases” (red) catalyze the transport of lipids toward the cytoplasm and require ATP, “floppases” (green) catalyze the ATP-dependent transport of lipids away from the cytoplasm. *PAF*, platelet-activating factor; *SM*, sphingomyelin; *PL*, phospholipid

1.4.2 *Aspergillus nidulans*

Over the last few decades, invasive infections caused by filamentous fungus have increased and affecting mainly immunocompromised patients (Debourgogne et al., 2016). Invasive aspergillosis is mainly caused by *Aspergillus fumigatus* in individuals with initial immunodeficiency, further by *A. nidulans*, due to its ability to cause infection in patients with chronic granulomatous disease (Seyedmousavi et al., 2018). Similar to *S. cerevisiae* P4 ATPase family also expresses in *A. nidulans*, including DnfA (Dnf1/2), DnfB (Drs2), DnfC (Dnf3) and DnfD (Neo1) (Schultzhaus et al., 2015). In *A. nidulans* Spitzenkörper is primarily composed of secretory vesicles that regulate fungal secretion and growth in the growing cell tip. DnfA and DnfB are localize to this organelle (Schultzhaus et al. 2017; Schultzhaus et al., 2015). In this

fungus DnfB promotes sexual reproduction and has no regulatory role in conidiation, while DnfA regulate asexual sporulation, polarized growth and pigmentation. Deletion of both *DNFA* and *DNFB* cause lethality in *A. nidulans* (Schultzhaus et al., 2015). DnfA and DnfB regulate the PS asymmetry of membrane and localize at different sets of vesicles. As DnfA is presented in the peripheral region, DnfB is distributed within the Spitzenkörper core (Schultzhaus et al., 2017; Schultzhaus et al., 2015). Similar to *S. cerevisiae*, deletion of beta subunit Cdc50 lead to defect in hyphal tip organization and morphology, secretion (Schultzhaus et al., 2017). Further Schultzhaus and collaborators analyzed mutants carrying single and pairwise deletions of P4 ATPases. It has been found that alteration of *DNFD* (ortholog of the essential *S. cerevisiae* *NEO1*) also resulted in a strong conidiation deficiency. Lethal phenotype displayed by cells on deletion of both *DNFB* and *DNFD* (Schultzhaus et al. 2019). Recently role of DnfD in cellular growth and development also demonstrated (Schultzhaus et al. 2019). DnfDp is required for morphological changes during conidiation and also important in trafficking processes (Schultzhaus et al. 2019). It localizes to the late Golgi and is also regulated early stages of conidiophore development (Schultzhaus et al. 2019).

1.4.3 Cryptococcus neoformans

C. neoformans major causative agent of meningoencephalitis also have *APT1*, *APT2*, *APT3* and *APT4* act as P4 ATPases, (Hu and Kronstad, 2010). Apt1 is similar to Drs2 from *S. cerevisiae* revealed by phylogenetic analysis and interestingly, in *S. cerevisiae* *drs2Δ/Δ* mutant strain partially restored the growth on expression of *C. neoformans* *APT1*. In *C. neoformans*, modification in Apt1 and its potential subunit, Cdc50, affect various fungal physiology and virulence related traits.

Deletion of *APT1* effected vesicle trafficking, endocytosis, and actin distribution, as well as fungal survival inside macrophages (Hu and Kronstad, 2010). *apt1* mutant have no significant

role in release of extracellular vesicles, but these vesicles show reduced concentration of glucuronoxylomannan (GXM) (Rizzo et al., 2014). Its deletion also lead to intra-vacuolar accumulation and pigment-containing vesicles as well as abnormalities in vacuolar membranes (Rizzo et al., 2018). Apt1 also regulated some virulence related trait as modification in this gene resulted in attenuated virulence in a mice model of infection, and altered synthesis of virulence associated lipids (Rizzo et al., 2014; 2018).

C. neoformans Cdc50 shows similarity to both *S. erevisiae* Cdc50 and Lem3 (Hu et al., 2017). In *C. neoformans* Cdc50 is localized at the plasma membrane, ER and endosome-like structures (Hu et al., 2017; Huang et al., 2016). Deletion of Cdc50 lead to increase sensitivity for trafficking inhibitors and echinocandin caspofungin (Huang et al., 2016). Cdc50p also play important role in activation of the Rim signaling pathway. By this pathway *C. neoformans* distinguish and responds to alterations in the extracellular pH, as well as in its evasion of the host immune response (O'Meara et al., 2013).

Individually deletion of *APT1*, *APT2*, *APT3* or *APT4* genes shared same phenotypical features with *C. neoformans* mutant cells lacking *CDC50*. Interestingly, *cdc50Δ* and *apt1Δ* cells share several phenotypic traits, reduced GXM secretion, attenuated survival in macrophages, and increased sensitivity to antifungal drugs, including azoles, cinnamycin and amphotericin B, iron-chelating drug curcumin, to trafficking inhibitors (brefeldin A and monensin) and growth defect in alkaline pH, (Hu and Kronstad, 2010; Rizzo et al., 2014; Hu et al., 2017; Huang et al., 2016). Additionally, both *cdc50Δ* and *apt1Δ* strains were hypovirulent in a murine model of infection, and unable to reach the brain, which is the fatal outcome of cryptococcosis (Hu and Kronstad, 2010; Rizzo et al., 2014; Hu et al., 2017; Huang et al., 2016). These findings introduced Cdc50

as a beta subunit of Apt1, which form a functional flippase complex that may use as a novel target for development of antifungals.

APT paralog genes *APT2*, *APT3*, and *APT4* is not well characterized. Contrasting to Apt1 and Cdc50, Apt2, Apt3, and Apt4 do not important for growth at alkaline pH, iron acquisition, and resistance to curcumin (Hu et al., 2017). *cdc50*Δ mutant showed increased susceptibility to brefeldin A than *apt1*Δ and *apt3*Δ mutants. Additionally double mutant (*apt1*Δ*apt3*Δ) was more sensitive to brefeldin A than each single mutant (Hu et al., 2017).

1.4.4 *Candida albicans*

Role of P4 ATPases in different cellular mechanism is studied in others pathogenic and nonpathogenic fungus but information in this aspect are limited in opportunistic human pathogenic fungus, *C. albicans*. This fungus by virtue of its plasma membrane asymmetry can evade toxicity of copper, generally used by immune system to attack pathogenic microbes (Festa et al., 2014). Deletion of *DRS2* in *C. albicans* leads to increase sensitivity to fluconazole and also effect bud to hyphal transition (Labbaoui et al., 2017). Cdc50 beta subunit of P4 ATPase also regulates susceptibility for different drugs in *C. albicans*. Alteration in *CDC50* results in increased susceptibility for sodium dodecyl sulfate a membrane perturbing agent, as well as to the azoles, caspofungin, and terbinafine. Besides this *cdc50* mutant also exhibit diminished virulence in mouse model of systemic infection and defective hyphal development (Xu et al., 2019).

1.5 AIM OF PRESENT WORK

Fungal pathogens are eukaryotes that share biological processes with the human host they infect, thus exhibiting a challenge to human health. *Candida albicans* is one such human opportunistic pathogen that resides as a natural component of the human flora and is major cause of life-threatening infections in immunosuppressed patients. Candidiasis is treated by different antifungal drugs like azoles, polyenes, fluoropyrimidines, and echinocandins. However, among several *Candida* species, the presence of intrinsic and developed resistance against these antifungals has been reported. In this way acquisition of drug resistance and prevalence of fungal infections is increasing, emphasizing on the need for identifying novel targets for developing antifungals. Fungal cell membrane is used as a drug development target for many years because of their effectiveness. Till date major success for treatment of this disease has been achieved by drugs that affect cell membrane integrity (for example antifungals such as polyenes and azoles) (Muller et al., 2013).

Biological membrane is made up of lipid bilayers, in which lipids are distributed in an asymmetrical manner between the two leaflets. This asymmetric distribution of phospholipids on the membrane is maintained by balance inward (flip) and outward (flop) translocation of phospholipids across the membrane. Between the two leaflets asymmetric pattern maintained with presence of aminophospholipids phosphatidylethanolamine (PE) and phosphatidylserine (PS) restricted to the cytosolic leaflet while sphingolipids and phosphatidylcholine (PC) enriched in the outer leaflet (Panatala et al., 2015; Kobayashi and Menon, 2018). Asymmetric arrangement of lipids provides different characteristics to outer and inner membrane and govern multiple cellular processes, like cell division, lipid metabolism, regulation of membrane traffic, and lipid signaling (Panatala et al., 2015; Hankins et al., 2015; Lopez-Marques et al., 2014).

Any perturbations in the asymmetric distribution of phospholipids on the plasma membrane serves as a trigger for activating multiple cellular events (Nichols, 2002).

Lipid transporters are the proteins that guide asymmetric distribution of lipids across the cellular membrane. These transporters are divided into two groups on the basis of requirement of ATP hydrolysis for transportation (i) ATP-driven transporters (ATP-binding cassette transporters and P-type ATPases) that actively translocate specific lipids between two leaflet and (ii) ATP-independent transporters, known as scramblases (Pomorski and Menon, 2016; López-Marqués et al., 2015). P4 ATPases are not found in eubacteria and archaea and are thus unique to eukaryotes. Interestingly P4 ATPases have been found in every eukaryotic genome that has been sequenced so far (Andersen et al., 2016). An interesting fact known about these P4 ATPases is their association with beta subunit known as Cdc50 proteins, resulting in a heterodimeric complex. This association of P4 ATPases with Cdc50 family proteins is essential for activity of the pump and their proper localization but seems not to affect their substrate specificity (Puts et al., 2012; Lopez-Marqués et al., 2010; Saito et al., 2004; Bryde et al., 2010; Lenoir et al., 2009).

In *S. cerevisiae* Dnf1, Dnf2, and Dnf3 are well identified as PE and PC flippases while Drs2p transports PS and PE across the lipid bilayer of plasma membrane (Pomorski et al., 2003; Zhou and Graham, 2009). It has been reported that Dnf1 and Dnf2 complex with their beta subunit Lem3 for transportation of phosphatidylethanolamine, phosphatidylcholine and monohexosyl glycosphingolipids (Riekhof et al., 2007; Kato et al., 2002; Hanson et al., 2003). It has been reported that cellular events like membrane budding and endocytosis are governed by phospholipid translocation. Yeast cells lacking P4 ATPases Dnf1, Dnf2 and Drs2 display a cold-sensitive defect in endocytosis (Pomorski et al., 2003; Gall et al., 2002). Loss of Drs2 is also known to decrease the clathrin-coated vesicle budding from the trans-Golgi network (Natarajan

et al., 2004; Gall et al., 2002). Furthermore, in *A. nidulans* DnfA is important for polarized growth and pigmentation, asexual sporulation, while DnfB play crucial role in sexual reproduction and has no importance in conidiation; a double deletion mutant of *DNFA* and *DNFB* is lethal in this pathogenic fungus. Deletion of DnfA flippase beta-subunit Cdc50 leads to defect in morphology and secretion, hyphal tip organization (Schultzhaus et al., 2015; 2017). In another fungal pathogen *C. neoformans* deletion of P4 ATPases Apt1 and its beta subunit Cdc50 affects the actin distribution, endocytosis, vesicle trafficking and virulence related traits and fungal survival inside macrophages (Hu et al., 2017; Huang et al., 2016). Recently, the role of *C. albicans* P4 ATPase subunit Cdc50, which in *S. cerevisiae* is shown to associate with Drs2, is essential for antifungal drug resistance and some pathogenic traits (Xu et al., 2019).

Considering the lesser known role of lipid asymmetry and lipid transporters in *C. albicans*, the goal of current study was to identify and characterize the putative membrane lipid transporter Lem3 in this pathogenic fungus. It is evident that better understanding of these biological membranes, metabolic pathways and membrane-associated biosynthetic pathways can play an important role in identifying new treatment alternatives for fungal infections. In addition, these advanced antifungal targets may also form the basis of new combination therapy to enhance the efficacy of currently used antifungal drugs.

Previous report from our laboratory has shown Rta3, a 7-transmembrane receptor protein, as the determinant of biofilm development in *C. albicans*. Furthermore, loss of Rta3 perturbs the dynamic equilibrium of PC by increasing its inwardly-directed (flip) movement across the plasma membrane. We later in this study hypothesized that Rta3 regulates the activity of an unknown PC-specific flippase in order to maintain the asymmetric distribution of PC across the plasma membrane, which we predicted could be Lem3 (Srivastava et al., 2017). Lem3 has been

identified as a member of Cdc50 family in the PFAM database (protein families database accession number P42838). Considering the significance of flippases and its beta subunit in regulating biological membrane asymmetry and other morphological, virulence related traits, an unexplored area, the goal of the current work was to focus on elucidating the role of P4 ATPase beta subunit, Lem3 in *C. albicans*. The immediate goal of this study therefore is

(1) To establish the role of Lem3 in regulating the transbilayer movement of phosphatidylcholine across the plasma membrane in *C. albicans*.

(2) If aim one is proven, then we hypothesized that changes in the asymmetric distribution of PC may have an impact on drug susceptibility and pathogenicity related traits. To this end, we would analyze the role of *LEM3* in the aforesaid cellular processes.

(3) To determine if Lem3 is regulated by the 7-transmembrane receptor protein Rta3.

2.0 MATERIALS AND METHODS

2.1. Materials

2.1.1 Strains, chemicals and growth conditions

The *C. albicans* strains used in the present study are listed in Table 1.

Table 1: Strains used in this study

Strain	Parent	Genotype	Source of reference
SC5314		Wild type	(Gillum et al., 1984)
PA10	SC5314	<i>LEM3/lem3Δ::SAT1-FLIP</i>	This study
PA11	PA10	<i>LEM3/lem3Δ::FRT</i>	This study
PA12	PA11	<i>lem3Δ::SAT1-FLIP/lem3Δ::FRT</i>	This study
PA13	PA12	<i>lem3Δ::FRT /lem3Δ::FRT</i>	This study
PA14	PA13	<i>lem3Δ::FRT/LEM3-SAT1-FLIP</i>	This study
PA15	PA14	<i>lem3Δ::FRT/LEM3::FRT</i>	This study
PA16	SC5314	<i>LEM3-Myc-FRT-SAT1-FLIP</i>	This study
PA17	PA16	<i>LEM3-Myc-FRT</i>	This study
GU5	Clinical isolate (fluconazole resistant)	Wild type	(Franz et al., 1998)
PA18	GU5	<i>LEM3/lem3Δ::SAT1-FLIP</i>	This study
PA19	PA18	<i>LEM3/lem3Δ::FRT</i>	This study
PA20	PA19	<i>lem3Δ::SAT1-FLIP/lem3Δ::FRT</i>	This study
PA21	PA20	<i>lem3Δ::FRT/lem3Δ::FRT</i>	This study
PA22	PA21	<i>lem3Δ::FRT/LEM3-SAT1-FLIP</i>	This study

PA24	PA13	<i>RTA3/rta3Δ::SAT1-FLIP</i>	This study
PA25	PA24	<i>RTA3/rta3Δ::FRT</i>	This study
PA26	PA25	<i>rta3Δ::SAT1-FLIP/rta3Δ::FRT</i>	This study
PA27	PA26	<i>rta3Δ::FRT/rta3Δ::FRT</i>	This study
PA28	PA27	<i>rta3Δ::FRT/LEM3-SAT1-FLIP</i>	This study
AS13	AS12	<i>rta3Δ::FRT/rta3Δ::FRT</i>	(Srivastava et al., 2017)
AS18	SC5314	<i>SC5314-TDH3-RTA3::NAT1</i>	(Srivastava et al., 2017)
PA29	SC5314	<i>SC5314-TDH3-LEM3::NAT1</i>	This study
PA30	PA13	<i>lem3Δ/Δ-TDH3-RTA3::NAT1</i>	This study
PA31	AS13	<i>rta3Δ/Δ-TDH3-LEM3::NAT1</i>	This study

The strains were maintained as frozen stocks and propagated at 30 °C in the liquid media and/or agar plates mentioned in Table 2. YEPD plates containing 200 µg/ml nourseothricin (Werner Bioreagents) were used for the selection of deletion mutants. To obtain nourseothricin sensitive derivatives of transformants strains were grown in YPM (Table 2) for 8 hours and plated on 25 µg/ml nourseothricin.

Table 2: Culture media compositions.

S.No.	Culture media name	Component	Composition (%-wt/vol)
1.	YEPD/YPM (Yeast extract peptone dextrose/ maltose)	Yeast extract	1 g
		Bactopeptone	2 g
		D-glucose/Maltose	2 g
		Bacto-agar	2.5 g

2.	SDC media	Yeast nitrogen base (w/o amino acids)	0.67 g
		Glucose	2 g
		Bactoagar	2.5 g
		Drop out mix	0.2 g
3.	SC media	Yeast nitrogen base (w/o amino acids)	0.67 g
		Sorbitol	2 g
		Drop out mix	0.2 g
4.	Spider Medium (pH set to 7.0)	Nutrient broth	1 g
		Mannitol	1 g
		K ₂ HPO ₄	0.2 g
		Bacto agar	2.5 g
5.	RoswellPark Memorial Institute medium (RPMI) preparation	RPMI powder	13.48 g
		Sodium bicarbonate	2.8 g

RPMI-1640 (containing L-glutamine, without bicarbonate) was prepared at 10.4 g/L, buffered with 0.165 mol/L MOPS (3-[N-morpholino] propanesulfonic acid), and pH adjusted to 7.0 using 1 mol/L sodium hydroxide. RPMI and sodium bicarbonate was mixed in autoclaved MQ, filtered through 0.22 μ nitrocellulose membrane filter and stored at 4 °C.

The drugs/supplements used in the study are listed in Table 3. These were added to the media/buffer at concentrations mentioned.

Table 3: Drugs/dyes used in the study

Drug/Dye/Standard	Solvent	
Miltefosine	Methanol	Sigma
Fluconazole	Methanol	Sigma
Ketoconazole	Methanol	Sigma
Voriconazole	DMSO	Sigma
Tunicamycin	DMSO	Sigma
DTT	Water	SRL
Caspofungin	Water	Biobasic
Congo red	Water	Sigma
Calcofluor white	Water	Biobasic
Norseothricin	Water	Werner bioreagents
Amphotericin B	Ethanol	Sigma
Ampicillin	50% Ethanol	Sigma
Chloramphenicol	Ethanol	Sigma
β -mecaptoethanol	-	Sigma
Sodium dithionite	Water	Sigma
Sodium azide	Water	Sigma

2.2 Methods

2.2.1 PCR Amplification

Polymerase chain reaction was used to amplify the desired gene sequences. **(i) Standard PCR conditions** were the following: the initial duration given was 94 °C for 5 minutes, which continued at 95 °C for 1 minute, followed by reannealing temperature of 55 °C for 1 minute and an extension temperature of 72 °C for 2 minutes each for 30 cycles. Final extension was given for 7 minutes and the final hold was carried out at 4 °C. Reaction Constituents: DNA (100 ng/μl) = 2.0 μl, Forward Primer (5 picomoles/μl) = 1.0 μl Reverse Primer (5 picomoles /μl) = 1.0 μl, dNTPs (10 mM) = 1.0 μl, 10X Reaction Buffer = 5.0 μl, Taq Polymerase (2.5 U/μl) = 0.5 μl, MQ = 39.5 μl. The total volume for a PCR reaction was set at 50 μl. Reaction conditions were altered for amplicons greater than 1 kb. PCR products were checked by agarose gel electrophoresis and purified by Qiagen MiniElute PCR Purification Kit before downstream applications. Amplification was done by high fidelity DNA polymerase in experiments where gene expression was required. Final clones in all vectors were sequenced before proceeding. **(ii) PCR conditions with long primers** - PCR conditions (for long primers) were as follows: Initial denaturation is at 98 °C for 5 minutes. Next, for cycle 1-5, denaturation is at 98 °C for 10 seconds, annealing is at 58 °C for 30 seconds and extension is at 72 °C for 5 minutes. Further for cycle 6-30, denaturation is at 98 °C for 10 seconds, extension is at 72 °C for 5 minutes and final extension is at 72 °C for 10 minutes. Final hold is at 4 °C. The oligonucleotides used for cloning and quantitative real time PCR are listed in Table 4.

Table 4. Oligonucleotide used in this study

Oligonucleotide	Description	Sequence (5' - 3')
<i>LEM3P1</i>	Forward primer for amplifying 5' <i>LEM3^{ORF}</i> bearing KpnI site	5'-GGTACCATACAAACTCTGAGCTGA-3'
<i>LEM3P2</i>	Reverse primer for amplifying 5' <i>LEM3^{ORF}</i> bearing XhoI site	5'-CTCGAGCACAAGGATAAATTCTTT-3'
<i>LEM3P3</i>	Forward primer for amplifying 3' <i>LEM3^{ORF}</i> bearing SacII site	5'-CCGCGGAACGTGGTATATACCAAATA-3'
<i>LEM3P4</i>	Reverse primer for amplifying 3' <i>LEM3^{ORF}</i> bearing SacI site	5'-GAGCTCACAATCTTTAATATAGACTTCAA-3'
<i>LEM3P5</i>	Forward primer for amplifying 5' <i>LEM3^{NCR}</i> + <i>LEM3^{ORF}</i> bearing ApaI site	5'-GGGCCCATAGGACAGATACCAGGACA- 3'
<i>LEM3P6</i>	Reverse primer for amplifying 5' <i>LEM3^{ORF}</i> bearing XhoI site	5'-CTCGAGTCATTTTTCAAATCCAGTG- 3'
<i>LEM3</i> mycF Nostop	To amplify 65 bp <i>LEM3</i> ORF myc tag region	5'AGAAGACAAAGAGAGATGAACAAAGTGCTGC AGCTGCTGAGGGTGTCCACCACTGGATTTGAAAA ACGGATCCCCGGGTTAATTAACGG-3'
<i>LEM3</i> mycR UTR	To amplify 65 bp <i>LEM3</i> UTR myc tag region	5'CCAACATTTATTACAACACAATCTTTAATAT AGACTTCAAAGAGAATTCATACTCAAATAA ACTGGCGGCCGCTCTAGAACTAGTGGATC-3'
DET <i>LEM3F</i>	To detect <i>LEM3</i> myc construct integration	5'-ACAAAATAGATTTAAGAAA-3'

DET <i>LEM3</i> R	To detect <i>LEM3</i> myc construct integration	5'-ATTGTACCTTGAAAGAACGG-3'
AHO300	To detect <i>LEM3</i> myc construct integration	5'-CCGTTAATTAACCCGGGGATC-3'
AHO301	To detect <i>LEM3</i> myc construct integration	5'GGAACTTCAGATCCACTAGTTCTAGAGC-3'
AHO302	To detect <i>LEM3</i> myc construct integration	5'-TCACTAGTGAATTCGCGCTCGAG-3'
AHO283	To detect <i>LEM3</i> myc construct integration/amplicon sequencing	5'GGCGGCCGCTCTAGAACTAGTGGATC-3'
<i>LEM3</i> myc(150bp upstream of stop codon)	To detect <i>LEM3</i> myc construct integration/amplicon sequencing	5'-TTTATATTAGGATTAGCCTT-3'
<i>LEM3</i> -F-OE-Ag- NAT-Ag-TEF1p	Forward primer for <i>LEM3</i> ^{OE}	5'GACAAAAGTTCTTATACTAAGGGGACGATC GGATATATTTTTTCCAACCAATAGGACAGAT ACCAGGACACATAGCCCCTGTTTCATTATCCC CATAATCATCAAGCTTGCCTCGTCCCC 3'
<i>LEM3</i> -R-OE-Ag- NAT-Ag-TDH3p	Reverse primer for <i>LEM3</i> ^{OE}	5'ATGATTCATATTCTCCCTCCTGTGCATACTC ATCTAATACACCTTCTCGCTGTTGATCTCCAT TATCAATTTGTTGTGCATCATCTGCTGTTTCGT GACATATTTGAATTCAATTGTGATG 3'
<i>LEM3</i> -OE-F-det	Detection primer for Overexpression	5'-AGCTTAACACGACTGAACAG-3'
<i>RTA3</i> -F-OE-Ag-NAT-Ag-TEF1p	Forward primer for <i>RTA3</i> ^{OE}	5'-ATAAGTTATTCCTAATCTGCTAAAAAA AAGAAACATGGTACTCTTAGAATAGTTATAGA TCCACACGGAACCTCGGAAATTATGCACTGAATG TAAATCAAGCTTGCCTCGTCCCC-3'
<i>RTA3</i> -R-OE-Ag-NAT-Ag-TDH3p	Reverse primer for <i>RTA3</i> ^{OE}	5'AAGCTGGGGCATAAGTTGCAGCAATGGTGGAT AGAGTTGTTGAAGTTGCAGTTGAGGTAGGAGTC CTTCTGTAATTACCGCAAGATCCATAGTATTCAT ATTTGAATTCAATTG TGATG-3'
<i>RTA3</i> -OE-F-det	Detection primer for OE	5'-CATGGTACTCTTAGAATAGTTAT -3'

Nat-OE-R-det2-CJN	Detection primer for OE	5'-GAAACAACAACGAAACCAGC-3'
<i>ACT1</i> /RT/F	Primer for qPCR	5'-GAAGCCCAATCCAAAAGAGG-3'
<i>ACT1</i> /RT/R	Primer for qPCR	5'-CTTCTGGAGCAACTCTCAAT-3'
<i>LEM3</i> /RT/F	Primer for qPCR	5'-ATGTCACGAACAGCAG-3'
<i>LEM3</i> /RT/R	Primer for qPCR	5'-CTCGTCATCGTAATCTG-3'
<i>RTA3</i> /RT/F	Primer for qPCR	5'-TACAGAATGGACTCCTACCT-3'
<i>RTA3</i> /RT/R	Primer for qPCR	5'-CCCGTACCATTTAATCGA-3'
<i>ERF1</i> /RT/F	Primer for qPCR	5'-AAAAGCATGGTAGAGGTGGTCAA-3'
<i>ERF1</i> /RT/R	Primer for qPCR	5'-ATTGTGTCTCTTTTCCTCTCTTAAACG-3'

2.2.2 DNA purification by gel extraction

Thermo Scientific™ DNA extraction kit was used for DNA purification by following the manufacturer protocol. DNA fragment from agarose gel was excised by cutting the fragment of interest with a clean, sharp scalpel. The gel slice was weighed in an Eppendorf tube and corresponding volume (1:1) of binding buffer was added to the same. The tube was then incubated at 55 °C to let the gel dissolve completely (light vortexing in between was suggested to enhance the mixing). Once mixed, the solution was transferred into a column, followed with centrifugation for 1 minute at 11,000 rpm. Flow through was discarded and wash buffer (600 µl) containing ethanol was added to the tube and recentrifuged for 1 minute. DNA was eluted in 20-30 µl of MQ or elution buffer (depending upon the further applications) after centrifugation.

2.2.3 Preparation of competent cells

For preparation of competent cells, single colony of *E. coli* DH5-α from a freshly streaked plate was inoculated into 10 ml of LB broth in a sterile 50 ml falcon (primary culture) and allowed to

grow at 37 °C combined with vigorous shaking at 220 rpm (in a rotary shaker) overnight, for bacterial growth. Secondary culture was obtained by inoculating 2 ml primary culture into 200 ml of fresh LB broth (1%) and was incubated for 37 °C, at 220 rpm shaking, till optical density of the culture reached between 0.4 and 0.6 (approximately 2.5 hours). Culture was taken out and let to cool down on ice for 20 minutes and transferred to 50 ml falcon, following the centrifugation at 6500 rpm for 5 minutes. Supernatant was discarded and cell pellet was washed twice with ice-cold sterile water. 12 ml of 0.1M CaCl₂ and 4 ml of 0.1M MgCl₂ was added to the washed pellet and mixed well by gentle pipetting. Cells were incubated on ice for 30 minutes and centrifuged at 6500 rpm for 5 minutes. Supernatant was removed and the cells were suspended in 480 µl of 0.1M CaCl₂ and 144 µl of 30% glycerol and incubated another time on ice for 30 minutes in order to improve competent efficiency. 200 µl of these competent cells were transferred into chilled microfuge tubes and were stored in -80 °C till required.

2.2.4 Transformation of competent *E. coli*

Bacterial transformation was carried out in pre-prepared competent cells. Competent cells were allowed to defrost on ice. Once defrosted, DNA to be transformed (100 ng approx.) was added to the cells followed by the heat shock at 42 °C for 90 seconds in a temperature regulated water bath. Tubes were quickly transferred to ice bucket and allowed to incubate there for 2 minutes. 900 µl of LB broth was added to each tubes and culture was incubated at 37 °C for 1 hour to allow the bacteria to recover from shock and to allow the bacteria to express the antibiotic resistance marker encoded by the plasmid. The culture was pelleted down by centrifugation at 6000 rpm for 3 minutes and spare media was removed. The pellet was resuspended in the residual media (100 µl) and transformed cells were gently and uniformly plated on the surface of ampicillin agar plate, using a sterile L rod. Plates were incubated overnight at 37 °C and were examined for Amp^R transformants on the following day.

2.2.5 Gel electrophoresis

2.2.5.1 Agarose gel electrophoresis

1% agarose gel was routinely used in the experiments. 1% agarose gel was casted by dissolving 0.5 g of agarose in 50 ml of 1X TAE buffer. The buffer was then boiled in the microwave oven to completely dissolve agarose. Meanwhile the gel apparatus was set up for 50 ml gel. After cooling the agarose by continuous swirling or stirring under the tap water, 2 μ l of EtBr (10 mg/ml) was added and the buffer was then mixed and poured into gel rack fitted with appropriate comb. After solidification of gel, combs were carefully removed. The holes that remained after removing out the combs were the wells or slots. The gel tank was filled with 1X TAE buffer and gel was also immersed in 1X TAE. 2 μ l of the respective samples along with 2 μ l of loading dye was loaded into each well. After setting up the tank completely, the power pack was switched on, and the gel was run at 80-90 V. The colored dye in the DNA ladder and DNA samples act as “front wave” that runs faster than DNA itself. When the “front wave” approached the end of the gel, the current was stopped. The gel was then viewed under UV light, observed on Gel Documentation, from Bio-Rad.

2.2.5.2 RNA gel electrophoresis

To prepare 1.2 % formaldehyde agarose gel, 1.2 g of agarose was dissolved in 100 ml 1X formaldehyde gel buffer and heated till gel gets dissolved. After gel cools down, 1.8 ml of 37% formaldehyde and 1 μ l of 10 mg/ml EtBr were added to the gel. After thorough mixing gel was poured onto a gel support. Before running the gel, it was equilibrated in 1X formaldehyde agarose gel running buffer for at least 30 minutes. Meanwhile samples were prepared by mixing 1 volume of 5X loading buffer with 4 volumes of RNA sample (for example 10 μ l of loading buffer and 40 μ l of RNA) and mixed well, followed with incubation for 3–5 minutes at 65 °C

followed by cooling and finally loaded on the equilibrated formaldehyde agarose gel buffer. Gel was observed under UV light or photographed under Gel Documentation system from Biorad.

2.2.6 Yeast transformation by Electroporation

Single colony of desired background strain of *C. albicans* was taken and grown in 10 ml of YEPD media over night at 30 °C, serving as a primary culture. 2 µl of primary culture was inoculated in 50 ml of YEPD media and allowed to grow for 14 hours (OD₆₀₀ of 1.6-1.8) to obtain a secondary culture of actively growing cells. Cells were harvested by centrifugation at 3000 rpm for 5 minutes and the pellet was suspended in 8 ml of ice-cold sterile MQ water, 1 ml of 10X TE (10 mM Tris and 1mM EDTA; pH 8.0) and 1 ml of 1 M lithium acetate (LiAc). The cells were incubated at 30 °C for 30-45 minutes on a shaking incubator. Cells were taken out and washed with ice-cold MQ water twice. Washed cell pellet was resuspended in 25 ml of 1 M sorbitol. Centrifuged at 3000 rpm for 5 minutes and the supernatant was discarded, following dissolving the pellet in minimum volume of sorbitol left in the falcon. 40 µl of the electrocompetent cells and 5 µl (approximately 1µg) linearized gel eluted DNA was mixed well and transferred to a electroporation cuvette; 0.2 mm (Bio-Rad) and electroporated using Bio-Rad Genepulser at electric pulse of 1.5 kV (Reuß et al. 2004). Electroporated cells were resuspended in YEPD, followed with revival on 30 °C for 4-5 hours/overnight. In the end culture was plated on selection plates (YEPD + 200 µg/ml nourseothricin). Plates were incubated at 30 °C for 48 hours to allow transformants to grow. Nourseothricin resistant (NouR) transformants were picked and streaked on YEPD plates containing 100 µg/ml of nourseothricin and also inoculated for genomic DNA isolation in YEPD media. Single copy integration of each construct at the desired locus was confirmed by Southern hybridization (with gene-specific probes) or PCR (using gene-specific primer) for the transformants.

2.2.7 Yeast genomic DNA isolation

Yeast cultures (wild type/transformants) were grown overnight to saturation in 10 ml of YEPD media at 30 °C at 220 rpm in shaker. The cells were centrifuged at 4,000 rpm for 5 minutes and the supernatant was decanted. The pellet was resuspended in 500 µl of sterile distilled water and briefly vortexed to resuspend the pellet and then transferred to 2 ml eppendorf tube. 2 ml tube was centrifuged at 4,000 rpm for 1 minute then a pellet was resuspended in residual volume of water. 200 µg of acid washed glass beads (Sigma), 200µl of yeast lysis buffer (TENTS) and 200 µl of PCI (Phenol: Chloroform: Isoamyl alcohol [25:24:1]) were added. Cells were lysed using a cell disruptor for 5 to 6 minutes and centrifuged in a microfuge for 5 minutes at 13,000 rpm at 4 °C. Upper aqueous phase was transferred to a fresh 1.5 ml tube and filled up with 100% chilled ethanol, and mixed by inverting few times. Tube was centrifuged for 3 minutes in centrifuged at 13,000 rpm. Supernatant was discarded and the pellet was washed with 600 µl of 70% ethanol. The pellet was dried at heat block for 5 minutes at 60 °C and resuspended in 50 µl of TE (10 mM Tris-Cl, 1 mM EDTA; pH 8.0) plus 3 µl of 10 mg/ml RNase A (Sigma). Tubes were incubated at 55 °C for at least 30 minutes for proper RNase treatment. The yield of genomic DNA isolated ranges from 1-3 µg/µl of sample. Approximately 10 to 16 µl of this DNA was used for Southern analysis.

2.2.8 Bacterial plasmid DNA isolation (Mini-preparation)

Isolation of plasmid DNA was done by Alkaline Lysis Method (Sambrook and Russell, 2006). DH5α cells containing the desired plasmid construct was streaked on ampicillin (100 µg/ml) added LB plate and incubated overnight at 37 °C. Single colony of each was inoculated in 10 ml of LB + Ampicillin (100 µg/ml) liquid medium and grown overnight at 37 °C with shaking at 220 rpm. On the following day, 3 ml of the bacterial culture was transferred into 1.5 ml Eppendorf tubes and cells were recovered by centrifugation at 12000 rpm for 2 minutes at 4 °C.

Supernatant was discarded and cell pellets were resuspended in 100 µl of solution I (25mM Tris HCl, pH 8.0, 10 mM EDTA, pH 8.0, 50 mM Glucose) with vigorous vortexing. Freshly prepared solution II (0.2 N NaOH, 1% SDS), 200 µl was added to the tubes, mixed gently by inverting the tubes (5 times) and were kept at room temperature for few minutes. To this, ice cold solution III (5M Potassium Acetate, pH5.2 and Glacial Acetic Acid) was added. Contents were mixed thoroughly by gently inverting the tube 5-6 times and incubated on ice for 5 minutes. Tubes were centrifuged at 12,000 for 15 minutes at 4 °C and cell debris was removed by centrifugation. Supernatant was separated to fresh tubes and equal volume of PCI (Phenol, Chloroform, Isoamylalcohol in the ration 25:24:1) was added and mixed vigorously by vortexing. The tubes were then centrifuged at 12,000 rpm for 5 minutes. The aqueous phase obtained after centrifugation was precipitated by adding 0.7 volume of isopropanol and was gently mixed by inverting. Precipitated DNA was collected by centrifugation carried at 12,000 rpm for 15 minutes at 4 °C and supernatant was discarded. The DNA pellet was rinsed with 70% ethanol allowed to air dry for 10 minutes. The pellet was finally resuspended in 20 µl of MQ containing RNase and quality was assessed on agarose gel. Plasmids were stored at -20 °C till further use. Plasmids used in the study are listed in Table 5.

Table 5: Plasmids used in this study

Plasmid	Description	Source or reference
pSFS2B	<i>SAT1</i> flipper carrying nourseothricin resistance gene	(Reuß et al., 2004)
pPA1	pSFS2B flanked 5' and 3' <i>LEM3</i> ^{ORF} for disruption of first allele of <i>LEM3</i>	This study
pPA2	<i>LEM3</i> reconstitution construct	This study
pADH34	C-terminal Myc tagging plasmid	(Nobile et al., 2009)
pCJN542	<i>NAT1-TDH3</i> promoter plasmid	(Nobile et al., 2008)

2.2.9 Strain construction

2.2.9.1. Deletion cassette construction

The first and second allele of the *LEM3* gene was disrupted using the *SAT1* flipper in the plasmid pSFS2B. For the *LEM3* disruption construct, a 300 bp 5' ORF region of *LEM3* (5' *LEM3*^{ORF}) was amplified from SC5314 genomic DNA with primers *LEM3*P1 and *LEM3*P2 (Table 4), with introduced KpnI and XhoI restriction sites. A 350 bp ORF region of 3' *LEM3* was amplified with primers *LEM3*P3 and *LEM3*P4, with introduced SacII and SacI sites. All amplicons (5' *LEM3*^{ORF} and 3'*LEM3*^{ORF}) were docked in pGEMT easy vector from which they were digested and cloned into the 5' and 3' ends of the *CaSAT1-FLIP* cassette respectively using the mentioned enzymes. This procedure created the *LEM3* knockout construct plasmid pPA1 (Table 5), which was digested with KpnI and SacI to release the 4.8 kb disruption construct. The wild type SC5314 strain was electroporated with the disruption construct. The *CaSAT1* construct was flipped out from *LEM3/lem3Δ::SAT1-FLIP* strain before disruption of the second allele. For the disruption of second allele we used the same deletion cassette. Second round of electroporation and integration generated the null mutant.

2.2.9.2. C-Myc tagging of *LEM3*

The C-terminal Myc-tagging plasmid, pADH34, containing a 13X Myc epitope tag preceding the *SAT1*-flipper cassette was used for epitope tagging as previously described (Nobile et al., 2009). The PCR amplicon obtained with primers *LEM3*mycFnostop and *LEM3*mycRUTR constitutes a 13X Myc epitope tag, *SAT1* flipper cassette, 65 bp region homologous to *LEM3* ORF minus its stop codon on the 5' end of the Myc tag and a 65 bp region homologous to *LEM3* UTR downstream of the stop codon on the 3' end of the *SAT* flipper cassette. This PCR product was transformed into SC5314 (wild type) to obtain strains PA16. Correct integration of the C-

terminal 13X Myc epitope tag and *SAT1* flipper was verified by colony PCR using detection primers *LEM3*upstreamcheckF, AHO300, *LEM3*downstreamR and AHO301. The primer pairs *LEM3*downstreamR and AHO302 were used in colony PCR to confirm the flipping out of the *SAT1*-flipper cassette. To obtain PA17 *CaSAT* was flipped out from PA16. The 13X Myc epitope tag and the region of homology to the 3' end of *LEM3* used for integration of the *SAT1*-flipper cassette was confirmed by sequencing the PCR product generated using primers *LEM3*upstreamcheckF and AHO283.

2.2.9.3. Overexpression strain construction

The *TDH3-LEM3* and *TDH3-RTA3* overexpression *C. albicans* strains (Table 1) were constructed using plasmid pCJN542 (Nobile et al. 2008) (Primers listed in Table 4). These primers amplify the *AshbyagossypiiTEF1* promoter, the *C. albicans NAT1* ORF, the *A. gossypii TEF1* terminator and the *C. albicans TDH3* promoter with 100 bp of hanging homology to promoter region of *LEM3* and *RTA3*. The transformation into *C. albicans* strains was done as described earlier and nourseothricin positive transformants were screened using detection primers listed in Table 4.

2.2.10 Southern Blot Analysis

C. albicans cells were grown in 10 ml YEPD at 30 °C overnight with shaking at 220 rpm. Genomic DNA was isolated by harvesting the cells after centrifugation. 10 µg of genomic DNA was digested with HindIII, separated on a 1% agarose gel, transferred onto a nylon membrane and fixed by ultraviolet crosslinking. The gel purified 350 bp 3' *LEM3*^{ORF} fragment obtained by digesting pPA1 with *SacII* and *SacI*, used as a probe. The probe was labeled with [³²P] dATP. All blots were hybridized at 65 °C in a solution containing 0.5 M NaH₂PO₄ (pH 7.2), 7% sodium dodecyl sulfate, and 1 mM EDTA. After hybridization, the membranes were washed thrice with

2X SSC and 0.1% SDS and expose the membrane in a PhosphorImager cassette for visualization and finally quantified on Fujifilmphosphorimager (Amersham Biosciences).

2.2.11 Microscopy

For confocal microscopy, an Olympus FluoViewTMFV1000 microscope (100X oil immersion objective) was used and photographs were processed with the Olympus FV110A SW 1.7 viewer software. For visualizing nucleus and GFP tagged protein, cells were grown to mid-log phase, and stained with 4, 6-diamidino-2-phenylindole (DAPI). DAPI was added to a concentration of 20 nM and 1 µg/ml respectively and incubated for 20 minutes for staining. After staining, cells were washed thrice and re-suspended in 1X PBS (phosphate buffered saline). The fluorescence excitation/emission for DAPI was 358/461 nm.

2.2.12 Antifungal susceptibility tests

2.2.12.1 Spot analysis

Strains were streaked on YEPD overnight and on the following day single colonies grown in YEPD overnight and OD₆₀₀ was set to 0.1 in 0.9% saline solution and serially diluted in saline four dilutions (5×10^3 to 5×10^5 cells). Five microliters of the corresponding dilutions were finally spotted onto YEPD plates containing the indicated drugs. Plates were incubated at 30 °C for 48 hours and then photographed.

2.2.12.2 Minimum inhibitory concentration (MIC) assay

Minimum inhibitory concentration (MIC) was determined by broth microdilution methods described in CSLI guidelines. Round-bottomed 96-well microtitre plates were prepared for MIC estimation by equal volumes of RPMI-1640 (buffered with 0.165 mol/l MOPS) and serially diluted concentrations of drugs. Then, diluted cell suspensions (10^4 cells/ml) were added to the wells. The prepared plates with cell dilutions were incubated at 37 °C for 48 hours. The growth

was evaluated by reading the OD₆₀₀ in a microplate reader and MIC₈₀ is defined as the lowest drug concentration that gave 80% inhibition of growth compared with the growth of the drug-free controls.

2.2.13. Internalization of phospholipids into yeast cells

For labeling experiments strains were grown to early-log phase in SDC media at 30 °C, and labeled with 5 μM NBD-PC (DMSO solubilized) at OD₆₀₀ 1.0 for 45 minutes as described in (Hanson et al., 2002). Cells were washed three times with SDC and kept at 30 °C for additional 30 minutes. The cells were finally washed with ice-cold SC-azide three times and kept on ice until further analysis by microscopy or flow cytometry.

2.2.13.1 Flippase activity

Flow cytometric analysis of the flippase activity on wild type, *lem3Δ/Δ* and *lem3Δ/Δ+LEM3* cells was done by using NBD-PC and sodium dithionite, an impermeant reducing agent used to quench the NBD-PC exposed on the cell surface (Popescu et al., 2010). Early log phase cells of wild type and *lem3Δ/Δ* were labeled with 2 μM NBD-PC. At the indicated times, an aliquot of cells was transferred to tubes with and without 25 mM sodium dithionite in SDC and washed with cold SC-azide. Residual MFI (mean fluorescence intensity) of NBD-PC in the presence (F_D) or absence (F_{Total}) of dithionite was measured by flow cytometer. Percentage of internalized NBD-PC was represented as the normalized F_D/F_{Total} ratio. Triton X-100 (0.1%) was added to the dithionite group to allow quenching of internalized NBD-PC in control experiments. Residual F_D/F_{Total} ratio in permeabilized samples was less than 5%. Data are mean ± of more than or equal to 10000 gated events.

2.2.14 Flow cytometry assays

Flow cytometry was performed using a FACS Calibur flow cytometer (Becton Dickinson Immunocytometry Systems, San Jose, CA) equipped with an argon laser emitting at 488 nm.

Cells were grown to early-log phase (OD_{600} 1.0) in YEPD at 30 °C, labelled with desired fluorophore and analyzed. Fluorescence was measured on the FL1 fluorescence channel equipped with a 530 nm band-pass filter for NBD-PC staining. A total of 10,000 events were counted. The data was analyzed using CellQuest V software.

2.2.15 Efflux of rhodamine 6G

Approximately 10^7 yeast cells from each overnight culture were inoculated into 50 ml YEPD medium and allowed to grow for 5 hours. Cells were pelleted, washed twice with phosphate buffered saline (PBS) buffer (pH 7.0) and resuspended in 1X PBS to 2% cell suspension. Rhodamine 6G (R6G) was added at a final concentration of 10 μ M. Cell suspensions were incubated at 30 °C with shaking (200 rpm) for 3 hours under glucose starvation conditions. The de-energized cells were then washed and resuspended again in PBS at 2% cell suspension. At 10 minute intervals, 1 ml volume of cells were removed, centrifuged and absorption of supernatants were measured at 527 nm. Energy dependent efflux was measured after the addition of 2% glucose. Glucose-free controls were included in all experiments. Effluxed rhodamine 6G was calculated from a standard concentration curve of R6G.

2.2.16 Gene expression analysis

2.2.16.1 RNA isolation and cDNA synthesis

C. albicans strains were grown overnight in YEPD, subcultured from a starting OD_{600} of 0.3 in fresh YEPD and incubated at 30 °C till OD_{600} reached 1.0. Cells were harvested by centrifugation at 4000 rpm for 5 minutes at 4 °C from samples. Total RNA was isolated using the RNeasymini kit (Qiagen) followed by the treatment with DNase I (Thermo Scientific) to remove contaminating DNA. cDNA was synthesized with a RevertAid™ H MinusFirst Strand cDNA synthesis kit (Thermo Scientific) following the manufacturer's protocol.

2.2.16.2 Real-time PCR (qRT-PCR)

Real-time PCR reactions were performed in a volume of 25 μ l using Thermo Scientific Maxima SYBR Green mix in a 96-well plate. For relative quantification of gene expression, the comparative CT method was used, where the fold change was determined as $2^{-\Delta\Delta CT}$ (Schmittgen and Livak, 2008). *ACT1* was used as the internal control and transcript level of the gene of interest was normalized to *ACT1* levels. Fold changes are means \pm SD and are derived from three or four independent RNA preparations. The qRT-PCR primers used in this study were designed by Primer Express 3.0 and are listed in Table 4.

2.2.17 Steady state phospholipid analysis

Phospholipids were extracted from crude cell fractions and separated by TLC as described. Briefly, starter cultures were diluted to an OD₆₀₀ of 0.2 in YNB-glucose supplemented with 10 μ Ci/ml ³²Pi and grown at 30 °C for 24 hours. After a wash with H₂O₂, the yeast pellets were resuspended in breaking buffer, and disintegrated by vortexing with glass beads for 30 minutes at 4 °C. Phospholipids from equal amounts of labelled crude cell, as determined by liquid scintillation, were extracted with 2:1 chloroform/methanol by vortexing at room temperature for 1 hour. After phase separation, the lower organic phase was transferred to a new borosilicate tube and dried down under a stream of liquid nitrogen. Chloroform-resuspended samples were loaded onto silica gel thin-layer chromatography (TLC) plates and resolved. Statistical comparisons were performed using Sigma Plot 11 software (Systat Software, Inc.).

2.2.18 Protein extracts and immunoblot analysis

C. albicans was grown at 30 °C with starting OD₆₀₀ of 0.4 and cells were harvested when OD₆₀₀ reached 2.0. Culture was pelleted down (10,000 rpm; 4 °C), washed with 1X PBS once and resuspended in 200 μ l ice cold lysis buffer (50 mM Tris-HCl pH 7.5, 150 mM NaCl, 1 mM EDTA, 1% Triton 100X), 5 μ l protease inhibitor cocktail, 10 μ l phenylmethylsulfonyl fluoride

(PMSF, 0.1 M stock) and 200 μ l glass beads. Breaking was done for 1 minute on cell breaker with intermittent chilling on ice three times, followed by centrifuging at 13,000 rpm to obtain a clear lysate, which was transferred into fresh tube. To equalize the amount of protein loaded, samples were analyzed by measuring the absorbance at 280 nm and then by coomassie staining. Total protein was determined using Bio-Basic BCA assay kit according to manufacturer's instructions, and 100 μ g of total protein was fractionated by SDS-PAGE using 10% Mini-Protean TGX gels (Bio-Rad). Fractionated proteins were transferred to nitrocellulose/PVDF membranes and blocked with 50 mg/ml BSA (in 1X PBS) for 2 hours at room temperature. Membrane was incubated with 9B11 anti-Myc primary antibody for overnight (Cell Signalling Technology) and then horseradish peroxidase (HRP)-conjugated secondary antibody for 2 hours (Bio-Rad). Blots were visualized with the ECL plus Western blotting detection system (Bio-Rad). Ponceau S staining was used as loading control, to show the equal loading of total amount of protein in each well.

2.2.19 Virulence testing assays

2.2.19.1 Morphogenesis assays

These experiments were done in liquid as well as solid media. Cells from an overnight culture grown in YEPD were used to subculture from a starting OD_{600} of 0.3, in fresh spider media and incubated for 4-5 hours at 37 °C with continuous shaking. Aliquots of the cells were taken out at 1 hour interval for 4 hours, washed with 1X PBS and observed under light microscope for changes in filamentation patterns.

For filamentation on solid media, cells from an overnight culture grown in YEPD were washed, and approximately 50-100 cells of each strain were plated on YEPD, 10% serum, and spider agar media and incubated at 37 °C for 5 days. Colonies were observed after 5 days for filamentation

changes. Cells and colonies were photographed by using a Zeiss microscope equipped with a digital camera for displayed filamentation pattern in different strains.

2.2.19.2 *In vitro* biofilm formation

In vitro biofilm assays were carried out in Spider medium by growing the biofilm directly on the bottom on the 96 well polystyrene plates, as described previously (Fox et al., 2015; Lohse et al., 2017). Briefly, strains were grown overnight in YEPD at 30 °C for 12-14 hours and diluted to an optical density at OD₆₀₀ of 0.5 in Spider medium. The inoculated plate was covered with a breathable film and incubated at 37 °C for 90 minutes at 250 rpm agitation on an ELMI incubator (ELMI, Ltd. Riga, Latvia) for initial adhesion of cells. Post adhesion, the cells were washed with 200 µl of 1X PBS, and 200 µl of fresh Spider medium was added. The plate was covered with a fresh breathable film and incubated at 37 °C for an additional 24 hours at 250 rpm agitation to allow for biofilm formation. Following incubation, the film and medium were removed and the OD₆₀₀ was measured using a standard plate reader to determine the extent of biofilm formation. A well containing medium alone was included as a contamination control. Statistical significance (P values) was calculated using a Student's one-tailed paired t-test. P values are as follows: n.s is not significant, ** < 0.005 and *** < 0.0005.

2.2.19.3 *In vivo* virulence testing in mice model

C. albicans strains SC5314, *lem3*Δ/Δ and *LEM3* revertant were cultivated overnight in YEPD. Each strain ($3-5 \times 10^5$ cfu/ml) was injected by the tail vein in four groups of 10 OF1 (Oncins France 1) mice (6–8 weeks old) (IFFA CREDO/now Charles River Laboratories, L'Arbresle, France). Mice survival was monitored for 10 days.

3.0 RESULTS

3.1 Evolutionary relationship of *CaLem3* to other fungal orthologs

The mechanism of phosphatidylcholine synthesis is well established in eukaryotic cells while its transport and metabolism remain unresolved. In *S. cerevisiae*, a membrane localized protein Lem3/Ros3 comprising of two transmembrane domains is a key player that directs the transbilayer movement of phosphatidylcholine and phosphatidylethanolamine (PE) by virtue of its flippase activity (Ono et al., 2009). *C. albicans* Lem3 is designated as a putative membrane protein in Candida Genome Database (CGD).

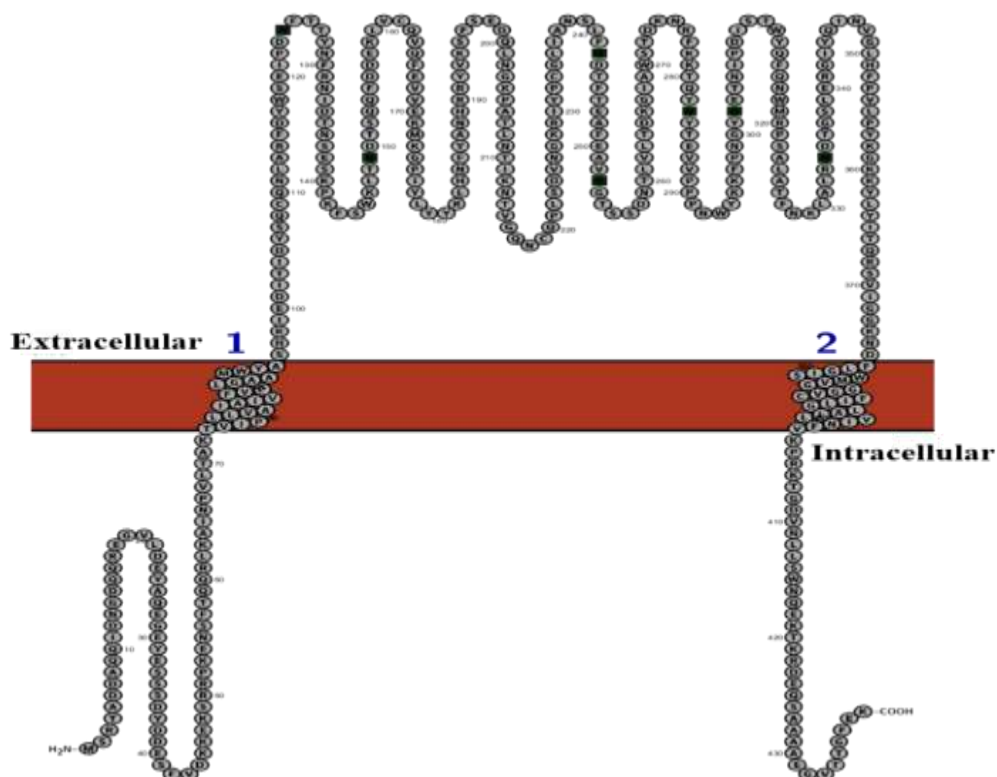


Figure 3.1: Predicted topology of Lem3. A prediction for the organization of Lem3 made by the Protter program. N-linked glycosylation sites in the sequence are represented by the green square.

Topological analysis of this protein by THHMM revealed the presence of two membrane-spanning segments, an extended extracellular region and C-terminal cytoplasmic tail, suggesting that *CaLem3* may be an integral membrane protein (Figure 3.1).

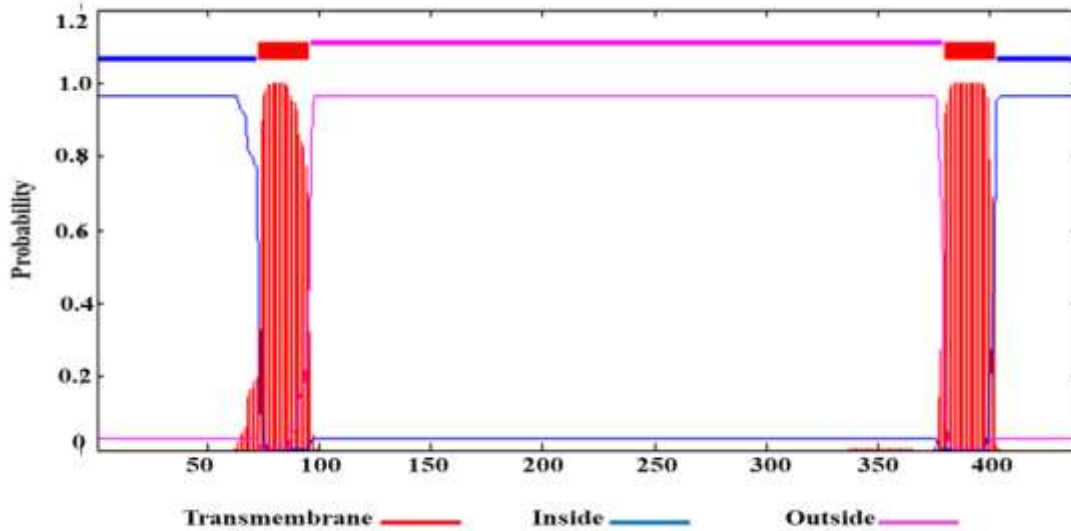


Figure 3.2: A prediction for the transmembrane domain organization of Lem3 as deduced from Transmembrane Helices Hidden Markov Models (THHMM)

We further evaluated the sequence similarity of Lem3 with other fungal orthologs by using Clustal Omega (a multiple sequence alignment program). For this *C. albicans* Lem3 (Gene ID: 3643456) protein sequence was aligned with the protein sequence of *ScLem3* (Gene ID: 855393) and its human ortholog, TMEM30A (Gene ID: 55754). While *CaLem3* shared 45.80% similarity and 40.80% identity (Figure 3.3) with *ScLem3*, it shared 36.0% similarity and 29.0% identity (Figure 3.3) with TMEM30A. Additionally, *CaLem3* was 44% and 96% similar and 40.7% and 95.8% identical to *C. glabrata* (CGD Gene ID: CAGL0D02442g) and *C. dubliniensis* Lem3 (CGD Gene ID: Cd36_19620). Percent similarity index to other fungal orthologs is presented in Table 6. The phylogenetic tree based on fungal Lem3 protein sequence were constructed by Neighbour Joining (NJ) method by using clustal omega (Figure 3.4). The phylogenetic analysis

of Lem3 demonstrates that *CaLem3* protein is most closely related to *C. dubliniensis*.

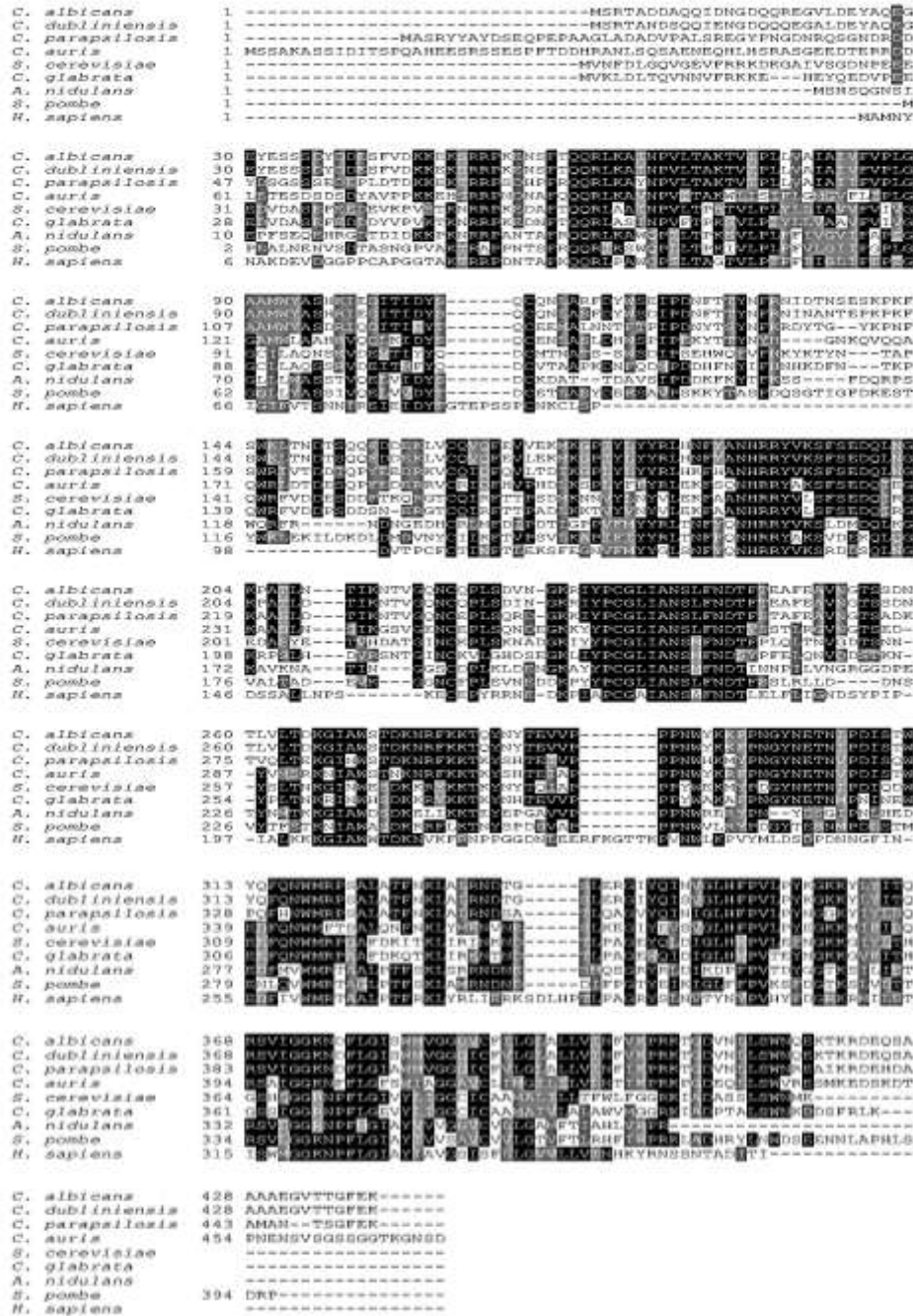


Figure 3.3: Sequence alignment of *C. albicans* Lem3 with its orthologs by CLUSTAL OMEGA.

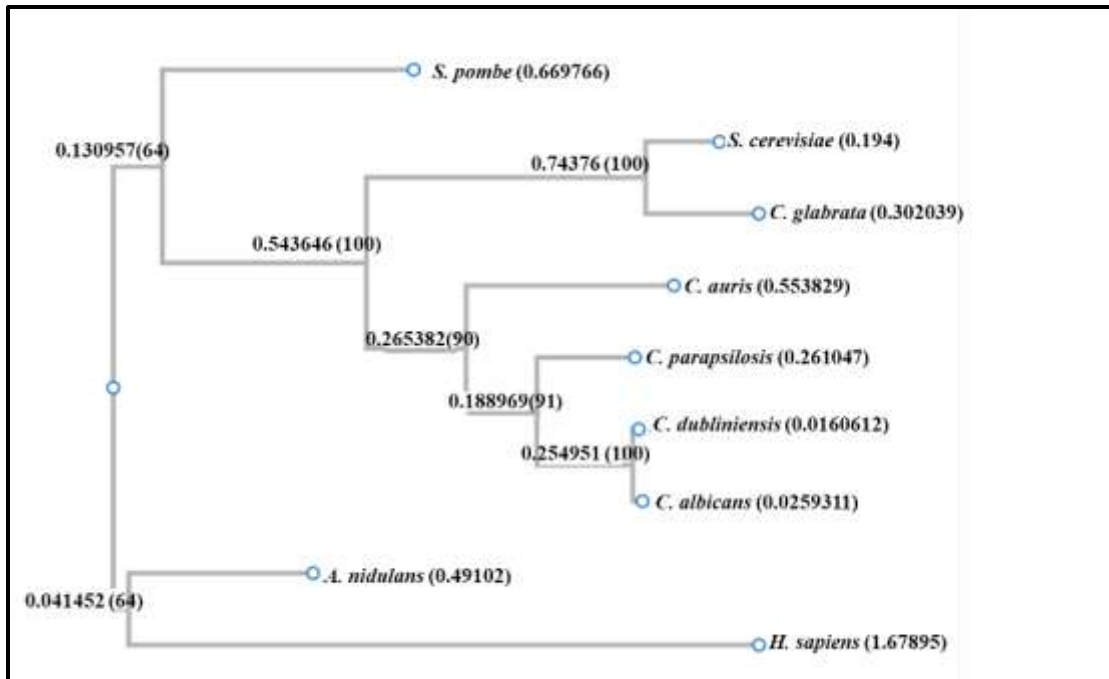


Figure 3.4: Phylogenetic analysis. *C. albicans*, *C. dubliniensis*, *C. parapsilosis*, *C. auris*, *S. cerevisiae*, *C. glabrata*, *A. nidulans*, *S. pombe*, *H. sapiens* Lem3 orthologs constitute a mutually distinct subfamily.

TABLE 6: Similarity of *CaLem3* with others fungal and human orthologs

S. No.	Orthologues	CGD Gene Id	Similarity (%)	Identity (%)
1	<i>C. dubliniensis</i>	Cd36_19620	96.0	95.8
2	<i>C. parapsilosis</i>	CPAR2_206640	69.0	65.3
3	<i>C. auris</i>	B9J08_002485	54.0	50.7
4	<i>S. cerevisiae</i>	SGD:S000005267	45.8	40.8
5	<i>C. glabrata</i>	CAGL0D02442g	44.0	40.7
6	<i>A. nidulans</i>	AN5100	43.0	37.3
7	<i>S. pombe</i>	SPBC1773.11c	43.0	38.8
8	<i>H. sapiens</i>	Gene ID: 55754	36.0	29.0

Based on the conservation in the amino acid residues and membrane topology with other orthologs, we propose that the defining feature of Lem3 in *S. cerevisiae* remain conserved in *C. albicans* Lem3.

3.2. *LEM3* influences miltefosine susceptibility in *C. albicans*

Phospholipids are distributed asymmetrically among two bilayers of the biological membrane. In eukaryotic plasma membrane, aminophospholipids such as phosphatidylcholine (PC) and sphingolipids reside predominantly in the outer leaflet, whereas phosphatidylethanolamine (PE) and phosphatidylserine (PS) are present in the cytoplasmic leaflet (Balasubramanian and Schroit, 2003). The asymmetric distribution of these phospholipids is maintained by their inward and outward translocation across the biological membrane facilitated by P4-ATPases in an energy dependent manner. In *S. cerevisiae*, five P4-ATPases i.e. Drs2, Dnf1, Dnf2, Dnf3 and Neo1 are recognized as flippases, and with the exception of Neo1, all of these require Cdc50 family proteins as non-catalytic subunits for their localization and flippase activity. For Drs2, interaction with Cdc50 is required for exit of the complex from the endoplasmic reticulum (ER). Consistently, Cdc50 is retained in the ER of *drs2Δ/Δ* cells and so these two proteins are codependent for their exit from the ER. Lem3 chaperones both Dnf1 and Dnf2 out of the ER while Crf1 chaperones Dnf3 (Saito et al., 2004; Furuta et al., 2007).

To functionally characterize Lem3 in *C. albicans*, we constructed *lem3Δ/Δ* in wild type (SC5314) strain by using *SAT1* flipper strategy (Reuß et al., 2004). *SAT1* flipper strategy is a highly efficient, convenient and widespread technique for targeted gene disruption in *C. albicans*. Disruption cassettes constructed as described in materials and methods contained gene-specific regions to facilitate homologous recombination on *LEM3* genomic locus. This cassette also contains an antibiotic selection marker, *SAT* (nourseothricin resistance gene) to facilitate selection of transformants. As *C. albicans* is a diploid fungus, two rounds of deletion was performed to generate homozygous null mutants (*lem3Δ::FRT/lem3Δ::FRT*). Wild type *LEM3* was reconstituted into its native locus in *lem3Δ/Δ* background by transforming the reconstituted cassette to obtain a revertant strain *lem3Δ::FRT/LEM3-SAT1-FLIP*. Each step of gene deletion

and reconstitution was confirmed by Southern blot analysis (figure 3.5).

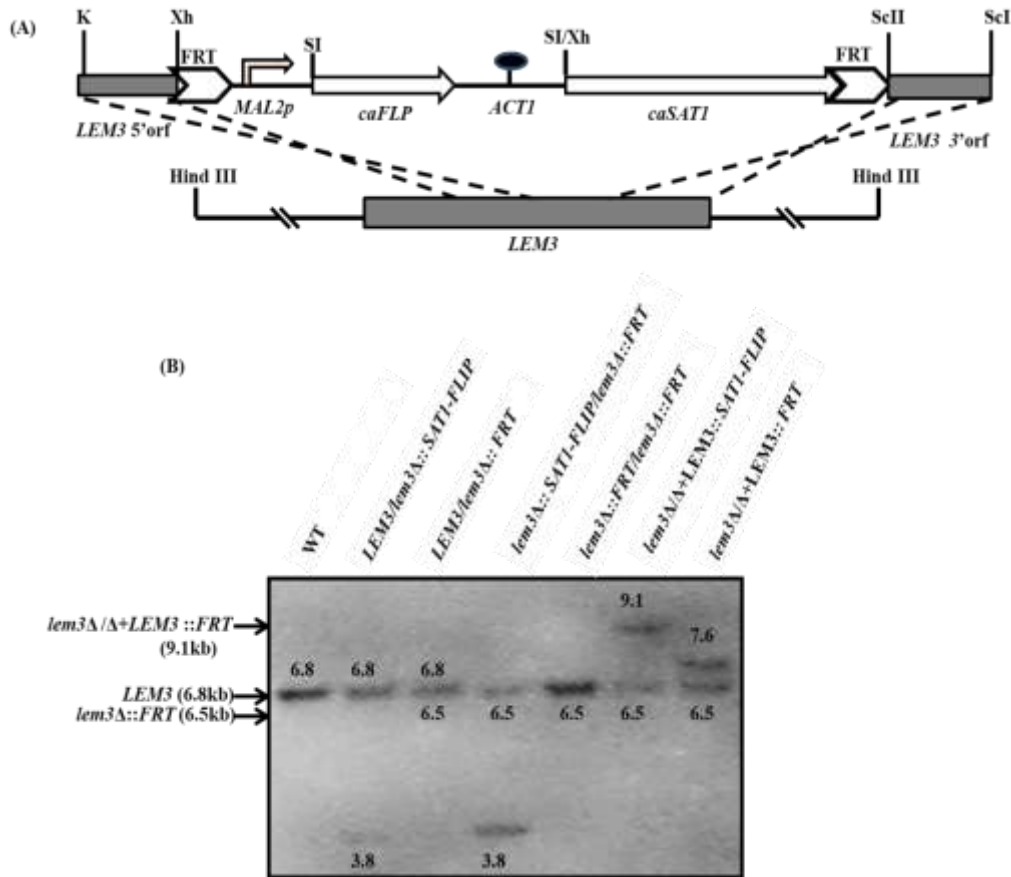


Figure 3.5: Disruption of *LEM3*. (A) Schematic representation of disruption strategy (B) Southern hybridization showing genomic configuration of *LEM3* in the wild type locus and its deletion derivatives. Genomic DNA from strains were digested with HindIII.

Lane 1, wild type (SC5314); Lane 2, *LEM3/lem3Δ::SAT1-FLIP*; Lane 3, *LEM3/lem3Δ::FRT*; Lane 4, *lem3Δ::SAT1-FLIP /lem3Δ::FRT*; Lane 5, *lem3Δ::FRT/ lem3Δ::FRT*; Lane 6, *lem3Δ/Δ+LEM3:: SAT1-FLIP*; Lane 7, *lem3Δ/Δ+LEM3::FRT*.

Earlier reports demonstrate that deleting *LEM3/ROS3* in *S. cerevisiae* renders this yeast resistant to miltefosine (Stevens et al., 2008), an alkylphosphocholine class of drug with promising antifungal activity. It inhibits *C. albicans* biofilm formation and displays activity against preformed biofilm (Vila et al., 2015). Beside antifungal activity these alkylphospholipids have anticancer activity and are widely used as anti-leishmaniasis drugs (Hanson et al., 2003; Seifert et al., 2001). Additionally, Lem3 also functions as the transporter of miltefosine in *S. cerevisiae* (Hanson et al., 2003; Kato et al., 2002). Considering these reports we tested the *C. albicans*

lem3Δ/Δ for any alteration in susceptibility to miltefosine. To our observation *lem3Δ/Δ* cells displayed decreased susceptibility to miltefosine when compared to wild type and reconstituted strains (Figure 3.6), pointing that impact Lem3 may have in modulating susceptibility to the alkylphosphocholine class of drugs in *C. albicans*.

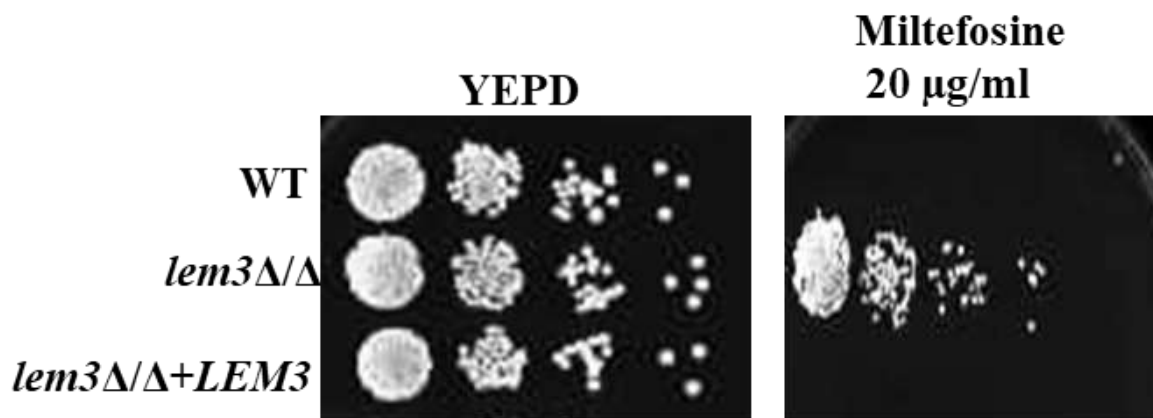


Figure 3.6: Spot assay of *lem3Δ/Δ* for miltefosine susceptibility. Fivefold serial dilutions of cell suspensions were spotted onto YEPD plates supplemented with miltefosine and incubated at 30 °C for 48 hours.

Deletion of *LEM3* also resulted in increased susceptibility to the azole antifungals, which is discussed below.

3.2.1. Absence of *LEM3* impacts intracellular accumulation of M-C6-NBD-PC while cellular phospholipid levels remain unchanged

In *S. cerevisiae* resistance to miltefosine is associated with defects in internalization of NBD-labelled PC (its fluorescent structural analogue) (Hanson et al., 2002). NBD-PC is the fluorescent lipid analogue of miltefosine that shares similar glycerophosphocholine structure and degree of hydrophobicity with miltefosine. In mammalian and yeast cells NBD-labelled lipids are regularly used as reporters to study transport and intracellular trafficking of phospholipids (Haldar and Chattopadhyay, 2012). Studies in *S. cerevisiae* also suggest an involvement of Lem3 in internalization of NBD-PC through plasma membrane (Hanson et al., 2003). Taking into consideration the previous studies we also measured alteration in NBD-phospholipid

internalization in *lem3Δ/Δ*. Change in internalization of NBD-PC was monitored by confocal microscopy and flow cytometry.

For analyzing time-dependent distribution of NBD-PC by confocal microscopy, strains were grown in SDC media till OD 1.0, incubated with NBD-PC for 45 min followed by subsequent washing with ice cold SC-azide (Synthetic Complete). Microscopy results revealed that while wild type cells displayed successful accumulation of NBD-PC, *lem3Δ/Δ* strain displayed a compromised NBD-PC accumulation. The phenotype was restored back to wild type levels by *LEM3* reconstitution (Figure 3.7). Flow cytometry results were consistent with the microscopy results, wherein there was a 12-fold reduced in the mean intracellular fluorescence intensity (MFI) of NBD-PC in *lem3Δ/Δ* strain, compared to the mean MFI of the wild type and reconstituted strain (Figure 3.7).

As low MFI in *lem3Δ/Δ* cells is reflective of decreased intracellular NBD-PC accumulation, we hypothesize that this could be due to a decrease in inward directed transbilayer movement (flip) of NBD-PC across the plasma membrane, thus justifying the decreased susceptibility of *lem3Δ/Δ* cells to miltefosine. We further analyzed whether a decrease in accumulation of NBD-PC would have any effect on the total cellular phospholipid levels. For this we checked the steady state levels of phospholipids. Wild type, mutant and reconstituted strain were grown in ³²Pi containing media. Total phospholipids were extracted from the whole cell extract and separated by thin layer chromatography (TLC). To our observation cellular phospholipid levels were not altered in the mutant (Figure 3.8).

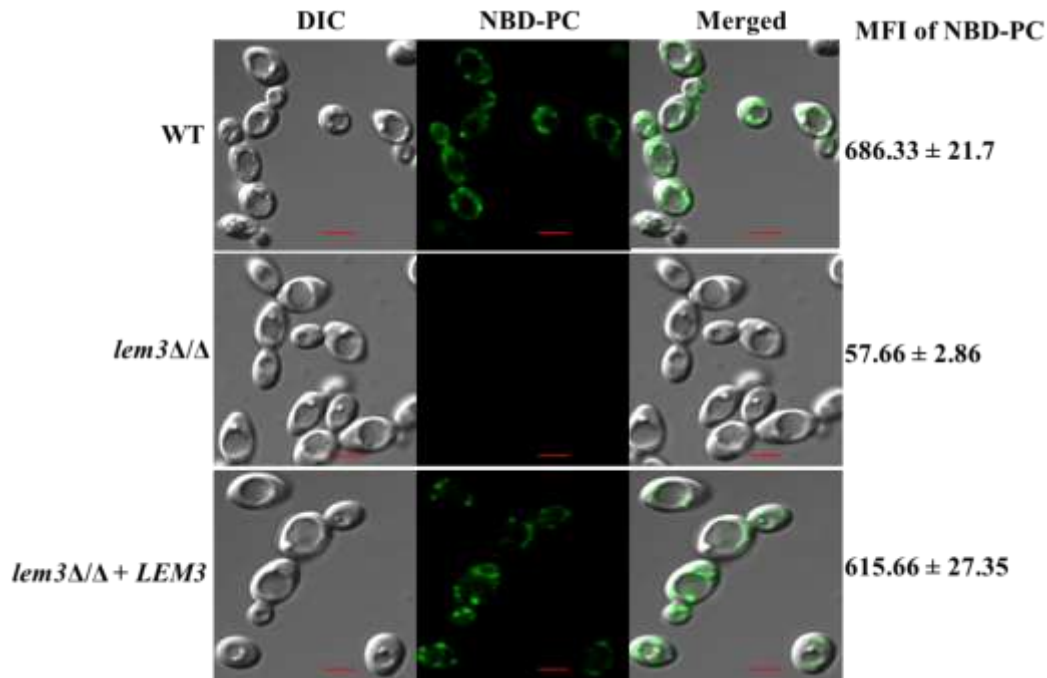


Figure 3.7: Internalization of NBD-PC in *lem3Δ/Δ* cells. SC5314, *lem3Δ/Δ* cells and *lem3Δ/Δ+LEM3* cells were labeled with 5 μ M of NBD-labeled PC. Strains were grown till O.D₆₀₀ of 1, incubated with NBD-PC for 45 min at 30 °C in SDC media, and washed with ice cold SC-azide. Samples were then incubated in SC media at 30 °C for 30 min and visualized under confocal microscope. Values on the left indicate mean \pm S.D (n=3) fluorescence measurements by flow cytometry. Data represent the mean \pm S.D of three independent experiments. Approximately 200 cells were visualized using confocal microscopy.

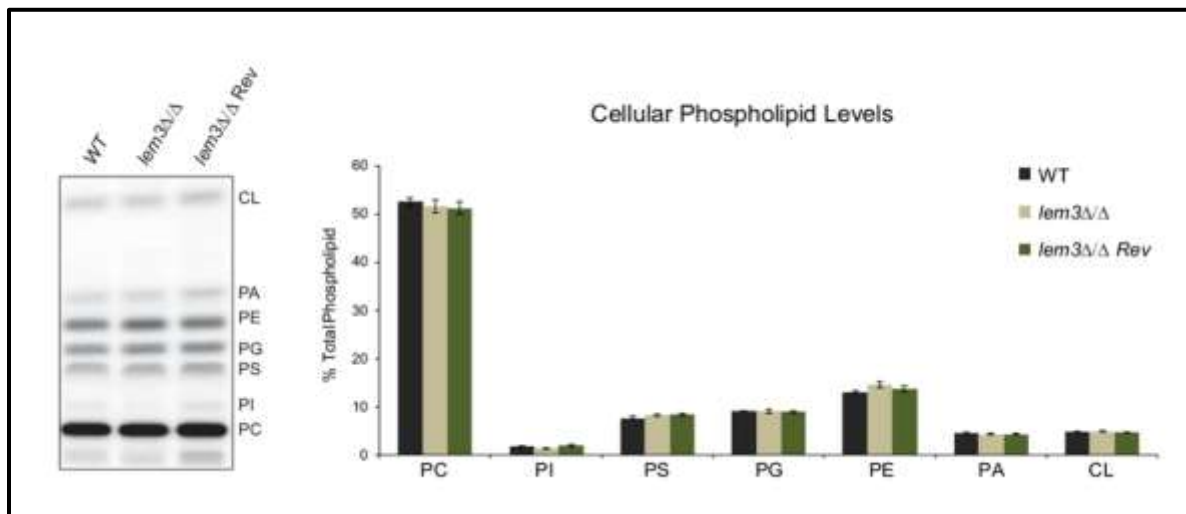


Figure 3.8: Steady state phospholipid analysis. Indicated yeast cells were cultivated in YNB-glucose in the presence of 32 Pi. Phospholipids were extracted from crude cellular fractions and separated by TLC. Steady state phospholipid species were determined. CL: Cardiolipin, PA: Phosphatidic acid, PE: Phosphatidylethanolamine, PS: Phosphatidylserine, PI: phosphatidylinositol, PC: phosphatidylcholine, PG: Phosphatidylglycerol, CDP-DAG: cytidinediphosphate diacylglycerol, LPC: Lysophosphatidylcholine, LPI: Lysophosphatidylinositol. Amounts of each lipid relative to total phospholipids were determined and represented in percentage. Values are mean \pm SD (n=6). P value <0.01 (students t-test).

Taken together, our results demonstrate a role for Lem3 in influencing the asymmetric distribution of PC across the plasma membrane, probably by its direct involvement in regulating the transbilayer movement of this phospholipid in *C. albicans*.

3.2.2. Reduced internalization of NBD-PC is attributed to decreased PC-specific flippase activity

Lem3 facilitates the localization and flippase activity of Dnf1 and Dnf2 in *S. cerevisiae* (Kato et al., 2002; Saito et al., 2004). Therefore, we hypothesized that compromising Lem3 function results in decreased intracellular accumulation of PC because of its effect on PC-specific flippase activity in *C. albicans*. To assess if the reduced flip of NBD-PC in *lem3Δ/Δ* cells was due to a decrease in the flippase activity that affects the transbilayer movement of PC, we measured NBD-PC fluorescence by flow cytometry in presence or absence of sodium dithionite (an impermeant reducing agent and quencher of NBD). This is a routinely used method to measure flippase activity in *S. cerevisiae* (McIntyre and Sleight, 1991; Popescu et al., 2010).

Dithionite produces nonfluorescent derivatives when it binds with the fluorescent lipid present in the outer leaflet. As, the total lipid upload is dependent on the adsorption of NBD-PC in outer leaflet of the plasma membrane and the flippase activity that transports it across the bilayers. This method provides information about the proportion of the fluorescent lipid incorporated in the outer leaflet and that which has migrated to locations within the cell. Accordingly, the lower the movement of the fluorescent lipid into the inner leaflet (decreased flip), the more be the dithionite quenching thereby keeping the lipid would be quenched by dithionite, and the intracellular MFI would continue to remain low with time. Flippase activity, therefore, can be assessed by measuring the intracellular MFI of NBD-PC in the presence (F_D) or absence (F_{Total}) of dithionite as measured by flow cytometry as described in the experimental procedure. We observed that percent flippase activity was comparably low in *lem3Δ/Δ* cells at T_0 (43.17 ± 1.58

vs. 53 ± 0.98) with respect to wild type, while there was a significant difference in MFI at T₃₀ (55 ± 3.09 vs. 71 ± 2.24) (Figure 3.9). The flippase activity in reconstituted strain remained to be similar to the wild type. **These results shows that loss of *LEM3* is the basis of the decrease in PC-specific flippase activity**

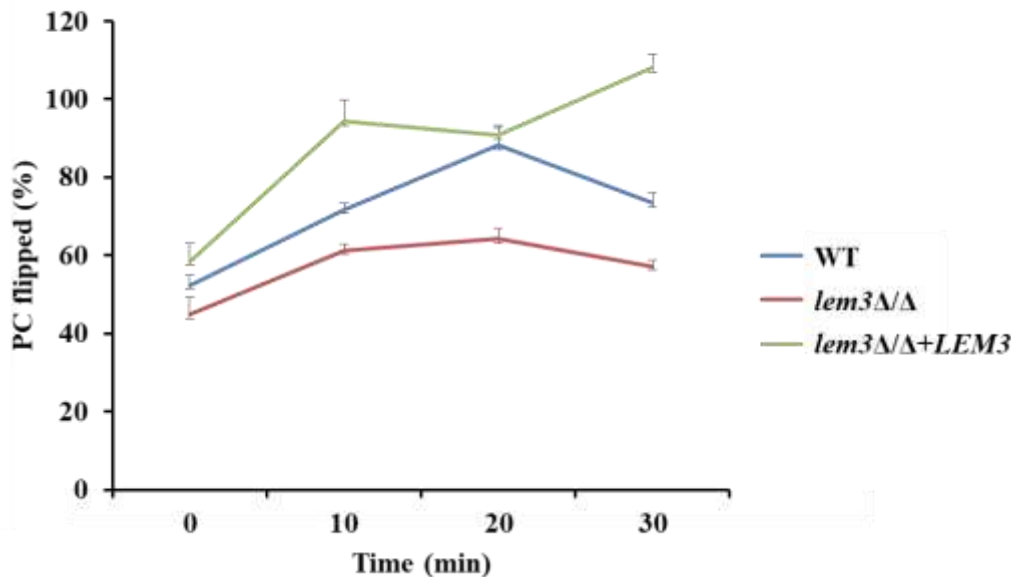


Figure 3.9: Flippase Activity. Flippase activity was measured in indicated strains by using 2- μ M NBD-PC and the impermeant quencher sodium dithionite (25 mM). At indicated times, MFI of NBD-PC in the presence or absence of dithionite was measured by flow cytometry. Percentage of internalised NBD-PC (or PC flipped in %) was represented as the normalised F_D/F_{total} ratio. For 20 and 30 min time points, % PC flipped in *lem3Δ/Δ* were found to be significant compared to wild type. NBD=nitrobenz-2-oxa-1,3-diazol-4-yl; PC= phosphatidylcholine.

3.3 Increased azole susceptibility of *lem3Δ/Δ* cells is due to decreased activity of *CDR1* efflux pump

Loss of lipid flippase component Cdc50 function leads to enhanced fluconazole sensitivity and several types of stress in *C. neoformans* (Huang et al. 2016). Similar studies in *S. cerevisiae* have shown that Cdc50-mediated lipid flippase regulates ergosterol distribution and trafficking in the Golgi network (Hankins et al., 2015). When treated with fluconazole, disruption of Cdc50 function could lead to altered ergosterol distribution on the membrane to cause lethality. Furthermore, disruption of both *CDC50* and genes acting at late steps of the ergosterol

biosynthesis pathway (*ERG2* and *ERG6*) results in synthetic lethality (Kishimoto et al., 2005). As Lem3 is a member of Cdc50 family of proteins (a subunit of P4 ATPases lipid flippases), we next sought to elucidate the role of *LEM3* in antifungal susceptibility. **We show that *lem3Δ/Δ* mutant exhibited increased susceptibility to various azole antifungals (Figure 3.10).**

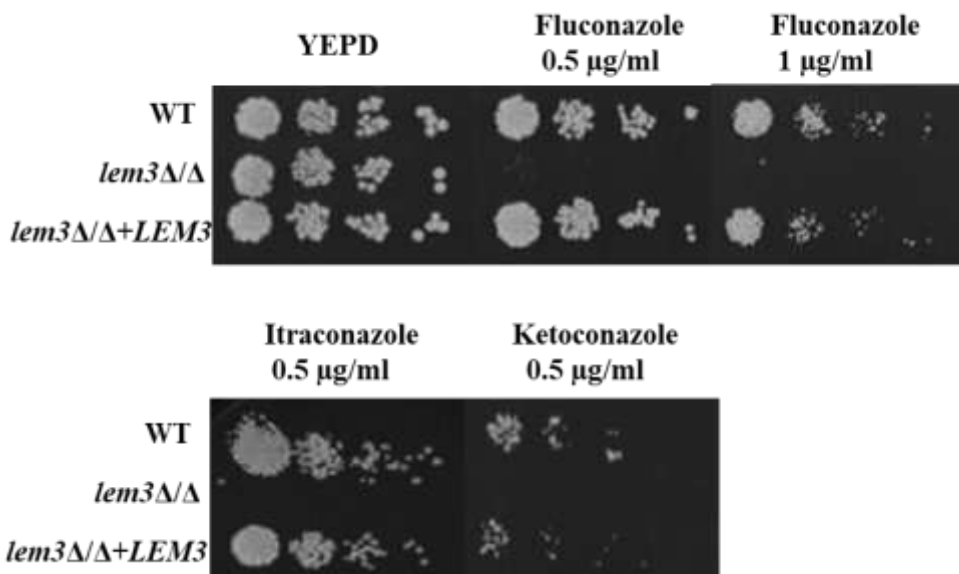


Figure 3.10: Spot assay of *lem3Δ/Δ* for fluconazole susceptibility. Fivefold serial dilution of cell suspensions were spotted onto YEPD plates supplemented with azoles and incubated at 30 °C for 48 hours.

Tolerance to azole antifungals is directly linked to the efflux activity of drug efflux pumps, *CDR1* and *CDR2* (ABC transporters) and *MDR1* (MFS transporter) in *C. albicans* (Prasad and Goffeau, 2012). We therefore hypothesized that increased susceptibility of the mutant to azole antifungals could be attributed to reduced activity of drug efflux pumps. To this end, we further compared the activity of *CDR1* between *lem3Δ/Δ* and wild type cells by rhodamine 6G (R6G; a substrate of *CDR* pumps) efflux assay (Nakamura et al., 2001).

R6G is a highly fluorescent dye often used to determine the transport activity of yeast membrane efflux pumps. Accumulation of R6G in growing *C. albicans* cells inversely correlates with the level of the ABC transporter *Candida drug resistance 1* (*CDR1*) mRNA expression and its activity. Measuring intracellular R6G levels can be used for successful identification of azole-

resistant strains. In both azole resistant and sensitive strains R6G migrates from extracellular into the intracellular compartment when incubated in glucose free condition. On addition of glucose, efflux of R6G from azole resistant strains is significantly enhanced, compared to its low efflux from azole sensitive strains (Maesaki et al., 1999). No significant R6G efflux is observed without the addition of glucose in any type of strain.

In our experiment, on glucose addition, an increase in extracellular concentration of R6G was observed from 2.7 nanomoles/ml to 4.2 nanomoles/ml in 30 min (1.5 fold increase) in the wild type. Similarly, 1.3 fold increase in extracellular concentration of R6G was observed in the reconstituted strain. We used *cdr1Δ/Δ* as a positive control as deletion of *CDR1* should not allow extracellular accumulation of R6G. Interestingly, similar to *cdr1Δ/Δ* (0.9 fold increase), *lem3Δ/Δ* mutant did not exhibit any significant change (0.9-fold) in extracellular R6G. These observations indicate that a deficiency in R6G transport is probably due to reduced activity of *CDR1* in *lem3Δ/Δ* cells (figure 3.11); underlying basis for the increased susceptibility of *lem3Δ/Δ* to azole antifungals.

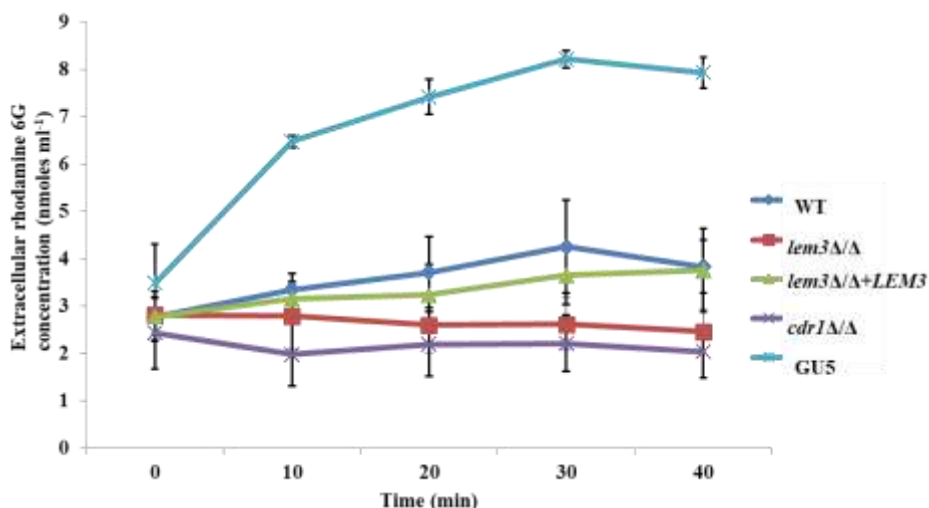


Figure 3.11. Reduced *CDR1* pump activity in *lem3Δ/Δ*. Efflux of fluorescent rhodamine 6G, a substrate of *CDR1* pumps. All strains were grown overnight in YEPD, starved for 2 hours in PBS buffer, incubated with rhodamine 6G (10 μ M), and then transferred to Phosphate buffered saline (PBS) buffer, pH 7. At 10 min, glucose was added to cultures and efflux of fluorescent rhodamine was measured subsequently for a total of 40 min.

Considering the aforesaid background, we were prompted to investigate the contribution of *LEM3* to the development of azole resistance in clinical isolates. To this end, we deleted this gene by *SAT*-flipper strategy in azole-resistant clinical isolate GU5 (Franz et al., 1998). Deletions were confirmed by Southern hybridization (Figure 3.12). This *C. albicans* isolate was derived from different episodes of oropharyngeal candidiasis (OPC) in AIDS patients who, after successful treatment (with 100 µg fluconazole) of the initial episodes, failed to respond to fluconazole therapy (Franz et al., 1998). The GU5/*lem3*Δ/Δ cells exhibited increased susceptibility to fluconazole as reflected by spot assay (Figure 3.14) and in MIC₈₀ values (Table 7). The MIC₈₀ value for GU5/*lem3*Δ/Δ was reduced by 32-fold for fluconazole, compared to GU5. **This demonstrates that susceptibility of azole-resistant clinical isolates to azole antifungals can be significantly increased by deleting *LEM3*.**

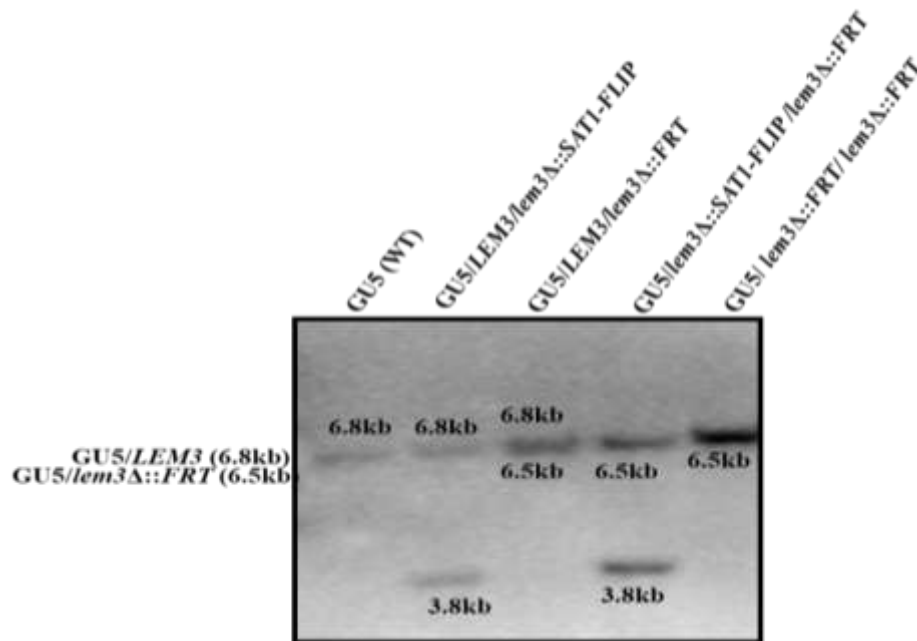


Figure 3.12: Disruption of *LEM3* in azole-resistant clinical isolate GU5. Southern hybridization showing genomic configuration of *LEM3* in the GU5 wild type locus and its deletion derivatives. Genomic DNA from strains were digested with HindIII.

Lane 1, wild type (GU5); Lane 2, GU5/*LEM3/lem3*Δ::*SAT1-FLIP*; Lane 3, GU5/*LEM3/lem3*Δ::*FRT*; Lane 4, GU5/*lem3*Δ::*SAT1-FLIP /lem3*Δ::*FRT*; Lane 5, GU5/*lem3*Δ::*FRT /lem3*Δ::*FRT*.

Table 7. Minimum inhibitory concentration (MIC₈₀) of *lem3Δ/Δ* in GU5 background with fluconazole.

MIC ₈₀ (μg/ml)			
Drug	GU5	<i>lem3Δ/Δ</i>	Fold change
Fluconazole	128	4	32

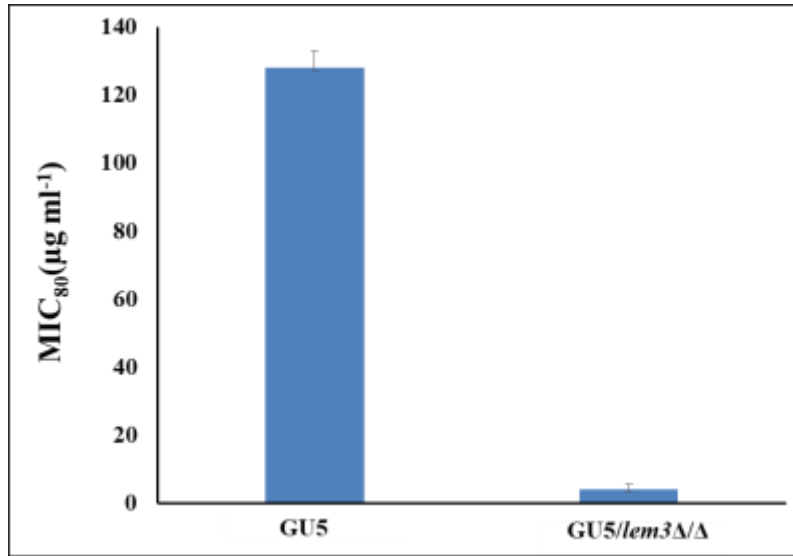


Figure 3.13: Minimum inhibitory concentration (MIC) assay.

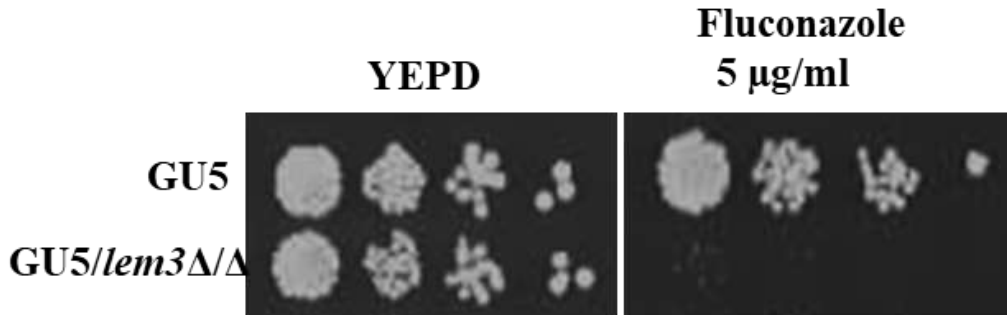


Figure 3.14: Spot assay of *lem3Δ/Δ* in clinical isolate for fluconazole susceptibility. Fivefold serial dilutions of cell suspensions were spotted onto YEPD plates supplemented with fluconazole and incubated at 30 °C for 48 hours.

3.4 *LEM3* influences pathogenicity in *C. albicans*

Previous studies suggest that flippase and floppase activity lead to the asymmetric distribution of phospholipids on plasma membrane in eukaryotic cells, and alteration in flippase activity of P4-ATPases leads to defects in cellular morphology in erythrocytes (Devaux, 1991; Murate et al.,

2015). Modification of *ATP10A* P4-ATPases of HeLa cells result in the imbalance of lipid levels between the two leaflets of biological membrane bilayer because of which membrane curvature is perturbed causing plasma membrane to bend inwards, leading to adhesion defects (Takada et al., 2018). As perturbations in the membrane asymmetry results in adhesion defect and biofilm formation, we expected that any change in PC asymmetry across the plasma membrane may also impact hyphal morphogenesis, an important virulence parameter. As the role of Lem3 in regulating the transbilayer movement of PC has been established above (Figure 3.7), we hypothesized compromising Lem3 function may contribute to pathogenicity-related traits in *C. albicans*.

The ability to switch between yeast and filamentous forms is thought to be tightly linked with virulence in *Candida* (Kornitzer, 2019). Filamentous cells are more invasive and easily undergo tissue penetration, while yeast cells are delivered and disseminated in the bloodstream. In infected tissues, both yeast-form and filamentous cells are found. Considering Lem3 as a lipid flippase subunit of Cdc50 family, we explored the ability of *lem3Δ/Δ* to filament in various filamentation-inducing medium as well as its ability to form biofilms. Considering this, we assessed *lem3Δ/Δ* for its ability to (i) filament (ii) form biofilms and (iii) cause infection in a mice model of systemic infection. For morphogenesis we evaluated the growth of all strains on YEPD (nutrient rich) and solid and liquid spider (nitrogen limiting media) medium. To our observation, *lem3Δ/Δ* cells produced compromised filaments in liquid media at 37 °C at different time intervals in contrast to wild type cells that were able to form normal filaments (Figure 3.15). A similar defect in filamentation was observed in solid spider medium at 37 °C, grown upto 6 days (Figure 3.16). The defect in both liquid as well as solid medium was successfully complemented back to wild type levels in the reconstituted strain.

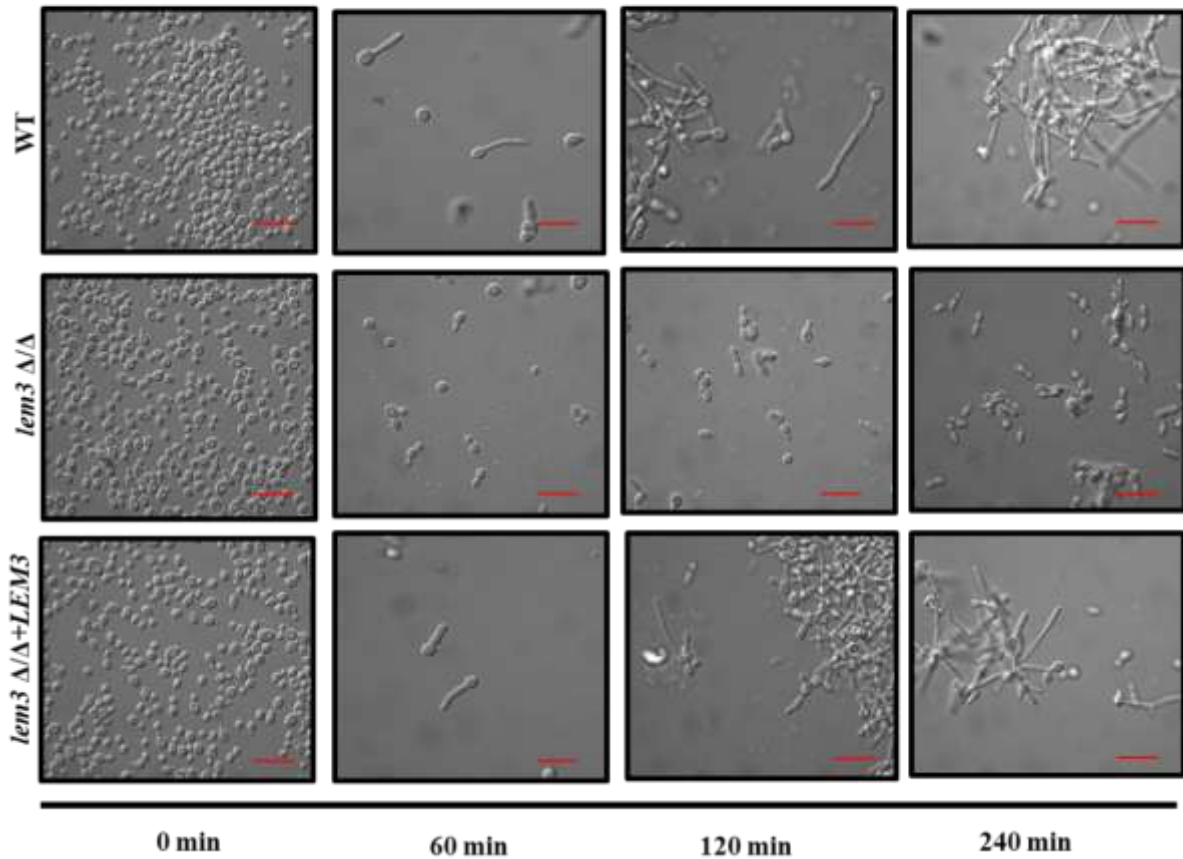


Figure 3.15: Bud-to-hyphae switch is compromised in absence of *LEM3* in liquid Spider medium. (A) SC5314, *lem3* Δ/Δ cells and *lem3* Δ/Δ +*LEM3* were incubated in spider medium (pH 7.4) at 37 °C and images were captured at 0 min, 60 min, 120 min, 240 min.

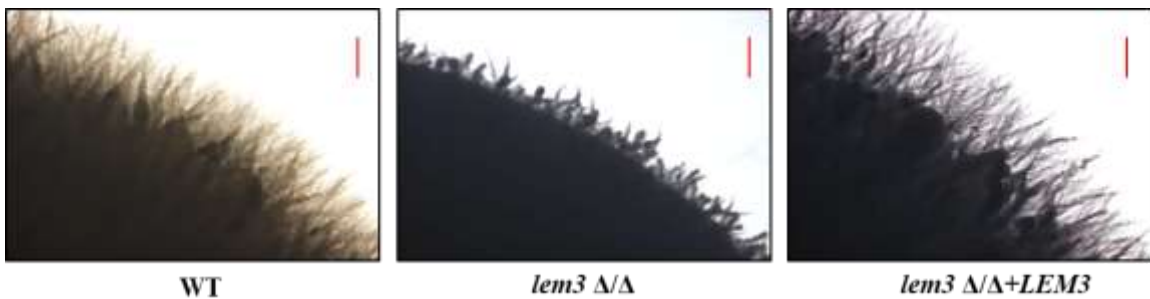


Figure 3.16: Bud-to-hyphae switch is compromised in absence of *LEM3* on solid spider media. SC5314, *lem3* Δ/Δ cells and *lem3* Δ/Δ +*LEM3* were spotted on spider agar plates and incubated at 37 °C for 6 days.

The influence of lipid flippase subunit Cdc50 on virulence has been demonstrated in *C. neoformans* (Huang et al., 2016). Considering that Lem3 is a member of Cdc50 family and

affects hyphal morphogenesis *in vitro*, we wanted to investigate if *in vitro* filamentation defects could be associated with virulence defects in a mice model of systemic infection. There was no significant difference in the survival between the *lem3Δ/Δ* mutant, wild type and the reconstituted strain indicating that Lem3 is dispensable for establishing an infection in the mouse systemic model of infection (Figure 3.17).

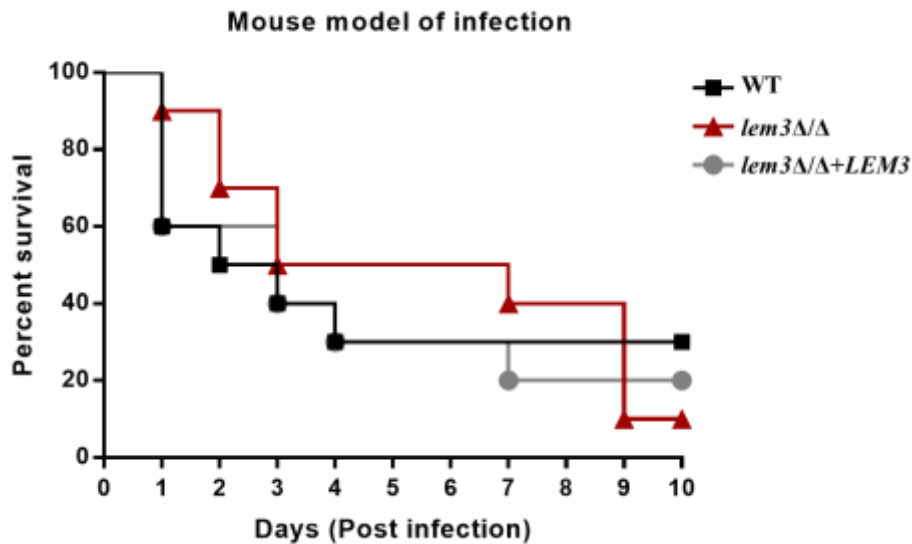


Figure 3.17: In vivo virulence analysis of *lem3Δ/Δ* strain in mice model of systemic infection. Mice were infected with the *C. albicans* strains via the tail vein, and disease progression was monitored.

In *C. albicans* dynamic modification in lipid profiles also have detrimental effects on cellular shape and cell physiology (Rizzo et al., 2019). Considering the altered PC flippase activity in *lem3Δ/Δ* cells, we used scanning electron microscopy (SEM) to analyze changes on the cell surface of the mutant. No significant alterations on the cell surface were observed in *lem3Δ/Δ* mutant with respect to wild type cells (Figure 3.18).

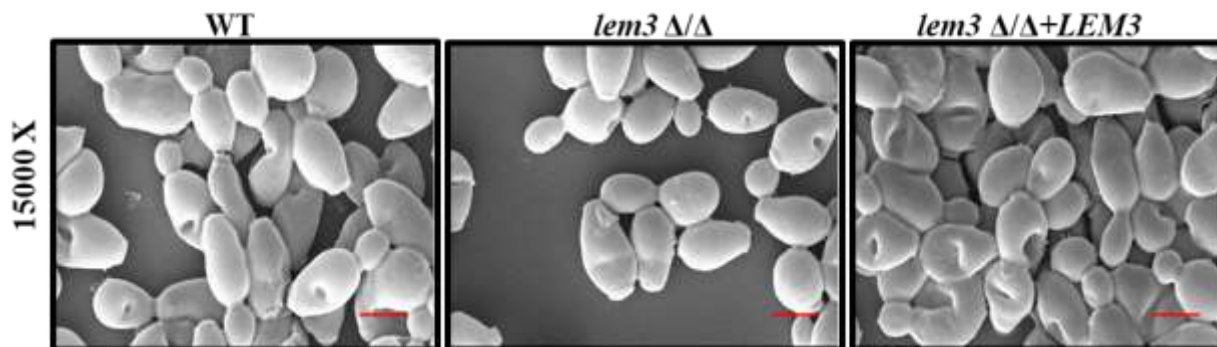


Figure 3.18: Cellular morphology is not affected in *lem3Δ/Δ*. Scanning electron micrographs of WT, *lem3Δ/Δ*, *lem3Δ/Δ+LEM3*.

Furthermore, any change in the PC: PE ratio may also influence cell adhesion properties resulting in biofilm defects in *C. albicans* (Nobile and Johnson, 2015). Cells in the biofilm mode of growth display a larger increase in the PC:PE ratio (2-fold) as opposed to a small increase (0.2-fold) in the planktonic cells, in both early and late phases of biofilm development (Alim et al., 2018).

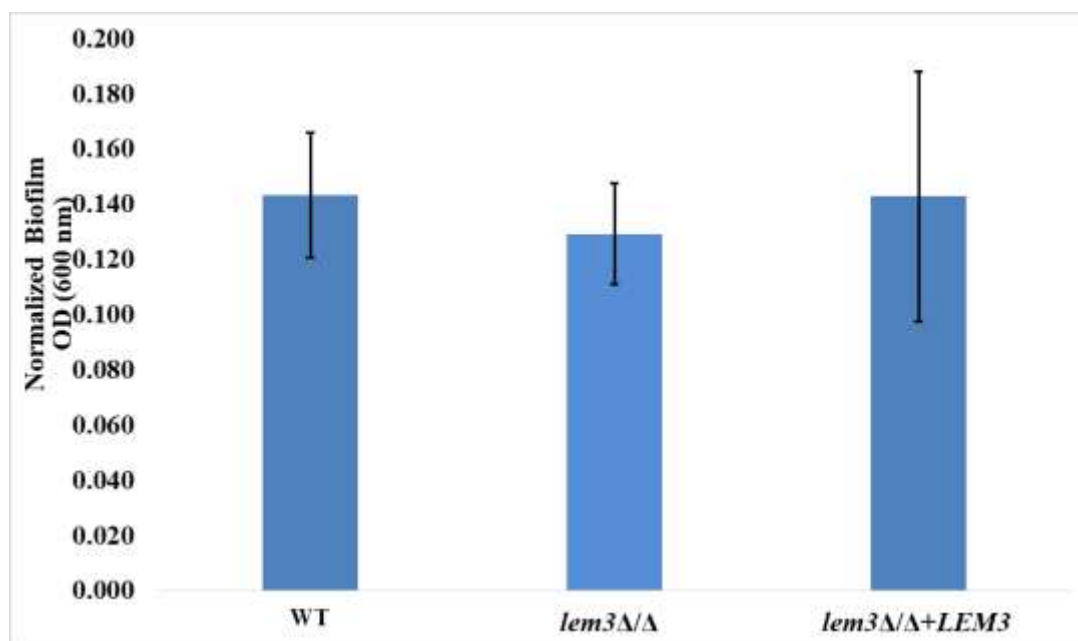


Figure 3.19: *in vitro* biofilm formation in *lem3Δ/Δ*: *In vitro* biofilm assay was carried out in Spider medium by growing the biofilm directly on the bottom on the 96 well polystyrene plates. Strains were grown and diluted to an optical density at OD₆₀₀ of 0.5 in 200 μl Spider medium. After incubation, the film and medium were removed and the OD₆₀₀ was measured using a standard plate reader to determine the extent of biofilm formation.

As deletion of *LEM3* may alter the lipid distribution across the plasma membrane, we next analyzed the mutant for its ability to form biofilm in vitro. We performed in vitro biofilm formation assay by growing the biofilm directly in spider medium in 96 well plate. After incubation for 24 hours no significant biofilm defects was observed in the *lem3Δ/Δ* mutant, compared to wild type (Figure 3.19). **Taken together, our results suggest that although deletion of *LEM3* impacts filamentation in vitro, it is not required for virulence in vivo. Additionally, compromising Lem3 function did not affect either cell surface morphology or the ability to form biofilm in vitro. Thus, we conclude that Lem3 may not be a contributor of pathogenicity-associated traits in *C. albicans*.**

3.5 Lem3 activity is regulated by Rta3, a 7-transmembrane receptor protein of *C. albicans*

Targeting membrane proteins especially those that affect membrane asymmetry could be beneficial as this would lead to the modulation of protein-protein, protein-lipid and protein-nucleic acid interactions, thus sensitizing cells to existing antifungals. Preliminary data from our laboratory has implicated Rta3, a 7-transmembrane receptor protein, unique to the fungal kingdom, as the determinant of biofilm development in *C. albicans*. Additionally, it was reported that *rta3Δ/Δ* cells exhibit increased susceptibility to miltefosine, an alkylphosphocholine drug (Srivastava et al., 2017). By using short chain fluorescent labelled phosphatidylcholine reporter; nitrobenz-2-oxa-1,3-diazol-4-yl (NBD)-phosphatidylcholine (PC), a link was established between Rta3 and maintenance of asymmetric distribution of phosphatidylcholine (PC) across the plasma membrane. We demonstrated that compromising Rta3 function results in enhanced PC-specific flippase activity (Srivastava et al., 2017). As Lem3 is one of the well-established PC-specific flippase in *S. cerevisiae* (Saito et al., 2004), we hypothesized that Rta3 may be

regulating the activity of *C. albicans* Lem3 to maintain PC asymmetry in the plasma membrane. Thus, to evaluate this hypothesis and also to further ascertain the role of Lem3 as a PC-specific flippase, we deleted *LEM3* in *rta3Δ/Δ* background by using *SAT*-flipper strategy. We posit that if Lem3 is the flippase that is regulated by Rta3, then deleting *LEM3* in the *rta3Δ/Δ* strain will lead to the abrogation of the increase in flippase activity in *rta3Δ/Δ* mutant. We found that *lem3Δ/Δrta3Δ/Δ* cells exhibit decreased susceptibility to miltefosine similar to *lem3Δ/Δ* (Figure 3.20). Concordantly, the double mutant also was compromised in the internalization of NBD-PC, confirming that Rta3 negatively regulates Lem3 and thus contributes to the maintenance of PC asymmetry in the plasma membrane in *C. albicans* (Figure 3.21).

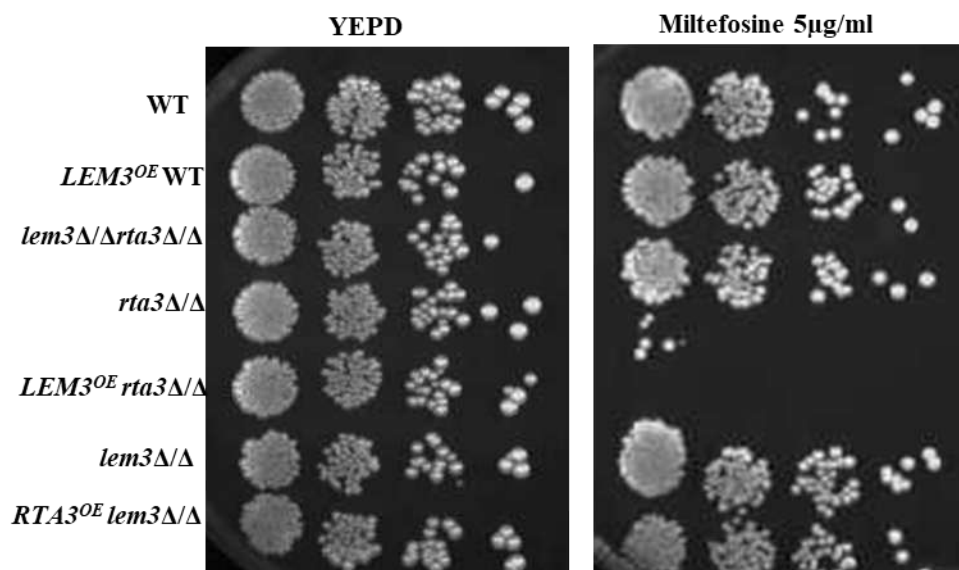


Figure 3.20: Spot assay for miltefosine susceptibility. Fivefold serial dilutions of cell suspensions were spotted onto YEPD plates supplemented with miltefosine and incubated at 30 °C for 48 hours.

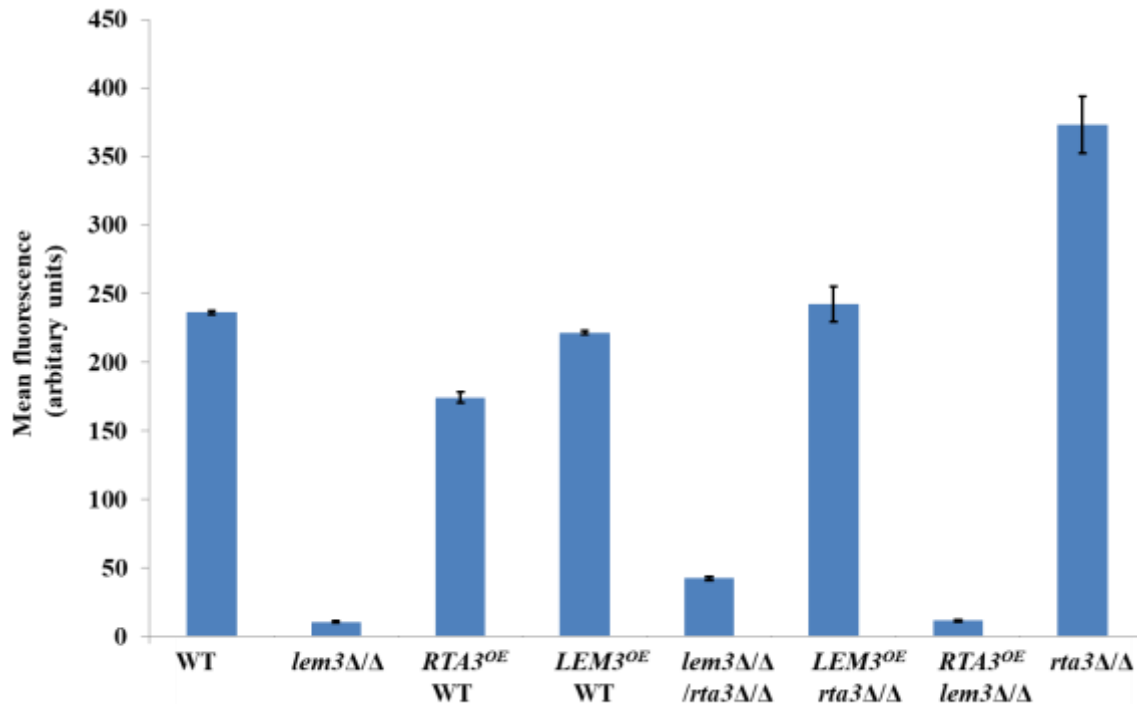


Figure 3.21: Intracellular accumulation of M-C6-NBD-PC in *lem3Δ/Δrta3Δ/Δ* cells. Cells were labeled with 5 μM of NBD-labeled PC. Strains were grown till O.D₆₀₀ of 1, incubated with NBD-PC for 45 min at 30 °C in SDC media, and washed with ice cold SC-azide. Samples were then incubated in SC media at 30 °C for 30 min and fluorescence measurements done by flow cytometry.

Next, to determine if *LEM3* and *RTA3* function in a common or parallel pathway to regulate the transbilayer movement of PC across the plasma membrane, we constructed and analyzed a mutant that lacked both *LEM3* and *RTA3*. We then sought to analyze the susceptibility of *lem3Δ/Δrta3Δ/Δ* mutant also on fluconazole, followed by testing its ability to undergo hyphal morphogenesis on solid Spider medium. While deletion of *RTA3* in wild type exhibited no alteration in azole susceptibility, *lem3Δ/Δrta3Δ/Δ* showed increased susceptibility to azoles, similar to *lem3Δ/Δ* (Figure 3.22). Similarly, *rta3Δ/Δ* cells showed no defect in hyphal growth while *lem3Δ/Δrta3Δ/Δ* showed abrogated hyphal growth, similar to *lem3Δ/Δ* (Figure 3.23). Considering that the *lem3Δ/Δrta3Δ/Δ* mutant had the same phenotype (decreased susceptibility to miltefosine, increased susceptibility to fluconazole and inhibition in hyphal morphogenesis) as the *lem3Δ/Δ* single mutant, it is likely that Lem3 and Rta3 function in the same pathway.

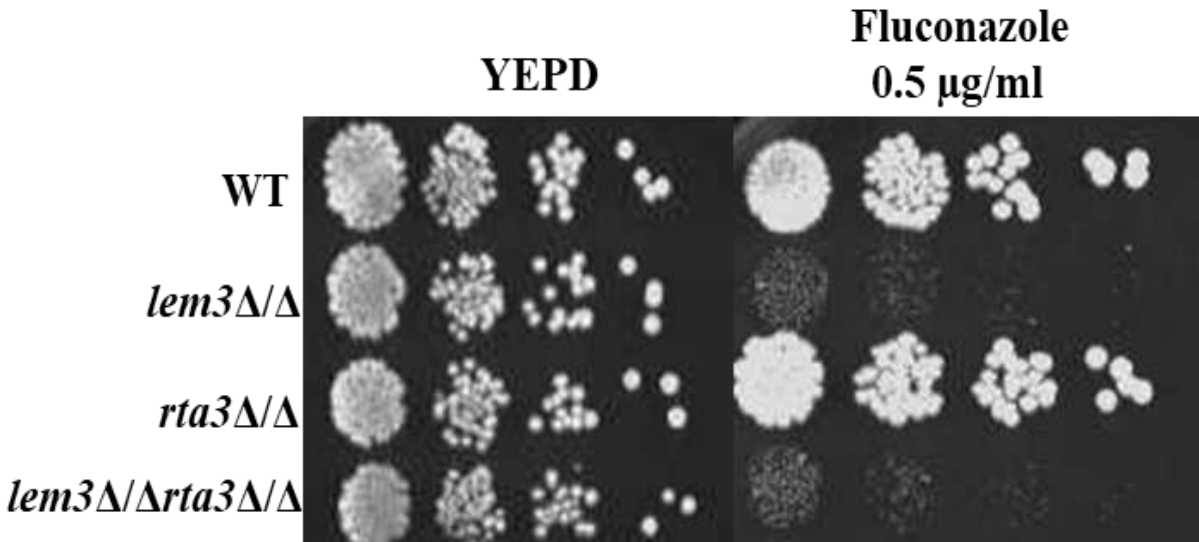


Figure 3.22: Spot assay for fluconazole susceptibility. Fivefold serial dilution of cell suspensions were spotted onto YEPD plates supplemented with fluconazole and incubated at 30 °C for 48 hours.

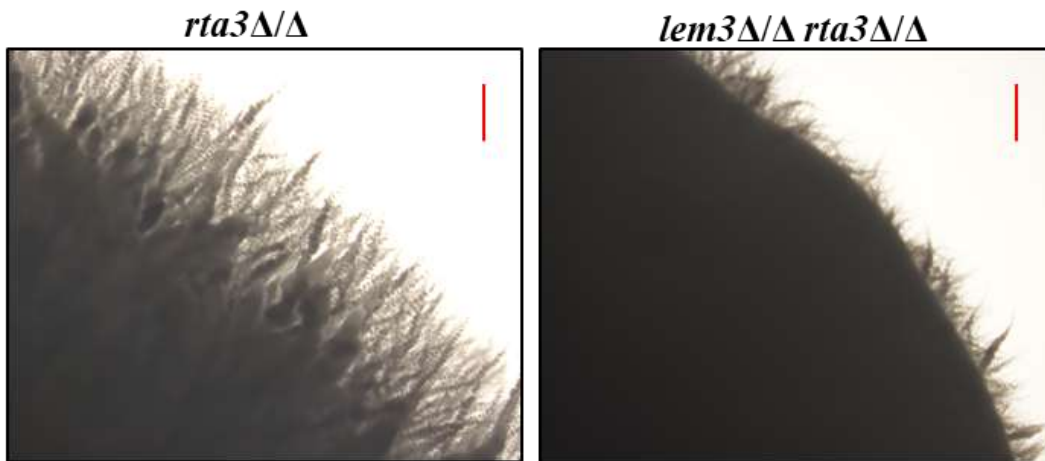


Figure 3.23: Bud-to-hyphae switch is compromised in absence of *LEM3*. Strains were spotted on spider agar plates and incubated at 37 °C for 6 days.

To determine whether Lem3 is upstream or downstream of Rta3, we overexpressed *LEM3* in *rta3Δ/Δ* and *RTA3* in *lem3Δ/Δ* cells by replacing the endogenous promoter of both the genes with the constitutively active *TDH3* promoter (Table 1). The forced expression of *LEM3* in *rta3Δ/Δ* did not restore sensitivity to miltefosine. On the other hand, overexpression of *RTA3* in *lem3Δ/Δ* had no effect on resistance to miltefosine (Figure 3.20). Susceptibility to miltefosine in

the respective strains correlated well with the accumulation of NBD-PC such that *LEM3^{OE}rta3Δ/Δ* exhibited decreased accumulation of NBD-PC as opposed to *RTA3^{OE}lem3Δ/Δ* that displayed increased accumulation of NBD-PC (Figure 3.21). Coupled together, our results suggest that Lem3 governs the transbilayer transport of PC across the plasma membrane at least in part by functioning downstream to Rta3 in *C. albicans*.

4.0 DISCUSSION

Plasma membrane of all eukaryotes has an asymmetrical distribution of phospholipids that is maintained by ATP-driven phospholipid translocases. P4-ATPases regulate this asymmetric distribution by translocating phospholipids from the outer leaflet to the inner/cytoplasmic leaflet of the plasma membrane. The P4-ATPase Drs2 of *S. cerevisiae* interacts with its non-catalytic subunit Cdc50 to maintain the asymmetrical distribution of phospholipids on the plasma membrane (Saito et al., 2004; Lenoir et al., 2009; Tanaka et al., 2010). Likewise, the P4-ATPase Dnf1 forms a complex with the non-catalytic subunit Lem3 and localizes to the plasma membrane (Noji et al., 2006). Lem3 is required for the exit of Dnf1 from the endoplasmic reticulum (ER) and together Dnf1-Lem3 regulate the flip of phosphatidylcholine, phosphatidylserine and phosphatidylethanolamine in *S. cerevisiae* (Pomorski et al., 2003). Parallel studies on P4-ATPases and their cognate non-catalytic partners are limited in the pathogenic fungus *C. albicans*. With the exception of a recent study where the role of Cdc50 in regulating antifungal resistance, virulence, endocytosis and hyphal morphogenesis has been demonstrated, characterization of other flippase complexes has not been initiated in *C. albicans*. Herein, we have identified the *C. albicans* *LEM3* gene encoding a protein of 439 amino acids with two conserved transmembrane domains. Given the sequence homology of CaLem3 with ScLem3 (Figure 3.3), we presumed that the function of CaLem3 may also be conserved in this pathogenic fungus. Consistent with this, we demonstrate the role of Lem3 in regulating the transbilayer movement (flip) of PC across the plasma membrane. The proposal that Lem3 is involved in flipping PC across the lipid bilayer stems from the following observations. First that loss of Lem3 results in decreased susceptibility to the alkylphosphocholine drug miltefosine

(Figure 3.6), hinting towards the possibility of the involvement of Lem3 in regulating PC movement across the plasma membrane in *C. albicans*. Second, the internalization of NBD-PC decreases in the *lem3Δ/Δ* cells (Figure 3.7). Third, the PC-specific flippase activity was abrogated in the absence of Lem3 (Figure 3.9) and fourth, the increase internalization of NBD-PC in *rta3Δ/Δ* also was abrogated upon deleting *LEM3* in this strain (Figure 3.21). This data combined infer a significant role for Lem3 in the transbilayer translocation of PC across the plasma membrane in *C. albicans*.

We observed that Lem3 plays a role in modulating the susceptibility of *C. albicans* to azole antifungals such that disruption of Lem3 function rendered *C. albicans* sensitive to azole antifungals (Figure 3.10). Previous studies in *S. cerevisiae* show that disruption of Lem3 function does not affect azole susceptibility. On the contrary, Cdc50 of *C. neoformans* and *S. cerevisiae* plays role in azole sensitivity by regulating the distribution and trafficking of ergosterol in the Golgi network (Hankins et al., 2015). Herein, we propose that disruption of Lem3 will lead to altered distribution of PC thereby affecting membrane permeability. Additionally, although not tested in this study but Lem3 may also have a role in regulating ergosterol distribution on the membrane similar to Cdc50, which in turn may cause cell death upon treatment with fluconazole; a questions that needs to be addressed. Earlier studies in *C. albicans* also have revealed a correlation between changes in membrane lipid composition and the activity of the drug efflux pump Cdr1 (Mukherjee et al., 2003). Concordantly, Cdr1 activity was abrogated in the *lem3Δ/Δ* cells (Figure 3.11). Thus, it is possible that the overall outcome of altered PC asymmetry in *lem3Δ/Δ* cells is abrogated activity of the drug efflux pump resulting in azole sensitivity in *C. albicans*. Whether alterations in PC asymmetry affect localization of Cdr1 or affects the functioning of this efflux pump via another mechanism will require further

investigation.

Besides its role in modulating azole susceptibility, we also tested the requirement of *C. albicans* Lem3 for regulating pathogenicity traits. Despite the reduced hyphal growth of the *lem3Δ/Δ* mutant in vitro (Figure 3.15), virulence was not attenuated in vivo mice model of systemic infection (Figure 3.17). Furthermore, the biofilm forming ability of the mutant also was not affected (Figure 3.19) pointing to the dispensability of Lem3 in regulating *C. albicans* pathogenesis. This is in contrast to the well defined role of *C. neoformans* Cdc50 in virulence in vitro as well as in vivo. The *cdc50Δ* cells are phagocytosed at a higher rate by the macrophages and thus are more sensitive to killing in vitro by macrophages (Huang et al., 2016). Likewise the *C. albicans* Cdc50 is also shown to be pivotal for establishing an infection in the mouse model of systemic infection (Xu et al., 2019). In *S. cerevisiae* the Lem3-Dnf1 and Cdc50-Drs2 complexes are functionally redundant as loss of function of both these complexes causes a synthetic lethal defect (Noji et al., 2006). Considering this background it is plausible that out of the two non-catalytic subunits of flippases, Cdc50 is a major contributor while Lem3 does not have a role to play in *C. albicans* pathogenesis.

In order to strengthen the role of Lem3 as a protein that may be associated with a PC-specific flippase in *C. albicans*, we made use of a mutant, *rta3Δ/Δ* generated in our laboratory (Srivastava et al., 2017). This mutant exhibits constitutively high PC-specific flippase activity that correlated well with an increased susceptibility to miltefosine and enhanced internalization of NBD-PC. Deleting *LEM3* in *rta3Δ/Δ* cells rendered cells resistant to miltefosine and decreased the PC-specific flippase activity, similar to *lem3Δ/Δ* cells (Figure 3.20, 3.21), affirming the role of Lem3 in regulating the transbilayer movement of PC across the plasma membrane in *C. albicans*. Considering that Rta3 is a plasma membrane localized regulatory

protein, we propose that Lem3 could be one of the downstream effectors of Rta3 on which this protein exerts its regulatory effect on to maintain the plasma membrane asymmetric distribution of PC in *C. albicans*. *lem3Δ/Δrta3Δ/Δ* cells exhibited a phenotype similar to *lem3Δ/Δ* cells confirming that both these genes function in a single pathway. Furthermore, *lem3Δ/Δ* cells continued to exhibit decreased susceptibility to miltefosine even upon overexpressing *RTA3* in the mutant (Figure 3.20) pointing to the role of Lem3 as one of the effectors of Rta3.

Perturbations in the asymmetric distribution of phospholipids on the plasma membrane serves as a trigger for activating multiple cellular events (Nichols 2002). Molecular entities that can function as flippases and their regulators remain unidentified in *C. albicans*. Therefore, the identification of Rta3 as a protein that may be crucial for maintaining asymmetric distribution of phosphatidylcholine via regulating the activity of Lem3 may prove to be an “emerging target” with therapeutic implication in the field of Candida biology. In *S. cerevisiae* the homologs of *RTA3* are referred to as the Rta1-family of proteins or the lipid translocating exporters (LTEs) (Manente and Ghislain, 2009). In addition to *RTA3*, *C. albicans* has three additional genes, *orf19.6224*, *RTA2* and *RTA4*, coding for the Rta1-family of proteins. Noteworthy is that these proteins lack an overall sequence conservation with the classical G-protein coupled-receptors (GPCRs) and are unique to the fungal kingdom. Considering that Rta3 is a regulatory protein and its deletion impacts multiple cellular processes (Figure 4.1), identification of proteins whose functions are regulated by Rta3 may provide additional molecular components that can be targeted in near future for antifungal therapies. We posit that one such interplay that can be exploited in order to disrupt events that are crucial for the pathogenesis of this fungus, is the cross-talk between Rta3 and its effector Lem3. The homologs of Rta3 and Lem3 are present across the fungal kingdom, indicating that this interaction, once it is demonstrated through this

study, may be conserved across the fungal kingdom and may be required for maintenance of PC asymmetry and biofilm formation. Interestingly, disrupting Lem3 function in a *C. albicans* azole-resistant clinical isolate rendered this strain azole-sensitive (Figure 3.14), pointing to the clinical impact of targeting Lem3. Thus, developing antifungals that target Rta3 and Lem3 may provide us with more effective broad spectrum antifungals that operate in a completely unexploited target space.

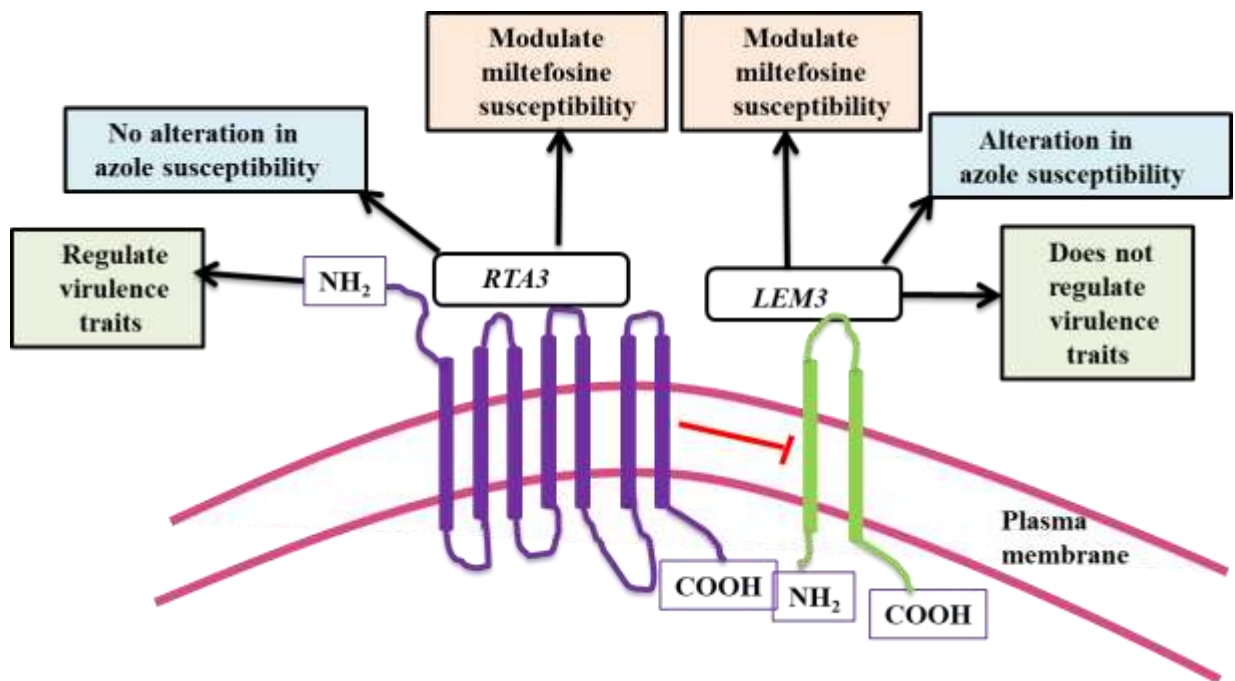


Figure 4.1. A model depicting roles of *LEM3* and its interaction with the membrane localized 7- transmembrane receptor protein Rta3 in *C. albicans*. Consistent with the presence of two transmembrane domains (by TMHMM Transmembrane Helices Hidden Markov Models) Lem3 may also be a putative membrane localized protein. Red arrow signifies negative regulation exerted by Rta3 on Lem3.

5.0 REFERENCES

Alder-Baerens, Nele, Quirine Lisman, Lambert Luong, Thomas Pomorski, and Joost CM Holthuis. 2006. “Loss of P4 ATPases Drs2p and Dnf3p Disrupts Aminophospholipid Transport and Asymmetry in Yeast Post-Golgi Secretory Vesicles.” *Molecular Biology of the Cell* 17 (4): 1632–1642.

Alexander, Barbara D., Melissa D. Johnson, Christopher D. Pfeiffer, Cristina Jiménez-Ortigosa, Jelena Catania, Rachel Booker, Mariana Castanheira, Shawn A. Messer, David S. Perlin, and Michael A. Pfaller. 2013. “Increasing Echinocandin Resistance in *Candida Glabrata*: Clinical Failure Correlates With Presence of FKS Mutations and Elevated Minimum Inhibitory Concentrations.” *Clinical Infectious Diseases* 56 (12): 1724–32. <https://doi.org/10.1093/cid/cit136>.

Alim, Darakshan, Shabnam Sircaik, and Sneha Lata Panwar. 2018. “The Significance of Lipids to Biofilm Formation in *Candida Albicans*: An Emerging Perspective.” *Journal of Fungi* 4 (4): 140.

Andersen, Jens P., Anna L. Vestergaard, Stine A. Mikkelsen, Louise S. Mogensen, Madhavan Chalat, and Robert S. Molday. 2016. “P4-ATPases as Phospholipid Flippases—Structure, Function, and Enigmas.” *Frontiers in Physiology* 7: 275.

Andes, David R., Nasia Safdar, John W. Baddley, Geoffrey Playford, Annette C. Reboli, John H. Rex, Jack D. Sobel, Peter G. Pappas, and Bart Jan Kullberg. 2012. “Impact of Treatment Strategy on Outcomes in Patients with Candidemia and Other Forms of Invasive Candidiasis: A Patient-Level Quantitative Review of Randomized Trials.” *Clinical Infectious Diseases* 54 (8): 1110–1122.

Anzai, Kazunori, Yasuyuki Yoshioka, and Yutaka Kirino. 1993. “Novel Radioactive Phospholipid Probes as a Tool for Measurement of Phospholipid Translocation across Biomembranes.” *Biochimica et Biophysica Acta (BBA)-Biomembranes* 1151 (1): 69–75.

Baddley, John W., Mukesh Patel, Sujata M. Bhavnani, Stephen A. Moser, and David R. Andes. 2008. “Association of Fluconazole Pharmacodynamics with Mortality in Patients with Candidemia.” *Antimicrobial Agents and Chemotherapy* 52 (9): 3022–3028.

Balasubramanian, Krishnakumar, and Alan J. Schroit. 2003. "Aminophospholipid Asymmetry: A Matter of Life and Death." *Annual Review of Physiology* 65 (1): 701–34. <https://doi.org/10.1146/annurev.physiol.65.092101.142459>.

Barbosa, Sónia, Dagmar Pratte, Heinz Schwarz, Rüdiger Pipkorn, and Birgit Singer-Krüger. 2010. "Oligomeric Dop1p Is Part of the Endosomal Neolp-Ysl2p-Arl1p Membrane Remodeling Complex." *Traffic* 11 (8): 1092–1106.

Basse, Francois, Patrick Gaffet, Francine Rendu, and Alain Bienvenue. 1993. "Translocation of Spin-Labeled Phospholipids through Plasma Membrane during Thrombin-and Ionophore A23187-Induced Platelet Activation." *Biochemistry* 32 (9): 2337–2344.

Bell, R. M., L. M. Ballas, and R. A. Coleman. 1981. "Lipid Topogenesis." *Journal of Lipid Research* 22 (3): 391–403.

Berman, Judith, and Peter E. Sudbery. 2002. "Candida Albicans: A Molecular Revolution Built on Lessons from Budding Yeast." *Nature Reviews. Genetics* 3 (12): 918–30. <https://doi.org/10.1038/nrg948>.

Bervers, E. M., T. Wiedmer, P. Comfurius, S. J. Shattil, H. J. Weiss, R. F. Zwaal, and P. J. Sims. 1992. "Defective Ca(2+)-Induced Microvesiculation and Deficient Expression of Procoagulant Activity in Erythrocytes from a Patient with a Bleeding Disorder: A Study of the Red Blood Cells of Scott Syndrome." *Blood* 79 (2): 380–88.

Bitbol, Michel, and Philippe F. Devaux. 1988. "Measurement of Outward Translocation of Phospholipids across Human Erythrocyte Membrane." *Proceedings of the National Academy of Sciences* 85 (18): 6783–6787.

Boon, J. Middleton, and Bradley D. Smith. 2002. "Chemical Control of Phospholipid Distribution across Bilayer Membranes." *Medicinal Research Reviews* 22 (3): 251–281.

Borst, P., and R. Oude Elferink. 2002. "Mammalian ABC Transporters in Health and Disease." *Annual Review of Biochemistry* 71 (1): 537–592.

Borst, P., N. Zelcer, and A. Van Helvoort. 2000. "ABC Transporters in Lipid Transport." *Biochimica et Biophysica Acta (BBA)-Molecular and Cell Biology of Lipids* 1486 (1): 128–144.

Bretscher, Mark S. 1972. "Asymmetrical Lipid Bilayer Structure for Biological Membranes." *Nature New Biology* 236 (61): 11.

Brown, G. D., D. W. Denning, and S. M. Levitz. 2012. "Tackling Human Fungal Infections." *Science* 336 (6082): 647–647. <https://doi.org/10.1126/science.1222236>.

Bryde, Susanne, Hanka Hennrich, Patricia M. Verhulst, Philippe F. Devaux, Guillaume Lenoir, and Joost CM Holthuis. 2010. "CDC50 Proteins Are Critical Components of the Human Class-1 P4-ATPase Transport Machinery." *Journal of Biological Chemistry* 285 (52): 40562–40572.

Bull, Laura N., Michiel JT van Eijk, Ludmila Pawlikowska, Joseph A. DeYoung, Jenneke A. Juijn, Mira Liao, Leo WJ Klomp, Noureddine Lomri, Ruud Berger, and Bruce R. Scharschmidt. 1998. "A Gene Encoding a P-Type ATPase Mutated in Two Forms of Hereditary Cholestasis." *Nature Genetics* 18 (3): 219.

Bütikofer, P., Z. W. Lin, D. T. Chiu, B. Lubin, and F. A. Kuypers. 1990. "Transbilayer Distribution and Mobility of Phosphatidylinositol in Human Red Blood Cells." *Journal of Biological Chemistry* 265 (27): 16035–16038.

Cauda, Roberto. 2009. "Candidaemia in Patients with an Inserted Medical Device." *Drugs* 69 (1): 33–38.

Chakrabarti, A., A. Ghosh, R. Batra, A. Kaushal, P. Roy, and H. Singh. 1996. "Antifungal Susceptibility Pattern of Non-Albicans Candida Species & Distribution of Species Isolated from Candidaemia Cases over a 5 Year Period." *The Indian Journal of Medical Research* 104 (August): 171–76.

Chakrabarti, A., B. Mohan, S. K. Shrivastava, R. S. K. Marak, A. Ghosh, and P. Ray. 2002. "Change in Distribution & Antifungal Susceptibility of Candida Species Isolated from Candidaemia Cases in a Tertiary Care Centre during 1996-2000." *The Indian Journal of Medical Research* 116 (July): 5–12.

Chantalat, Sophie, Sei-Kyoung Park, Zhaolin Hua, Ke Liu, Renée Gobin, Anne Peyroche, Alain Rambourg, Todd R. Graham, and Catherine L. Jackson. 2004. "The Arf Activator Gea2p and the P-Type ATPase Drs2p Interact at the Golgi in *Saccharomyces Cerevisiae*." *Journal of Cell Science* 117 (Pt 5): 711–22. <https://doi.org/10.1242/jcs.00896>.

Chen, Chih-Ying, Michael F. Ingram, Peter H. Rosal, and Todd R. Graham. 1999. "Role for Drs2p, a P-Type ATPase and Potential Aminophospholipid Translocase, in Yeast Late Golgi Function." *The Journal of Cell Biology* 147 (6): 1223–1236.

Chen, Sophie, Jiyi Wang, Baby-Periyannayagi Muthusamy, Ke Liu, Sara Zare, Raymond J. Andersen, and Todd R. Graham. 2006. "Roles for the Drs2p-Cdc50p Complex in Protein Transport and Phosphatidylserine Asymmetry of the Yeast Plasma Membrane." *Traffic (Copenhagen, Denmark)* 7 (11): 1503–17. <https://doi.org/10.1111/j.1600-0854.2006.00485.x>.

Cheng, Georgina, Karen Wozniak, Matthew A. Wallig, Paul L. Fidel, Suzanne R. Trupin, and Lois L. Hoyer. 2005. "Comparison between *Candida Albicans* Agglutinin-like Sequence Gene Expression Patterns in Human Clinical Specimens and Models of Vaginal Candidiasis." *Infection and Immunity* 73 (3): 1656–63. <https://doi.org/10.1128/IAI.73.3.1656-1663.2005>.

Coleman, Jonathan A., Michael CM Kwok, and Robert S. Molday. 2009. "Localization, Purification, and Functional Reconstitution of the P4-ATPase Atp8a2, a Phosphatidylserine Flippase in Photoreceptor Disc Membranes." *Journal of Biological Chemistry* 284 (47): 32670–32679.

Coleman, Jonathan A., Faraz Quazi, and Robert S. Molday. 2013. "Mammalian P4-ATPases and ABC Transporters And Their Role in Phospholipid Transport." *Biochimica et Biophysica Acta* 1831 (3): 555–74. <https://doi.org/10.1016/j.bbaliip.2012.10.006>.

Colleau, Martine, Paulette Hervé, Pierre Fellmann, and Philippe F. Devaux. 1991. "Transmembrane Diffusion of Fluorescent Phospholipids in Human Erythrocytes." *Chemistry and Physics of Lipids* 57 (1): 29–37.

Connor, Jerome, Charles H. Pak, R. F. Zwaal, and Alan J. Schroit. 1992. "Bidirectional Transbilayer Movement of Phospholipid Analogs in Human Red Blood Cells. Evidence for an ATP-Dependent and Protein-Mediated Process." *Journal of Biological Chemistry* 267 (27): 19412–19417.

Connor, Jerome, and Alan J. Schroit. 1987. "Determination of Lipid Asymmetry in Human Red Cells by Resonance Energy Transfer." *Biochemistry* 26 (16): 5099–5105.

Cornely, O. A., M. Bassetti, T. Calandra, J. Garbino, B. J. Kullberg, O. Lortholary, W. Meersseman, et al. 2012. "ESCMID* Guideline for the Diagnosis and Management of *Candida* Diseases 2012: Non-Neutropenic Adult Patients." *Clinical Microbiology and Infection* 18 (s7): 19–37. <https://doi.org/10.1111/1469-0691.12039>.

Daleke, David L., and Wray H. Huestis. 1985. "Incorporation and Translocation of Aminophospholipids in Human Erythrocytes." *Biochemistry* 24 (20): 5406–5416.

———. 1989. “Erythrocyte Morphology Reflects the Transbilayer Distribution of Incorporated Phospholipids.” *The Journal of Cell Biology* 108 (4): 1375–1385.

Dalle, Frederic, Betty Wächtler, Coralie L’Ollivier, Gudrun Holland, Norbert Bannert, Duncan Wilson, Catherine Labruère, Alain Bonnin, and Bernhard Hube. 2010. “Cellular Interactions of *Candida Albicans* with Human Oral Epithelial Cells and Enterocytes.” *Cellular Microbiology* 12 (2): 248–71. <https://doi.org/10.1111/j.1462-5822.2009.01394.x>.

Debourgogne, Anne, Joséphine Dorin, and Marie Machouart. 2016. “Emerging Infections Due to Filamentous Fungi in Humans and Animals: Only the Tip of the Iceberg?” *Environmental Microbiology Reports* 8 (3): 332–342.

Devaux, Philippe F. 1991. “Static and Dynamic Lipid Asymmetry in Cell Membranes.” *Biochemistry* 30 (5): 1163–1173.

Devaux, Philippe F., Pierre Fellmann, and Paulette Hervé. 2002. “Investigation on Lipid Asymmetry Using Lipid Probes: Comparison between Spin-Labeled Lipids and Fluorescent Lipids.” *Chemistry and Physics of Lipids* 116 (1–2): 115–134.

Doedt, Thomas, Shankarling Krishnamurthy, Dirk P. Bockmuhl, Bernd Tebarth, Christian Stempel, Claire L. Russell, Alistair JP Brown, and Joachim F. Ernst. 2004. “APSES Proteins Regulate Morphogenesis and Metabolism in *Candida Albicans*.” *Molecular Biology of the Cell* 15 (7): 3167–3180.

Donlan, Rodney M., and J. William Costerton. 2002. “Biofilms: Survival Mechanisms of Clinically Relevant Microorganisms.” *Clinical Microbiology Reviews* 15 (2): 167–193.

Engelman, Donald M. 2005. “Membranes Are More Mosaic than Fluid.” *Nature* 438 (7068): 578–80. <https://doi.org/10.1038/nature04394>.

Eppens, Elaine F., Saskia WC van Mil, J. Marleen L. de Vree, Kam S. Mok, Jenneke A. Juijn, Ronald PJ Oude Elferink, Ruud Berger, Roderick HJ Houwen, and Leo WJ Klomp. 2001. “FIC1, the Protein Affected in Two Forms of Hereditary Cholestasis, Is Localized in the Cholangiocyte and the Canalicular Membrane of the Hepatocyte.” *Journal of Hepatology* 35 (4): 436–443.

Fanning, Saranna, and Aaron P. Mitchell. 2012. “Fungal Biofilms.” *PLoS Pathogens* 8 (4). <https://doi.org/10.1371/journal.ppat.1002585>.

Farge, Emmanuel, and Philippe F. Devaux. 1992. "Shape Changes of Giant Liposomes Induced by an Asymmetric Transmembrane Distribution of Phospholipids." *Biophysical Journal* 61 (2): 347–357.

Farge, Emmanuel, David M. Ojcius, Agathe Subtil, and Alice Dautry-Varsat. 1999. "Enhancement of Endocytosis Due to Aminophospholipid Transport across the Plasma Membrane of Living Cells." *American Journal of Physiology-Cell Physiology* 276 (3): C725–C733.

Festa, Richard A., Marian E. Helsel, Katherine J. Franz, and Dennis J. Thiele. 2014. "Exploiting Innate Immune Cell Activation of a Copper-Dependent Antimicrobial Agent during Infection." *Chemistry & Biology* 21 (8): 977–87. <https://doi.org/10.1016/j.chembiol.2014.06.009>.

Fidel Jr, Paul L. 2007. "History and Update on Host Defense against Vaginal Candidiasis." *American Journal of Reproductive Immunology* 57 (1): 2–12.

Finkel, Jonathan S., and Aaron P. Mitchell. 2011. "Genetic Control of *Candida Albicans* Biofilm Development." *Nature Reviews. Microbiology* 9 (2): 109–18. <https://doi.org/10.1038/nrmicro2475>.

Fonzi, William A. n.d. "Isogenic Strain Construction and Gene Mapping in *Candida Albicans*," 12.

Fox, Emily P., Catherine K. Bui, Jeniel E. Nett, Nairi Hartooni, Michael C. Mui, David R. Andes, Clarissa J. Nobile, and Alexander D. Johnson. 2015. "An Expanded Regulatory Network Temporally Controls *Candida Albicans* Biofilm Formation." *Molecular Microbiology* 96 (6): 1226–1239.

Franz, Renate, Steven L. Kelly, David C. Lamb, Diane E. Kelly, Markus Ruhnke, and Joachim Morschhäuser. 1998. "Multiple Molecular Mechanisms Contribute to a Stepwise Development of Fluconazole Resistance in Clinical *Candida Albicans* Strains." *Antimicrobial Agents and Chemotherapy* 42 (12): 3065–3072.

Fujii, T., and A. Tamura. 1983. "Dynamic Behaviour of Amphiphilic Lipids to Penetrate into Membrane of Intact Human Erythrocytes and to Induce Change in the Cell Shape." *Biomedica Biochimica Acta* 42 (11–12): S81–5.

Furuta, Nobumichi, Konomi Fujimura-Kamada, Koji Saito, Takaharu Yamamoto, and Kazuma Tanaka. 2007. "Endocytic Recycling in Yeast Is Regulated by Putative Phospholipid Translocases and the Ypt31p/32p-Rcy1p Pathway." *Molecular Biology of the Cell* 18 (1): 295–312.

Gall, Walter E., Nathan C. Geething, Zhaolin Hua, Michael F. Ingram, Ke Liu, Sophie I. Chen, and Todd R. Graham. 2002. "Drs2p-Dependent Formation of Exocytic Clathrin-Coated Vesicles in Vivo." *Current Biology* 12 (18): 1623–1627.

Gascard, Philippe, Dien Tran, Monique Sauvage, Jean-Claude Sulpice, Kiyoko Fukami, Tadaomi Takenawa, Michel Claret, and Françoise Giraud. 1991. "Asymmetric Distribution of Phosphoinositides and Phosphatidic Acid in the Human Erythrocyte Membrane." *Biochimica et Biophysica Acta (BBA)-Biomembranes* 1069 (1): 27–36.

Gaur, Nand K., and Stephen A. Klotz. 1997. "Expression, Cloning, and Characterization of a *Candida Albicans* Gene, ALA1, That Confers Adherence Properties upon *Saccharomyces Cerevisiae* for Extracellular Matrix Proteins." *Infection and Immunity* 65 (12): 5289–5294.

Gilbert, Martin J., Christopher R. Thornton, Gavin E. Wakley, and Nicholas J. Talbot. 2006. "A P-Type ATPase Required for Rice Blast Disease and Induction of Host Resistance." *Nature* 440 (7083): 535.

Gillum, Amanda M., Emma YH Tsay, and Donald R. Kirsch. 1984. "Isolation of the *Candida Albicans* Gene for Orotidine-5'-Phosphate Decarboxylase by Complementation of *S. Cerevisiae* Ura3 and *E. Coli* PyrF Mutations." *Molecular and General Genetics MGG* 198 (1): 179–182.

Grossman, Nina T., Tom M. Chiller, and Shawn R. Lockhart. 2014. "Epidemiology of Echinocandin Resistance in *Candida*." *Current Fungal Infection Reports* 8 (4): 243–248.

Gummadi, Sathyanarayana N., and Anant K. Menon. 2002. "Transbilayer Movement of Dipalmitoylphosphatidylcholine in Proteoliposomes Reconstituted from Detergent Extracts of Endoplasmic Reticulum KINETICS OF TRANSBILAYER TRANSPORT MEDIATED BY A SINGLE FLIPPASE AND IDENTIFICATION OF PROTEIN FRACTIONS ENRICHED IN FLIPPASE ACTIVITY." *Journal of Biological Chemistry* 277 (28): 25337–25343.

Hachiro, Takeru, Takaharu Yamamoto, Kenji Nakano, and Kazuma Tanaka. 2013. "Phospholipid Flippases Lem3p-Dnf1p and Lem3p-Dnf2p Are Involved in the Sorting of the Tryptophan Permease Tat2p in Yeast." *Journal of Biological Chemistry* 288 (5): 3594–3608.

Hajjeh, Rana A., Andre N. Sofair, Lee H. Harrison, G. Marshall Lyon, Beth A. Arthington-Skaggs, Sara A. Mirza, Maureen Phelan, Juliette Morgan, Wendy Lee-Yang, and Meral A. Ciblak. 2004. "Incidence of Bloodstream Infections Due to *Candida* Species and in Vitro Susceptibilities of Isolates Collected from 1998 to 2000 in a Population-Based Active Surveillance Program." *Journal of Clinical Microbiology* 42 (4): 1519–1527.

Haldar, Sourav, and Amitabha Chattopadhyay. 2012. "Application of NBD-Labeled Lipids in Membrane and Cell Biology." In *Fluorescent Methods to Study Biological Membranes*, 37–50. Springer.

Hani, Umme, Hosakote G Shivakumar, Rudra Vaghela, Ali M. Osmani, and Atul Shrivastava. 2015. "Candidiasis: A Fungal Infection-Current Challenges and Progress in Prevention and Treatment." *Infectious Disorders-Drug Targets (Formerly Current Drug Targets-Infectious Disorders)* 15 (1): 42–52.

Hankins, Hannah M., Yves Y. Sere, Nicholas S. Diab, Anant K. Menon, and Todd R. Graham. 2015. "Phosphatidylserine Translocation at the Yeast Trans-Golgi Network Regulates Protein Sorting into Exocytic Vesicles." *Molecular Biology of the Cell* 26 (25): 4674–85. <https://doi.org/10.1091/mbc.E15-07-0487>.

Hanson, Pamela K., Althea M. Grant, and J. Wylie Nichols. 2002. "NBD-Labeled Phosphatidylcholine Enters the Yeast Vacuole via the Pre-Vacuolar Compartment." *Journal of Cell Science* 115 (13): 2725–2733.

Hanson, Pamela K., Lynn Malone, Jennifer L. Birchmore, and J. Wylie Nichols. 2003. "Lem3p Is Essential for the Uptake and Potency of Alkylphosphocholine Drugs, Edelfosine and Miltefosine." *Journal of Biological Chemistry* 278 (38): 36041–36050.

Holthuis, Joost C. M., and Anant K. Menon. 2014. "Lipid Landscapes and Pipelines in Membrane Homeostasis." *Nature* 510 (7503): 48–57. <https://doi.org/10.1038/nature13474>.

Holthuis, Joost CM, Thomas Pomorski, René J. Raggars, Hein Sprong, and Gerrit Van Meer. 2001. "The Organizing Potential of Sphingolipids in Intracellular Membrane Transport." *Physiological Reviews* 81 (4): 1689–1723.

Hrafnisdóttir, Sigrún, and Anant K. Menon. 2000. "Reconstitution and Partial Characterization of Phospholipid Flippase Activity from Detergent Extracts of the *Bacillus Subtilis* Cell Membrane." *Journal of Bacteriology* 182 (15): 4198–4206.

Hu, Guanggan, Mélissa Caza, Erik Bakkeren, Matthias Kretschmer, Gaurav Bairwa, Ethan Reiner, and James Kronstad. 2017. "A P4-ATPase Subunit of the Cdc50 Family Plays a Role in Iron Acquisition and Virulence in *Cryptococcus Neoformans*." *Cellular Microbiology* 19 (6): e12718.

Hu, Guanggan, and James W. Kronstad. 2010. "A Putative P-Type ATPase, Apt1, Is Involved in Stress Tolerance and Virulence in *Cryptococcus Neoformans*." *Eukaryotic Cell* 9 (1): 74–83.

Hua, Zhaolin, Parvin Fatheddin, and Todd R. Graham. 2002. "An Essential Subfamily of Drs2p-Related P-Type ATPases Is Required for Protein Trafficking between Golgi Complex and Endosomal/Vacuolar System." *Molecular Biology of the Cell* 13 (9): 3162–3177.

Hua, Zhaolin, and Todd R. Graham. 2003. "Requirement for Neo1p in Retrograde Transport from the Golgi Complex to the Endoplasmic Reticulum." *Molecular Biology of the Cell* 14 (12): 4971–4983.

Huang, Wei, Guojian Liao, Gregory M. Baker, Yina Wang, Richard Lau, Padmaja Paderu, David S. Perlin, and Chaoyang Xue. 2016. "Lipid Flippase Subunit Cdc50 Mediates Drug Resistance and Virulence in *Cryptococcus Neoformans*." *MBio* 7 (3): e00478–16.

Inglis, D. O., M. B. Arnaud, J. Binkley, P. Shah, M. S. Skrzypek, F. Wymore, G. Binkley, S. R. Miyasato, M. Simison, and G. Sherlock. 2012. "The *Candida* Genome Database Incorporates Multiple *Candida* Species: Multispecies Search and Analysis Tools with Curated Gene and Protein Information for *Candida Albicans* and *Candida Glabrata*." *Nucleic Acids Research* 40 (D1): D667–74. <https://doi.org/10.1093/nar/gkr945>.

Jacobsen, Ilse D., Duncan Wilson, Betty Wächtler, Sascha Brunke, Julian R. Naglik, and Bernhard Hube. 2012. "Candida Albicans Dimorphism as a Therapeutic Target." *Expert Review of Anti-Infective Therapy* 10 (1): 85–93. <https://doi.org/10.1586/eri.11.152>.

Jain, Shilpa, NaTaza Stanford, Neha Bhagwat, Brian Seiler, Michael Costanzo, Charles Boone, and Peter Oelkers. 2007. "Identification of a Novel Lysophospholipid Acyltransferase in *Saccharomyces Cerevisiae*." *Journal of Biological Chemistry* 282 (42): 30562–30569.

Kabir, M. Anaul, Mohammad Asif Hussain, and Zulfiqar Ahmad. 2012. "Candida Albicans: A Model Organism for Studying Fungal Pathogens." *ISRN Microbiology* 2012.

Kao, Annie S., Mary E. Brandt, W. Ruth Pruitt, Laura A. Conn, Bradley A. Perkins, David S. Stephens, Wendy S. Baughman, Arthur L. Reingold, Gretchen A. Rothrock, and Michael A.

Pfaller. 1999. "The Epidemiology of Candidemia in Two United States Cities: Results of a Population-Based Active Surveillance." *Clinical Infectious Diseases* 29 (5): 1164–1170.

Kato, Utako, Kazuo Emoto, Charlotta Fredriksson, Hidemitsu Nakamura, Akinori Ohta, Toshihide Kobayashi, Kimiko Murakami-Murofushi, Tetsuyuki Kobayashi, and Masato Umeda. 2002. "A Novel Membrane Protein, Ros3p, Is Required for Phospholipid Translocation across the Plasma Membrane in *Saccharomyces Cerevisiae*." *Journal of Biological Chemistry* 277 (40): 37855–37862.

Kibbler, C. C., S. Seaton, Rosemary A. Barnes, W. R. Gransden, R. E. Holliman, E. M. Johnson, John D. Perry, D. J. Sullivan, and J. A. Wilson. 2003. "Management and Outcome of Bloodstream Infections Due to *Candida* Species in England and Wales." *Journal of Hospital Infection* 54 (1): 18–24.

Kishimoto, Takuma, Takaharu Yamamoto, and Kazuma Tanaka. 2005. "Defects in Structural Integrity of Ergosterol and the Cdc50p-Drs2p Putative Phospholipid Translocase Cause Accumulation of Endocytic Membranes, onto Which Actin Patches Are Assembled in Yeast." *Molecular Biology of the Cell* 16 (12): 5592–5609. <https://doi.org/10.1091/mbc.e05-05-0452>.

Klein, R. S., C. A. Harris, C. B. Small, B. Moll, M. Lesser, and G. H. Friedland. 1984. "Oral Candidiasis in High-Risk Patients as the Initial Manifestation of the Acquired Immunodeficiency Syndrome." *The New England Journal of Medicine* 311 (6): 354–58. <https://doi.org/10.1056/NEJM198408093110602>.

Klose, Christian, Michal A. Surma, and Kai Simons. 2013. "Organelle Lipidomics--Background and Perspectives." *Current Opinion in Cell Biology* 25 (4): 406–13. <https://doi.org/10.1016/j.ceb.2013.03.005>.

Kobayashi, Toshihide, and Anant K. Menon. 2018. "Transbilayer Lipid Asymmetry." *Current Biology* 28 (8): R386–R391.

Koehler, Philipp, Daniela Tacke, and Oliver A. Cornely. 2014. "Our 2014 Approach to Candidaemia." *Mycoses* 57 (10): 581–583.

Kojic, Erna M., and Rabih O. Darouiche. 2004. "Candida Infections of Medical Devices." *Clinical Microbiology Reviews* 17 (2): 255–267.

Kolter, Thomas, Richard L. Proia, and Konrad Sandhoff. 2002. "Combinatorial Ganglioside Biosynthesis." *Journal of Biological Chemistry* 277 (29): 25859–25862.

Kornitzer, Daniel. 2019. "Regulation of *Candida Albicans* Hyphal Morphogenesis by Endogenous Signals." *Journal of Fungi* 5 (1). <https://doi.org/10.3390/jof5010021>.

Krishnamurthy, Smriti S., and Rajendra Prasad. 1999. "Membrane Fluidity Affects Functions of Cdr1p, a Multidrug ABC Transporter of *Candida Albicans*." *FEMS Microbiology Letters* 173 (2): 475–481.

Labbaoui, Hayet, Stéphanie Bogliolo, Vikram Ghugtyal, Norma V. Solis, Scott G. Filler, Robert A. Arkowitz, and Martine Bassilana. 2017. "Role of Arf GTPases in Fungal Morphogenesis and Virulence." *PLoS Pathogens* 13 (2): e1006205.

Lenoir, Guillaume, Patrick Williamson, Cathelene F. Puts, and Joost CM Holthuis. 2009. "Cdc50p Plays a Vital Role in the ATPase Reaction Cycle of the Putative Aminophospholipid Transporter Drs2p." *Journal of Biological Chemistry* 284 (27): 17956–17967.

Lepak, Alexander, and David Andes. 2011. "Fungal Sepsis: Optimizing Antifungal Therapy in the Critical Care Setting." *Critical Care Clinics* 27 (1): 123–147.

Li, Xiaogang, Zhun Yan, and Jianping Xu. 2003. "Quantitative Variation of Biofilms among Strains in Natural Populations of *Candida Albicans*." *Microbiology (Reading, England)* 149 (Pt 2): 353–62. <https://doi.org/10.1099/mic.0.25932-0>.

Lingwood, Daniel, and Kai Simons. 2010. "Lipid Rafts as a Membrane-Organizing Principle." *Science (New York, N.Y.)* 327 (5961): 46–50. <https://doi.org/10.1126/science.1174621>.

Liu, Ke, Zhaolin Hua, Joshua A. Nepute, and Todd R. Graham. 2007. "Yeast P4-ATPases Drs2p and Dnf1p Are Essential Cargos of the NPFXD/Sla1p Endocytic Pathway." *Molecular Biology of the Cell* 18 (2): 487–500.

Lo, H. J., J. R. Köhler, B. DiDomenico, D. Loebenberg, A. Cacciapuoti, and G. R. Fink. 1997. "Nonfilamentous *C. Albicans* Mutants Are Avirulent." *Cell* 90 (5): 939–49. [https://doi.org/10.1016/s0092-8674\(00\)80358-x](https://doi.org/10.1016/s0092-8674(00)80358-x).

Lohse, Matthew B., Megha Gulati, Ashley Valle Arevalo, Adam Fishburn, Alexander D. Johnson, and Clarissa J. Nobile. 2017. "Assessment and Optimizations of *Candida Albicans* in Vitro Biofilm Assays." *Antimicrobial Agents and Chemotherapy* 61 (5): e02749–16.

Lopez-Marqués, Rosa L., Lisbeth R. Poulsen, Susanne Hanisch, Katharina Meffert, Morten J. Buch-Pedersen, Mia K. Jakobsen, Thomas Günther Pomorski, and Michael G. Palmgren. 2010. "Intracellular Targeting Signals and Lipid Specificity Determinants of the ALA/ALIS P4-ATPase Complex Reside in the Catalytic ALA α -Subunit." *Molecular Biology of the Cell* 21 (5): 791–801.

López-Marqués, Rosa L., Lisbeth R. Poulsen, and Michael G. Palmgren. 2012. "A Putative Plant Aminophospholipid Flippase, the Arabidopsis P4 ATPase ALA1, Localizes to the Plasma Membrane Following Association with a β -Subunit." *PLoS One* 7 (4): e33042. <https://doi.org/10.1371/journal.pone.0033042>.

López-Marqués, Rosa L., Lisbeth Rosager Poulsen, Aurélien Bailly, Markus Geisler, Thomas Günther Pomorski, and Michael G. Palmgren. 2015. "Structure and Mechanism of ATP-Dependent Phospholipid Transporters." *Biochimica et Biophysica Acta (BBA)-General Subjects* 1850 (3): 461–475.

Lopez-Marques, Rosa L., Lisa Theorin, Michael G. Palmgren, and Thomas Günther Pomorski. 2014. "P4-ATPases: Lipid Flippases in Cell Membranes." *Pflügers Archiv-European Journal of Physiology* 466 (7): 1227–1240.

Lortholary, O., G. Petrikos, M. Akova, M. C. Arendrup, S. Arikan-Akdagli, M. Bassetti, J. Bille, et al. 2012. "ESCMID* Guideline for the Diagnosis and Management of Candida Diseases 2012: Patients with HIV Infection or AIDS." *Clinical Microbiology and Infection* 18 (s7): 68–77. <https://doi.org/10.1111/1469-0691.12042>.

Maesaki, S., P. Marichal, H. Vanden Bossche, D. Sanglard, and S. Kohno. 1999. "Rhodamine 6G Efflux for the Detection of CDR1-Overexpressing Azole-Resistant *Candida Albicans* Strains." *The Journal of Antimicrobial Chemotherapy* 44 (1): 27–31. <https://doi.org/10.1093/jac/44.1.27>.

Maier, Olaf, Volker Oberle, and Dick Hoekstra. 2002. "Fluorescent Lipid Probes: Some Properties and Applications (a Review)." *Chemistry and Physics of Lipids* 116 (1–2): 3–18.

Manente, Myriam, and Michel Ghislain. 2009. "The Lipid-Translocating Exporter Family and Membrane Phospholipid Homeostasis in Yeast." *FEMS Yeast Research* 9 (5): 673–687.

Mark, Vincent A. van der, Ronald P. J. Oude Elferink, and Coen C. Paulusma. 2013. "P4 ATPases: Flippases in Health and Disease." *International Journal of Molecular Sciences* 14 (4): 7897–7922. <https://doi.org/10.3390/ijms14047897>.

Maubon, Danièle, Cécile Garnaud, Thierry Calandra, Dominique Sanglard, and Muriel Cornet. 2014. “Resistance of *Candida* Spp. to Antifungal Drugs in the ICU: Where Are We Now?” *Intensive Care Medicine* 40 (9): 1241–1255.

McConnell, Harden M., and Roger D. Kornberg. 1971. “Inside-Outside Transitions of Phospholipids in Vesicle Membranes.” *Biochemistry* 10 (7): 1111–1120.

McIntyre, Jonathan C., and Richard G. Sleight. 1991. “Fluorescence Assay for Phospholipid Membrane Asymmetry.” *Biochemistry* 30 (51): 11819–11827.

Meer, Gerrit van. 2005. “Cellular Lipidomics.” *The EMBO Journal* 24 (18): 3159–65. <https://doi.org/10.1038/sj.emboj.7600798>.

Mermel, Leonard A., Michael Allon, Emilio Bouza, Donald E. Craven, Patricia Flynn, Naomi P. O’Grady, Issam I. Raad, Bart J. A. Rijnders, Robert J. Sherertz, and David K. Warren. 2009. “Clinical Practice Guidelines for the Diagnosis and Management of Intravascular Catheter-Related Infection: 2009 Update by the Infectious Diseases Society of America.” *Clinical Infectious Diseases: An Official Publication of the Infectious Diseases Society of America* 49 (1): 1–45. <https://doi.org/10.1086/599376>.

Mesa-Arango, Ana Cecilia, Liliana Scorzoni, and Oscar Zaragoza. 2012. “It Only Takes One to Do Many Jobs: Amphotericin B as Antifungal and Immunomodulatory Drug.” *Frontiers in Microbiology* 3: 286.

Middelkoop, Esther, Bertram H. Lubin, Jos AF Op den Kamp, and Ben Roelofsen. 1986. “Flip-Flop Rates of Individual Molecular Species of Phosphatidylcholine in the Human Red Cell Membrane.” *Biochimica et Biophysica Acta (BBA)-Biomembranes* 855 (3): 421–424.

Mora, Camilo, Derek P. Tittensor, Sina Adl, Alastair G. B. Simpson, and Boris Worm. 2011. “How Many Species Are There on Earth and in the Ocean?” Edited by Georgina M. Mace. *PLoS Biology* 9 (8): e1001127. <https://doi.org/10.1371/journal.pbio.1001127>.

Mukherjee, Pranab K., Jyotsna Chandra, Duncan M. Kuhn, and Mahmoud A. Ghannoum. 2003. “Mechanism of Fluconazole Resistance in *Candida Albicans* Biofilms: Phase-Specific Role of Efflux Pumps and Membrane Sterols.” *Infection and Immunity* 71 (8): 4333–40. <https://doi.org/10.1128/IAI.71.8.4333-4340.2003>.

Muller, Guilherme Gubert, Newton Kara-Jose, and Rosane Silvestre De Castro. 2013. "Antifungals in Eye Infections: Drugs and Routes of Administration." *Revista Brasileira de Oftalmologia*.

Muller, Peter, Thomas Pomorski, and Andreas Herrmann. 1994. "Incorporation of Phospholipid Analogs into the Plasma Membrane Affects ATP-Induced Vesiculation of Human Erythrocyte Ghosts." *Biochemical and Biophysical Research Communications* 199 (2): 881–887.

Murate, Motohide, Mitsuhiro Abe, Kohji Kasahara, Kazuhisa Iwabuchi, Masato Umeda, and Toshihide Kobayashi. 2015. "Transbilayer Distribution of Lipids at Nano Scale." *J Cell Sci* 128 (8): 1627–1638.

Murciano, Celia, David L. Moyes, Manohursingh Runglall, Priscila Tobouti, Ayesha Islam, Lois L. Hoyer, and Julian R. Naglik. 2012. "Evaluation of the Role of Candida Albicans Agglutinin-Like Sequence (Als) Proteins in Human Oral Epithelial Cell Interactions." *PLOS ONE* 7 (3): e33362. <https://doi.org/10.1371/journal.pone.0033362>.

Naglik, Julian R., David L. Moyes, Betty Wächtler, and Bernhard Hube. 2011. "Candida Albicans Interactions with Epithelial Cells and Mucosal Immunity." *Microbes and Infection* 13 (12–13): 963–76. <https://doi.org/10.1016/j.micinf.2011.06.009>.

Nakamura, Kenjiro, Masakazu Niimi, Kyoko Niimi, Ann R. Holmes, Jenine E. Yates, Anabelle Decottignies, Brian C. Monk, Andre Goffeau, and Richard D. Cannon. 2001. "Functional Expression of Candida Albicans Drug Efflux Pump Cdr1p in a Saccharomyces Cerevisiae Strain Deficient in Membrane Transporters." *Antimicrobial Agents and Chemotherapy* 45 (12): 3366–3374.

Natarajan, Paramasivam, Jiyi Wang, Zhaolin Hua, and Todd R. Graham. 2004. "Drs2p-Coupled Aminophospholipid Translocase Activity in Yeast Golgi Membranes and Relationship to in Vivo Function." *Proceedings of the National Academy of Sciences* 101 (29): 10614–10619.

Nichols, J. Wylie. 2002. "Internalization and Trafficking of Fluorescent-Labeled Phospholipids in Yeast." In *Seminars in Cell & Developmental Biology*, 13:179–184. Elsevier.

Nobile, Clarissa J., Emily P. Fox, Jeniel E. Nett, Trevor R. Sorrells, Quinn M. Mitrovich, Aaron D. Hernday, Brian B. Tuch, David R. Andes, and Alexander D. Johnson. 2012. "A Recently Evolved Transcriptional Network Controls Biofilm Development in Candida Albicans." *Cell* 148 (1–2): 126–38. <https://doi.org/10.1016/j.cell.2011.10.048>.

Nobile, Clarissa J., and Alexander D. Johnson. 2015. "Candida Albicans Biofilms and Human Disease." *Annual Review of Microbiology* 69: 71–92.

Nobile, Clarissa J., Jeniel E. Nett, Aaron D. Hernday, Oliver R. Homann, Jean-Sebastien Deneault, Andre Nantel, David R. Andes, Alexander D. Johnson, and Aaron P. Mitchell. 2009. "Biofilm Matrix Regulation by Candida Albicans Zap1." *PLoS Biology* 7 (6): e1000133. <https://doi.org/10.1371/journal.pbio.1000133>.

Nobile, Clarissa J., Heather A. Schneider, Jeniel E. Nett, Donald C. Sheppard, Scott G. Filler, David R. Andes, and Aaron P. Mitchell. 2008. "Complementary Adhesin Function in C. Albicans Biofilm Formation." *Current Biology: CB* 18 (14): 1017–24. <https://doi.org/10.1016/j.cub.2008.06.034>.

Noji, Takehiro, Takaharu Yamamoto, Koji Saito, Konomi Fujimura-Kamada, Satoshi Kondo, and Kazuma Tanaka. 2006. "Mutational Analysis of the Lem3p-Dnf1p Putative Phospholipid-Translocating P-Type ATPase Reveals Novel Regulatory Roles for Lem3p and a Carboxyl-Terminal Region of Dnf1p Independent of the Phospholipid-Translocating Activity of Dnf1p in Yeast." *Biochemical and Biophysical Research Communications* 344 (1): 323–331.

Odds, F. C. 1988. "Candida and Candidosis: A Review and Bibliography. 2nd Edition." *Candida and Candidosis: A Review and Bibliography. 2nd Edition*. <https://www.cabdirect.org/cabdirect/abstract/19892057780>.

O'Meara, Teresa R., Stephanie M. Holmer, Kyla Selvig, Fred Dietrich, and J. Andrew Alspaugh. 2013. "Cryptococcus Neoformans Rim101 Is Associated with Cell Wall Remodeling and Evasion of the Host Immune Responses." *MBio* 4 (1): e00522–12.

Ono, Yusuke, Ryouichi Fukuda, and Akinori Ohta. 2009. "Involvement of LEM3/ROS3 in the Uptake of Phosphatidylcholine with Short Acyl Chains in Saccharomyces Cerevisiae." *Bioscience, Biotechnology, and Biochemistry* 73 (3): 750–752.

Ozkan, Semiha, Fatma Kaynak, Ayse Kalkanci, Ufuk Abbasoglu, and Semra Kustimur. 2005. "Slime Production and Proteinase Activity of Candida Species Isolated from Blood Samples and the Comparison of These Activities with Minimum Inhibitory Concentration Values of Antifungal Agents." *Memórias Do Instituto Oswaldo Cruz* 100 (3): 319–324.

Palmgren, M. G., and K. B. Axelsen. 1998. "Evolution of P-Type ATPases." *Biochimica Et Biophysica Acta* 1365 (1–2): 37–45. [https://doi.org/10.1016/s0005-2728\(98\)00041-3](https://doi.org/10.1016/s0005-2728(98)00041-3).

Palmgren, Michael G., and Poul Nissen. 2011. "P-Type ATPases." *Annual Review of Biophysics* 40: 243–66. <https://doi.org/10.1146/annurev.biophys.093008.131331>.

Panatala, Radhakrishnan, Hanka Hennrich, and Joost CM Holthuis. 2015. "Inner Workings and Biological Impact of Phospholipid Flippases." *J Cell Sci* 128 (11): 2021–2032.

Pappas, Peter G., Carol A. Kauffman, David Andes, Daniel K. Benjamin, Thierry F. Calandra, John E. Edwards, Scott G. Filler, et al. 2009. "Clinical Practice Guidelines for the Management of Candidiasis: 2009 Update by the Infectious Diseases Society of America." *Clinical Infectious Diseases* 48 (5): 503–35.

Paramythiotou, Elisabeth, Frantzeska Frantzeskaki, Aikaterini Flevari, Apostolos Armaganidis, and George Dimopoulos. 2014. "Invasive Fungal Infections in the ICU: How to Approach, How to Treat." *Molecules* 19 (1): 1085–1119.

Park, Hyunsook, Carter L. Myers, Donald C. Sheppard, Quynh T. Phan, Angela A. Sanchez, John E. Edwards, and Scott G. Filler. 2005. "Role of the Fungal Ras-Protein Kinase A Pathway in Governing Epithelial Cell Interactions during Oropharyngeal Candidiasis." *Cellular Microbiology* 7 (4): 499–510. <https://doi.org/10.1111/j.1462-5822.2004.00476.x>.

Peman, Javier, Emilia Canton, and Ana Espinel-Ingroff. 2009. "Antifungal Drug Resistance Mechanisms." *Expert Review of Anti-Infective Therapy* 7 (4): 453–460.

Pfaller, M. A., and D. J. Diekema. 2007. "Epidemiology of Invasive Candidiasis: A Persistent Public Health Problem." *Clinical Microbiology Reviews* 20 (1): 133–63. <https://doi.org/10.1128/CMR.00029-06>.

Pfaller, Michael A., and Daniel J. Diekema. 2010. "Epidemiology of Invasive Mycoses in North America." *Critical Reviews in Microbiology* 36 (1): 1–53. <https://doi.org/10.3109/10408410903241444>.

Pfaller, Michael A., Ronald N Jones, Shawn A Messer, Michael B Edmond, and Richard P Wenzel. 1998. "National Surveillance of Nosocomial Blood Stream Infection Due to Species of *Candida* Other than *Candida Albicans*: Frequency of Occurrence and Antifungal Susceptibility in the SCOPE Program." *Diagnostic Microbiology and Infectious Disease* 30 (2): 121–29. [https://doi.org/10.1016/S0732-8893\(97\)00192-2](https://doi.org/10.1016/S0732-8893(97)00192-2).

Phan, Quynh T., Rutillio A. Fratti, Nemani V. Prasadarao, John E. Edwards, and Scott G. Filler. 2005. "N-Cadherin Mediates Endocytosis of *Candida Albicans* by Endothelial Cells."

The Journal of Biological Chemistry 280 (11): 10455–61.
<https://doi.org/10.1074/jbc.M412592200>.

Phan, Quynh T., Carter L. Myers, Yue Fu, Donald C. Sheppard, Michael R. Yeaman, William H. Welch, Ashraf S. Ibrahim, John E. Edwards Jr, and Scott G. Filler. 2007. “Als3 Is a *Candida Albicans* Invasin That Binds to Cadherins and Induces Endocytosis by Host Cells.” *PLoS Biology* 5 (3): e64.

Pomorski, Thomas Günther, and Anant K. Menon. 2016. “Lipid Somersaults: Uncovering the Mechanisms of Protein-Mediated Lipid Flipping.” *Progress in Lipid Research* 64: 69–84.

Pomorski, Thomas, Sigrún Hrafnisdóttir, Philippe F. Devaux, and Gerrit van Meer. 2001. “Lipid Distribution and Transport across Cellular Membranes.” In *Seminars in Cell & Developmental Biology*, 12:139–148. Elsevier.

Pomorski, Thomas, Ruben Lombardi, Howard Riezman, Philippe F. Devaux, Gerrit van Meer, and Joost CM Holthuis. 2003. “Drs2p-Related P-Type ATPases Dnf1p and Dnf2p Are Required for Phospholipid Translocation across the Yeast Plasma Membrane and Serve a Role in Endocytosis.” *Molecular Biology of the Cell* 14 (3): 1240–1254.

Popescu, Narcis I., Cristina Lupu, and Florea Lupu. 2010. “Extracellular Protein Disulfide Isomerase Regulates Coagulation on Endothelial Cells through Modulation of Phosphatidylserine Exposure.” *Blood* 116 (6): 993–1001. <https://doi.org/10.1182/blood-2009-10-249607>.

Poulsen, L. R., R. L. López-Marqués, and M. G. Palmgren. 2008. “Flippases: Still More Questions than Answers.” *Cellular and Molecular Life Sciences: CMLS* 65 (20): 3119–25. <https://doi.org/10.1007/s00018-008-8341-6>.

Prasad, Rajendra, and Andre Goffeau. 2012. “Yeast ATP-Binding Cassette Transporters Conferring Multidrug Resistance.” *Annual Review of Microbiology* 66: 39–63.

Prasad, Rajendra, and Sneha Lata Panwar. 2002. “Drug Resistance in Yeasts—an Emerging Scenario.”

Puts, Cathelene F., Guillaume Lenoir, Jeroen Krijgsveld, Patrick Williamson, and Joost CM Holthuis. 2009. “A P4-ATPase Protein Interaction Network Reveals a Link between Aminophospholipid Transport and Phosphoinositide Metabolism.” *Journal of Proteome Research* 9 (2): 833–842.

Puts, Catheleyne F., Radhakrishnan Panatala, Hanka Hennrich, Alina Tsareva, Patrick Williamson, and Joost CM Holthuis. 2012. "Mapping Functional Interactions in a Heterodimeric Phospholipid Pump." *Journal of Biological Chemistry* 287 (36): 30529–30540.

Rella, Antonella, Amir M. Farnoud, and Maurizio Del Poeta. 2016. "Plasma Membrane Lipids and Their Role in Fungal Virulence." *Progress in Lipid Research* 61: 63–72.

Reuß, Oliver, Aashild Vik, Roberto Kolter, and Joachim Morschhäuser. 2004. "The SAT1 Flipper, an Optimized Tool for Gene Disruption in *Candida Albicans*." *Gene* 341: 119–127.

Riekhof, Wayne R., and Dennis R. Voelker. 2006. "Uptake and Utilization of Lyso-Phosphatidylethanolamine by *Saccharomyces Cerevisiae*." *Journal of Biological Chemistry* 281 (48): 36588–36596.

Riekhof, Wayne R., James Wu, Miguel A. Gijón, Simona Zarini, Robert C. Murphy, and Dennis R. Voelker. 2007. "Lysophosphatidylcholine Metabolism In *Saccharomyces Cerevisiae* The Role Of P-Type ATPases In Transport And A Broad Specificity Acyltransferase In Acylation." *Journal of Biological Chemistry* 282 (51): 36853–36861.

Rizzo, Juliana, Ana C. Colombo, Daniel Zamith-Miranda, Vanessa KA Silva, Jeremy C. Allegood, Arturo Casadevall, Maurizio Del Poeta, Joshua D. Nosanchuk, James W. Kronstad, and Marcio L. Rodrigues. 2018. "The Putative Flippase Apt1 Is Required for Intracellular Membrane Architecture and Biosynthesis of Polysaccharide and Lipids in *Cryptococcus Neoformans*." *Biochimica et Biophysica Acta (BBA)-Molecular Cell Research* 1865 (3): 532–541.

Rizzo, Juliana, Débora L. Oliveira, Luna S. Joffe, Guanggan Hu, Felipe Gazos-Lopes, Fernanda L. Fonseca, Igor C. Almeida, Susana Frases, James W. Kronstad, and Marcio L. Rodrigues. 2014. "Role of the Apt1 Protein in Polysaccharide Secretion by *Cryptococcus Neoformans*." *Eukaryotic Cell* 13 (6): 715–726.

Rizzo, Juliana, Lyubomir Dimitrov Stanchev, Vanessa KA da Silva, Leonardo Nimrichter, Thomas Günther Pomorski, and Marcio L. Rodrigues. 2019. "Role of Lipid Transporters in Fungal Physiology and Pathogenicity." *Computational and Structural Biotechnology Journal*.

Robbins, Nicole, Priya Uppuluri, Jeniel Nett, Ranjith Rajendran, Gordon Ramage, Jose L. Lopez-Ribot, David Andes, and Leah E. Cowen. 2011. "Hsp90 Governs Dispersion and Drug Resistance of Fungal Biofilms." *PLoS Pathogens* 7 (9): e1002257. <https://doi.org/10.1371/journal.ppat.1002257>.

Roland, Bartholomew P., Tomoki Naito, Jordan T. Best, Cayetana Arnaiz-Yépez, Hiroyuki Takatsu, J. Yu Roger, Hye-Won Shin, and Todd R. Graham. 2019. “Yeast and Human P4-ATPases Transport Glycosphingolipids Using Conserved Structural Motifs.” *Journal of Biological Chemistry* 294 (6): 1794–1806.

Saito, Koji, Konomi Fujimura-Kamada, Nobumichi Furuta, Utako Kato, Masato Umeda, and Kazuma Tanaka. 2004. “Cdc50p, a Protein Required for Polarized Growth, Associates with the Drs2p P-Type ATPase Implicated in Phospholipid Translocation in *Saccharomyces Cerevisiae*.” *Molecular Biology of the Cell* 15 (7): 3418–3432.

Sambrook, Joseph, and David W. Russell. 2006. “Purification of Nucleic Acids by Extraction with Phenol: Chloroform.” *Cold Spring Harbor Protocols* 2006 (1): pdb–prot4455.

Sampaio, Julio L., Mathias J. Gerl, Christian Klose, Christer S. Ejsing, Hartmut Beug, Kai Simons, and Andrej Shevchenko. 2011. “Membrane Lipidome of an Epithelial Cell Line.” *Proceedings of the National Academy of Sciences of the United States of America* 108 (5): 1903–7. <https://doi.org/10.1073/pnas.1019267108>.

Sanguinetti, Maurizio, Brunella Posteraro, and Cornelia Lass-Flörl. 2015. “Antifungal Drug Resistance among *Candida* Species: Mechanisms and Clinical Impact.” *Mycoses* 58: 2–13.

Sardi, J. C. O., L. Scorzoni, T. Bernardi, A. M. Fusco-Almeida, and MJS Mendes Giannini. 2013. “*Candida* Species: Current Epidemiology, Pathogenicity, Biofilm Formation, Natural Antifungal Products and New Therapeutic Options.” *Journal of Medical Microbiology* 62 (1): 10–24.

Schmittgen, Thomas D., and Kenneth J. Livak. 2008. “Analyzing Real-Time PCR Data by the Comparative C T Method.” *Nature Protocols* 3 (6): 1101.

Schultzhaus, Z., G. A. Cunningham, R. R. Mouriño-Pérez, and B. D. Shaw. 2019. “The Phospholipid Flippase DnfD Localizes to Late Golgi and Is Involved in Asexual Differentiation in *Aspergillus Nidulans*.” *Mycologia* 111 (1): 13–25.

Schultzhaus, Zachary, Huijuan Yan, and Brian D. Shaw. 2015. “A *Aspergillus Nidulans* Flippase DnfA Is Cargo of the Endocytic Collar and Plays Complementary Roles in Growth and Phosphatidylserine Asymmetry with Another Flippase, DnfB.” *Molecular Microbiology* 97 (1): 18–32.

Schultzhaus, Zachary, Wenhui Zheng, Zonghua Wang, Rosa Mouriño-Pérez, and Brian Shaw. 2017. "Phospholipid Flippases DnfA and DnfB Exhibit Differential Dynamics within the A. Nidulans Spitzenkörper." *Fungal Genetics and Biology* 99: 26–28.

Seddiki, Sidi Mohammed Lahbib, Zahia Boucherit-Otmani, Kebir Boucherit, Souad Bads-Amir, Mourad Taleb, and Dennis Kunkel. 2013. "Assessment of the Types of Catheter Infectivity Caused by Candida Species and Their Biofilm Formation. First Study in an Intensive Care Unit in Algeria." *International Journal of General Medicine* 6: 1.

Seifert, Karin, Michael Duchêne, Walther H. Wernsdorfer, Herwig Kollaritsch, Otto Scheiner, Gerhard Wiedermann, Thomas Hottkowitz, and Hansjörg Eibl. 2001. "Effects of Miltefosine and Other Alkylphosphocholines on Human Intestinal Parasite *Entamoeba Histolytica*." *Antimicrobial Agents and Chemotherapy* 45 (5): 1505–10. <https://doi.org/10.1128/AAC.45.5.1505-1510.2001>.

Seigneuret, Michel, and Philippe F. Devaux. 1984. "ATP-Dependent Asymmetric Distribution of Spin-Labeled Phospholipids in the Erythrocyte Membrane: Relation to Shape Changes." *Proceedings of the National Academy of Sciences* 81 (12): 3751–3755.

Seyedmousavi, S., M. S. Lionakis, M. Parta, S. W. Peterson, and K. J. Kwon-Chung. 2018. "Emerging *Aspergillus* Species Almost Exclusively Associated with Primary Immunodeficiencies." In *Open Forum Infectious Diseases*, 5:ofy213. Oxford University Press US.

Sheppard, Donald C., Michael R. Yeaman, William H. Welch, Quynh T. Phan, Yue Fu, Ashraf S. Ibrahim, Scott G. Filler, Mason Zhang, Alan J. Waring, and John E. Edwards. 2004. "Functional and Structural Diversity in the Als Protein Family of *Candida Albicans*." *Journal of Biological Chemistry* 279 (29): 30480–30489.

Sleight, Richard G., and Richard E. Pagano. 1985. "Transbilayer Movement of a Fluorescent Phosphatidylethanolamine Analogue across the Plasma Membranes of Cultured Mammalian Cells." *Journal of Biological Chemistry* 260 (2): 1146–1154.

Smeets, Edgar F., Paul Comfurius, Edouard M. Bevers, and Robert FA Zwaal. 1994. "Calcium-Induced Transbilayer Scrambling of Fluorescent Phospholipid Analogs in Platelets and Erythrocytes." *Biochimica et Biophysica Acta (BBA)-Biomembranes* 1195 (2): 281–286.

Sobel, J. D. 1997. "Vaginitis." *The New England Journal of Medicine* 337 (26): 1896–1903. <https://doi.org/10.1056/NEJM199712253372607>.

Soll, David R. 2009. "Why Does *Candida Albicans* Switch?" *FEMS Yeast Research* 9 (7): 973–89. <https://doi.org/10.1111/j.1567-1364.2009.00562.x>.

Sonneborn, Anja, Dirk P. Bockmühl, and Joachim F. Ernst. 1999. "Chlamyospore Formation in *Candida Albicans* Requires the Efg1p Morphogenetic Regulator." *Infection and Immunity* 67 (10): 5514–5517.

Spampinato, Claudia, and Darío Leonardi. 2013. "Candida Infections, Causes, Targets, and Resistance Mechanisms: Traditional and Alternative Antifungal Agents." *BioMed Research International* 2013.

Srikantha, Thyagarajan, Luong K. Tsai, Karla Daniels, and David R. Soll. 2000. "EFG1 Null Mutants of *Candida Albicans* Switch but Cannot Express the Complete Phenotype of White-Phase Budding Cells." *Journal of Bacteriology* 182 (6): 1580–1591.

Srivastava, Archita, Shabnam Sircaik, Farha Husain, Edwina Thomas, Shivani Ror, Sumit Rastogi, Darakshan Alim, Priyanka Bapat, David R. Andes, and Clarissa J. Nobile. 2017. "Distinct Roles of the 7-Transmembrane Receptor Protein R Ta3 in Regulating the Asymmetric Distribution of Phosphatidylcholine across the Plasma Membrane and Biofilm Formation in *Candida Albicans*." *Cellular Microbiology* 19 (12): e12767.

Staab, J. F., S. D. Bradway, P. L. Fidel, and P. Sundstrom. 1999. "Adhesive and Mammalian Transglutaminase Substrate Properties of *Candida Albicans* Hwp1." *Science (New York, N.Y.)* 283 (5407): 1535–38. <https://doi.org/10.1126/science.283.5407.1535>.

Staib, Peter, and Joachim Morschhäuser. 2007. "Chlamyospore Formation in *Candida Albicans* and *Candida Dubliniensis*--an Enigmatic Developmental Programme." *Mycoses* 50 (1): 1–12. <https://doi.org/10.1111/j.1439-0507.2006.01308.x>.

Stevens, Haley C., Lynn Malone, and J. Wylie Nichols. 2008. "The Putative Aminophospholipid Translocases, DNF1 and DNF2, Are Not Required for 7-Nitrobenz-2-Oxa-1, 3-Diazol-4-Yl-Phosphatidylserine Flip across the Plasma Membrane of *Saccharomyces Cerevisiae*." *Journal of Biological Chemistry* 283 (50): 35060–35069.

Stoldt, Volker R., Anja Sonneborn, Christoph E. Leuker, and Joachim F. Ernst. 1997. "Efg1p, an Essential Regulator of Morphogenesis of the Human Pathogen *Candida Albicans*, Is a Member of a Conserved Class of BHLH Proteins Regulating Morphogenetic Processes in Fungi." *The EMBO Journal* 16 (8): 1982–91. <https://doi.org/10.1093/emboj/16.8.1982>.

Sudbery, Peter E. 2011. "Growth of *Candida Albicans* Hyphae." *Nature Reviews. Microbiology* 9 (10): 737–48. <https://doi.org/10.1038/nrmicro2636>.

Sudbery, Peter, Neil Gow, and Judith Berman. 2004. "The Distinct Morphogenic States of *Candida Albicans*." *Trends in Microbiology* 12 (7): 317–24. <https://doi.org/10.1016/j.tim.2004.05.008>.

Sun, Jianing N., Norma V. Solis, Quynh T. Phan, Jashanjot S. Bajwa, Helena Kashleva, Angela Thompson, Yaoping Liu, Anna Dongari-Bagtzoglou, Mira Edgerton, and Scott G. Filler. 2010. "Host Cell Invasion and Virulence Mediated by *Candida Albicans* Ssa1." *PLoS Pathogens* 6 (11): e1001181. <https://doi.org/10.1371/journal.ppat.1001181>.

Sundstrom, Paula, Jim E. Cutler, and Janet F. Staab. 2002. "Reevaluation of the Role of HWP1 in Systemic Candidiasis by Use of *Candida Albicans* Strains with Selectable Marker URA3 Targeted to the ENO1 Locus." *Infection and Immunity* 70 (6): 3281–83. <https://doi.org/10.1128/iai.70.6.3281-3283.2002>.

Taff, Heather T., Jeniel E. Nett, Robert Zarnowski, Kelly M. Ross, Hiram Sanchez, Mike T. Cain, Jessica Hamaker, Aaron P. Mitchell, and David R. Andes. 2012. "A *Candida* Biofilm-Induced Pathway for Matrix Glucan Delivery: Implications for Drug Resistance." *PLoS Pathogens* 8 (8): e1002848. <https://doi.org/10.1371/journal.ppat.1002848>.

Takada, Naoto, Tomoki Naito, Takanari Inoue, Kazuhisa Nakayama, Hiroyuki Takatsu, and Hye-Won Shin. 2018. "Phospholipid-flipping Activity of P4-ATPase Drives Membrane Curvature." *The EMBO Journal* 37 (9). <https://doi.org/10.15252/emboj.201797705>.

Takar, Mehmet, Yuantai Wu, and Todd R. Graham. 2016. "The Essential Neol Protein from Budding Yeast Plays a Role in Establishing Aminophospholipid Asymmetry of the Plasma Membrane." *Journal of Biological Chemistry* 291 (30): 15727–15739.

Takatsu, Hiroyuki, Keiko Baba, Takahiro Shima, Hiroyuki Umino, Utako Kato, Masato Umeda, Kazuhisa Nakayama, and Hye-Won Shin. 2011. "ATP9B, a P4-ATPase (a Putative Aminophospholipid Translocase), Localizes to the Trans-Golgi Network in a CDC50 Protein-Independent Manner." *Journal of Biological Chemistry* 286 (44): 38159–38167.

Tamaki, Hisanori, Atsushi Shimada, Yoshihiro Ito, Mihoko Ohya, Juri Takase, Masahiro Miyashita, Hisashi Miyagawa, Hiroyuki Nozaki, Reiko Nakayama, and Hidehiko Kumagai. 2007. "LPT1 Encodes a Membrane-Bound O-Acyltransferase Involved in the Acylation of Lysophospholipids in the Yeast *Saccharomyces Cerevisiae*." *Journal of Biological Chemistry* 282 (47): 34288–34298.

Tanaka, Kazuma, Konomi Fujimura-Kamada, and Takaharu Yamamoto. 2010. “Functions of Phospholipid Flippases.” *The Journal of Biochemistry* 149 (2): 131–143.

Tilley, Leann, Sophie Cribier, Ben Roelofsen, Jos A. F. Op den Kamp, and Laurens L. M. van Deenen. 1986. “ATP-Dependent Translocation of Amino Phospholipids across the Human Erythrocyte Membrane.” *FEBS Letters* 194 (1): 21–27. [https://doi.org/10.1016/0014-5793\(86\)80044-8](https://doi.org/10.1016/0014-5793(86)80044-8).

Toda, Mitsuru, Sabrina R. Williams, Elizabeth L. Berkow, Monica M. Farley, Lee H. Harrison, Lindsay Bonner, Kaytlynn M. Marceaux, Rosemary Hollick, Alexia Y. Zhang, and William Schaffner. 2019. “Population-Based Active Surveillance for Culture-Confirmed Candidemia—Four Sites, United States, 2012–2016.” *MMWR Surveillance Summaries* 68 (8): 1.

Tsai, Pei-Chin, Jia-Wei Hsu, Ya-Wen Liu, Kuan-Yu Chen, and Fang-Jen S. Lee. 2013. “Arl1p Regulates Spatial Membrane Organization at the Trans-Golgi Network through Interaction with Arf-GEF Gea2p and Flippase Drs2p.” *Proceedings of the National Academy of Sciences* 110 (8): E668–E677.

Van Meer, Gerrit, Dennis R. Voelker, and Gerald W. Feigenson. 2008. “Membrane Lipids: Where They Are and How They Behave.” *Nature Reviews Molecular Cell Biology* 9 (2): 112.

Vila, Taissa Vieira Machado, Ashok K. Chaturvedi, Sonia Rozental, and Jose L. Lopez-Ribot. 2015. “In Vitro Activity of Miltefosine against *Candida Albicans* under Planktonic and Biofilm Growth Conditions and In Vivo Efficacy in a Murine Model of Oral Candidiasis.” *Antimicrobial Agents and Chemotherapy* 59 (12): 7611–20. <https://doi.org/10.1128/AAC.01890-15>.

Wächtler, Betty, Duncan Wilson, Katja Haedicke, Frederic Dalle, and Bernhard Hube. 2011. “From Attachment to Damage: Defined Genes of *Candida Albicans* Mediate Adhesion, Invasion and Damage during Interaction with Oral Epithelial Cells.” *PLoS One* 6 (2): e17046. <https://doi.org/10.1371/journal.pone.0017046>.

Weng, Jian, Nathan L. Mata, Sassan M. Azarian, Radouil T. Tzekov, David G. Birch, and Gabriel H. Travis. 1999. “Insights into the Function of Rim Protein in Photoreceptors and Etiology of Stargardt’s Disease from the Phenotype in Abcr Knockout Mice.” *Cell* 98 (1): 13–23.

Wicky, Sidonie, Heinz Schwarz, and Birgit Singer-Krüger. 2004. “Molecular Interactions of Yeast Neolp, an Essential Member of the Drs2 Family of Aminophospholipid Translocases,

and Its Role in Membrane Trafficking within the Endomembrane System.” *Molecular and Cellular Biology* 24 (17): 7402–7418.

Williamson, Patrick, Edouard M. Bevers, Edgar F. Smeets, Paul Comfurius, Robert A. Schlegel, and Robert FA Zwaal. 1995. “Continuous Analysis of the Mechanism of Activated Transbilayer Lipid Movement in Platelets.” *Biochemistry* 34 (33): 10448–10455.

Xie, Zhihong, Angela Thompson, Takanori Sobue, Helena Kashleva, Hongbin Xu, John Vasilakos, and Anna Dongari-Bagtzoglou. 2012. “Candida Albicans Biofilms Do Not Trigger Reactive Oxygen Species and Evade Neutrophil Killing.” *The Journal of Infectious Diseases* 206 (12): 1936–45. <https://doi.org/10.1093/infdis/jis607>.

Xu, Dayong, Xing Zhang, Biao Zhang, Xin Zeng, Hongchen Mao, Haitao Xu, Linghuo Jiang, and Feng Li. 2019. “The Lipid Flippase Subunit Cdc50 Is Required for Antifungal Drug Resistance, Endocytosis, Hyphal Development and Virulence in Candida Albicans.” *FEMS Yeast Research* 19 (3): foz033.

Zachowski, Alain. 1993. “Phospholipids in Animal Eukaryotic Membranes: Transverse Asymmetry and Movement.” *Biochemical Journal* 294 (Pt 1): 1.

Zakikhany, Katherina, Julian R. Naglik, Andrea Schmidt-Westhausen, Gudrun Holland, Martin Schaller, and Bernhard Hube. 2007. “In Vivo Transcript Profiling of Candida Albicans Identifies a Gene Essential for Interepithelial Dissemination.” *Cellular Microbiology* 9 (12): 2938–54. <https://doi.org/10.1111/j.1462-5822.2007.01009.x>.

Zhou, Xiaoming, and Todd R. Graham. 2009. “Reconstitution of Phospholipid Translocase Activity with Purified Drs2p, a Type-IV P-Type ATPase from Budding Yeast.” *Proceedings of the National Academy of Sciences* 106 (39): 16586–16591.

Zhou, Zhimin, Kimberly A. White, Alessandra Polissi, Costa Georgopoulos, and Christian RH Raetz. 1998. “Function of Escherichia Coli MsbA, an Essential ABC Family Transporter, in Lipid A and Phospholipid Biosynthesis.” *Journal of Biological Chemistry* 273 (20): 12466–12475.

Zhu, Weidong, and Scott G. Filler. 2010. “Interactions of Candida Albicans with Epithelial Cells.” *Cellular Microbiology* 12 (3): 273–82. <https://doi.org/10.1111/j.1462-5822.2009.01412.x>.

Zordan, Rebecca, and Brendan Cormack. 2012. "Adhesins in Opportunistic Fungal Pathogens." In *Candida and Candidiasis, Second Edition*, 243–259. American Society of Microbiology.

6.0 APPENDICES

1. Phosphate-Buffer Saline (PBS)

Components	Amount
NaCl	137 mM
KCl	2.7 mM
Na ₂ HPO ₄	10 mM
KH ₂ PO ₄	2 mM

8 g of NaCl, 0.2 g of KCl, 1.44 g of Na₂HPO₄ and 0.24 g of KH₂PO₄ was dissolved in 800 ml of distilled water. pH was adjusted to 7.4 with the help of HCl. The resulting solution was autoclaved for 20 min. The buffer was stored at room temperature.

2. Tris Acetic Acid Electrophoresis (TAE) buffer

Components	Amount of 50X stock
Tris-base	242 g
Glacial acetic acid	57.1 ml of glacial acetic acid
EDTA	100 ml of 0.5 M EDTA (pH 8.0)

The above components were mixed for a 50X stock solution and autoclaved for 20 min. The autoclaved stock was stored at room temperature.

3. Ethidium Bromide stock (10 mg/ml)

0.1g of ethidium bromide was dissolved in 10 ml of water. The falcon was wrapped in aluminum foil and stored at room temperature.

4. 0.5M EDTA (pH 8.0)

Component	Quantity
Disodium ethylenediaminetetraacetate·2H ₂ O	186.1 g
ddH ₂ O	800 ml

Adjusted the pH to 8.0 with NaOH (~20 g of NaOH pellets). Aliquot and sterilized by autoclaving.

Comment - The disodium salt of EDTA would not go into solution until the pH of the solution was adjusted to approximately 8.0 by the addition of NaOH.

5. 1% Agarose for DNA gel electrophoresis

Components	Volume for 50 ml
1% Agarose	0.5 g
1X TAE	50 ml

6. FA (10X) for RNA gel electrophoresis buffer

Components	Volume for 1 litre
200mM MOPS	200 ml
50 mM NaAcetate	12.5 ml
10 mM EDTA	20 ml

Make up volume to 1 litre with RNAase treated ddH₂O. Dilution to 1X FA buffer: add 20 ml 37% formaldehyde after cooling.

7. Alkaline Lysis Solution I for mini preparation of plasmid DNA

Component	Quantity
Glucose	50 mM
Tris-Cl (pH 8.0)	5 mM
EDTA (pH 8.0)	10 mM

Prepared Solution I from standard stocks in batches of approx. 100 ml, autoclaved for 15 min at 15 psi (1.05 kg/cm²) on liquid cycle, and stored at 4 °C.

8. Alkaline Lysis Solution II

Component	Quantity
NaOH	0.2 N NaOH (freshly diluted from a 5 N stock)
SDS	1% (W/V)

Prepared Solution II fresh and used at room temperature.

9. Alkaline Lysis Solution III

Component	Quantity
Potassium acetate	5 M, 60.0 ml
Glacial acetic acid	11.5 ml
H ₂ O	28.5 ml

Stored the solution at 4°C and transferred it to an ice bucket just before use.

10. Yeast Lysis Buffer (TENTS Buffer)

Components	Volume for 100 ml
1 M Tris (pH 7.5)	1 ml
0.5 M EDTA (pH 8.0)	200 μ l
5 M NaCl	2 ml
Triton X-100	2 ml
10% SDS	10 ml
M.Q. water	Up to 100 ml

11. Southern hybridizing solutions

(1) 20 X SSC

Components	Amount
NaCl	175.3 g
Na Citrate	88.2 g

(2) Solution A (300 ml)

Components	Volume
0.25N HCl	6.25 ml HCl

Depurination – If the fragments of interest are larger than 15 kb, the DNA should be nicked by depurination prior to transfer. To depurinate the DNA, the gel was soaked in several gel volumes of Depurination Solution (0.2 N HCl) for 10 minutes at room temperature.

(3) Solution B (200 ml)

Components	Volume
1.5M NaCl	60 ml of 5M NaCl
0.5M NaOH	20 ml of 5N NaOH

Denaturation - The denaturation in an alkaline environment may improve binding of the negatively charged thymine residues of DNA to a positively charged amino groups of membrane, separating it into single DNA strands for later hybridization to the probe (see below), and destroys any residual RNA that may still be present in the DNA.

(4) Solution C (200 ml)

Components	Volume
1.5M NaCl	60 ml of 5M NaCl
0.5M Tris-HCl pH 7.5	100 ml 1M of Tris-Cl, pH 7.5

Neutralization – to neutralize residual alkaline solution.

(5) Wash Buffer (100 ml)

Components	Volume
2X SSC	10 ml of 20X SSC
0.1% SDS	1 ml of 10% SDS

(6) Pre-hybridization buffer (10 ml)

Components	Volume
30 mM NaH ₂ PO ₄	10 ml of 20X SSC
7% SDS	7 ml of 10% SDS



RESEARCH ARTICLE

WILEY

Ifu5, a WW domain-containing protein interacts with Efg1 to achieve coordination of normoxic and hypoxic functions to influence pathogenicity traits in *Candida albicans*

Sumit K. Rastogi^{1,2} | Lasse van Wijlick³ | Shivani Ror¹ | Keunsook K. Lee⁴ | Elvira Román⁵ | Pranjali Agarwal¹ | Nikhat Manzoor² | Neil A.R. Gow⁴ | Jesús Pla⁵ | Joachim F. Ernst³ | Sneh L. Panwar¹ 

¹Yeast Molecular Genetics Laboratory, School of Life Sciences, Jawaharlal Nehru University, New Delhi, India

²Medical Mycology Laboratory, Department of Biosciences, Jamia Millia Islamia University, New Delhi, India

³Department Biologie, Molekulare Mykologie, Heinrich-Heine-Universität, Düsseldorf, Germany

⁴The Aberdeen Fungal Group, MRC Centre for Medical Mycology, School of Medicine, Medical Sciences & Nutrition, Institute of Medical Sciences, University of Aberdeen, Aberdeen, UK

⁵Departamento de Microbiología y Parasitología-IRYCIS, Facultad de Farmacia, Universidad Complutense de Madrid, Madrid, Spain

Correspondence

Sneh L. Panwar, Yeast Molecular Genetics Laboratory, School of Life Sciences, Jawaharlal Nehru University, New Delhi, India.
Email: sneh@mail.jnu.ac.in

Funding information

Department of Biotechnology, Grant/Award Number: BT/PR5347/MED/29/629/2012

Abstract

Hypoxic adaptation pathways, essential for *Candida albicans* pathogenesis, are tied to its transition from a commensal to a pathogen. Herein, we identify a WW domain-containing protein, Ifu5, as a determinant of hypoxic adaptation that also impacts normoxic responses in this fungus. Ifu5 activity supports glycosylation homeostasis via the Cek1 mitogen-activated protein kinase-dependent up-regulation of *PMT1*, under normoxia. Transcriptome analysis of *ifu5Δ/Δ* under normoxia shows a significant up-regulation of the hypoxic regulator *EFG1* and *EFG1*-dependent genes. We demonstrate physical interaction between Ifu5 by virtue of its WW domain and Efg1 that represses *EFG1* expression under normoxia. This interaction is lost under hypoxic growth conditions, relieving *EFG1* repression. Hypoxic adaptation processes such as filamentation and biofilm formation are affected in *ifu5Δ/Δ* cells revealing the role of Ifu5 in hypoxic signalling and modulating pathogenicity traits of *C. albicans* under varied oxygen conditions. Additionally, the WW domain of Ifu5 facilitates its role in hypoxic adaptation, revealing the importance of this domain in providing a platform to integrate various cellular processes. These data forge a relationship between Efg1 and Ifu5 that fosters the role of Ifu5 in hypoxic adaptation thus illuminating novel strategies to undermine the growth of *C. albicans*.

KEYWORDS

Biofilm, cell wall integrity, hypoxia, Efg1, hyphal morphogenesis, WW domain

1 | INTRODUCTION

The ability of *Candida albicans*, a commensal pathogen, to adapt to environmental challenges while it colonises and infects the human host, is critical for its survival. One such challenge is to be able to adapt to a variety of oxygen concentrations that this pathogen may experience at various stages of establishing an infection in the

mammalian host. The response of *C. albicans* to hypoxic microenvironment is crucial for various virulence traits, starting from infection (commensal-to-pathogen transition) to biofilm formation (Ernst & Tielker, 2009; Grahl, Shepardson, Chung, & Cramer, 2012). Hypoxic responses are also critical for *C. albicans* to ensure its occupancy as a commensal in hypoxic niches such as the lower gastrointestinal tract, in its human host (Pierce & Kumamoto, 2012).

A body of studies has identified distinct transcription factors and regulatory circuits that function to facilitate the adaptation of *C.*

Sumit K. Rastogi and Lasse van Wijlick contributed equally to this work.

albicans exclusively under hypoxia and differ from those required under normoxia. In this fungus during hypoxia, genes involved in ergosterol and fatty acid biosynthesis, iron metabolism, cell wall regulation, glycolysis, and fermentation are up-regulated, whereas respiratory genes are repressed (Chang, Bien, Lee, Espenshade, & Kwon-Chung, 2007; Desai, van Wijlick, Kurtz, Juchimiuk, & Ernst, 2015; Setiadi, Doedt, Cottier, Noffz, & Ernst, 2006). Whereas, the transcription factor Upc2 directs an increase in the ergosterol biosynthesis transcripts (Synnott, Guida, Mulhern-Haughey, Higgins, & Butler, 2010), the regulators Tye7 and Efg1 activate the glycolytic and fermentation genes and unsaturated fatty acid metabolism, respectively during hypoxia (Askew et al., 2009; Bonhomme et al., 2011; Setiadi et al., 2006). The pleiotropic virulence regulator Efg1 is considered central for hypoxic adaptation in this fungus as Efg1 not only contributes to the regulation of half of all hypoxia-responsive genes but also prevents the expression of normoxia associated genes (Setiadi et al., 2006; Stichernoth & Ernst, 2009). Thus, compromising the function of the key hypoxia-regulated genes or regulators results in attenuated virulence in murine models of fungal infection (Askew et al., 2009; Desai et al., 2015).

The link between *C. albicans* ability to adapt to hypoxia with its pathogenesis is reinforced by the observation that hypoxic conditions enable *C. albicans* to establish a successful infection by inducing the masking of cell wall β -glucan. As a consequence, *C. albicans* is able to impede its clearance by evading recognition by the polymorphonuclear leukocytes, pointing to the contribution of hypoxic niches in enhancing virulence (Lopes et al., 2018; Pradhan et al., 2018). Additionally, the ability of this fungal pathogen to undergo the bud-to-hyphae transition and form biofilms in response to hypoxia also permits this pathogen to colonise hypoxic niches in the human host. Both these processes are regulated by Efg1 wherein although Efg1 promotes hypoxic filamentation and biofilm formation at 37°C, it inhibits hypoxic hypha formation during growth on agar specifically at temperatures $\leq 35^\circ\text{C}$ (Desai et al., 2015; Setiadi et al., 2006). The temperature-dependent inhibition on hypoxic hypha formation requires the concerted action of Efg1, Bcr1, Brg1, and Ace2 transcription factors (Desai et al., 2015). Furthermore, transcriptional induction of genes such as those involved in glucose metabolism, sulphur metabolism, peroxisomal functions, and iron uptake that make possible biofilm formation in hypoxic niches is also dependent on Efg1. Biofilm formation allows *C. albicans* to generate foci for infections in oxygen-limiting microenvironments and is considered a major cause of persistent infections (Nobile & Mitchell, 2006). Collectively, all these studies emphasise the contribution of Efg1 in regulating hypoxic adaptation in *C. albicans*. Despite this knowledge, molecular components influencing the hypoxic regulation of Efg1 remain unidentified.

Treating candida infections is not only impeded by the ability of *C. albicans* to adapt to environmental changes by switching between the planktonic and biofilm mode of growth in host microenvironments but also due to the highly drug recalcitrant nature of the biofilms. *C. albicans* develops resistance to existing azole antifungals due to the up-regulation of drug efflux pumps in both the planktonic as well as biofilm modes of growth. Induced expression of the drug efflux

pumps, Cdr1, and Cdr2 in drug resistant *C. albicans* isolates is often accompanied by the simultaneous induction of a subset of genes (*RTA3*, *IFU5*, and *HSP12*) regulated by the transcription factor Tac1 (Coste, Karababa, Ischer, Bille, & Sanglard, 2004). The significance of these coregulated genes remains largely unexplored in *C. albicans*, which prompted us to ask if these proteins contribute to the development of azole resistance in *C. albicans* by affecting the function of Cdr1 and Cdr2. A recent study from our laboratory demonstrates that the 7-TM receptor protein Rta3 does not contribute to azole tolerance at least in a wild type *C. albicans* strain (SC5314) but is required for biofilm development in vivo (Srivastava et al., 2017). Thus, in order to investigate the relevance of other Tac1 coregulated genes, we characterised Ifu5, a WW domain-containing protein, in this pathogenic fungus.

A large number of WW domain-containing proteins have been assigned relevance in *Saccharomyces cerevisiae* (Hesselberth et al., 2006), whereas they remain uncharacterised in *C. albicans*. WW domains are small modular domains that interact with peptide ligands that contain a core proline-rich sequence and are implicated in a plethora of cellular processes (Hesselberth et al., 2006). A typical WW domain consists of 35–40 amino acid residues with two highly conserved tryptophan residues separated by 20–23 amino acids followed by a proline residue in the protein. Ifu5 is a homolog of the *S. cerevisiae* WW domain-containing protein Wwm1 (73% similarity and 66% identity with Wwm1) that is implicated in apoptosis by means of interaction with a metacaspase (Figure S1; Szallies, Kubata, & Duszenko, 2002). Both Wwm1 and Ifu5 contain a single WW domain spanning 26 amino acid residues defined by two conserved tryptophan residues and a single proline residue (Figure 1). The WW domains are categorised into four groups based on the presence of signature residues within the domain and their ligand specificities (Figure 1; Hesselberth et al., 2006). In this study, we describe the role of WW domain-containing protein Ifu5 in mediating normoxic and hypoxic responses in *C. albicans* and demonstrate an alliance between Ifu5 and Efg1 that facilitates adaptation of this fungus to oxygen-limiting environments. Thus, our study uncovers a novel link between Ifu5 and Efg1 that is pivotal for modulating pathogenicity-related traits in *C. albicans*.

2 | RESULTS

2.1 | Tac1-regulated Ifu5 is involved in maintaining cell wall integrity

The up-regulation of the drug efflux proteins Cdr1 and Cdr2 by fluphenazine has been well documented (Coste et al., 2004). A genome wide transcriptome study showed that fluphenazine triggers the simultaneous up-regulation of *IFU5* with *CDR1* and *CDR2* via the transcription factor Tac1 (Coste et al., 2004). In order to confirm Tac1-dependent coordinate regulation of *CDR1* and *IFU5*, we first analysed their expression in *tac1 Δ /* cells and in a strain carrying the *TAC1^{HA}* (hyperactive Tac1) allele. Although the expression of *IFU5* and *CDR1* in *tac1 Δ /* was two-

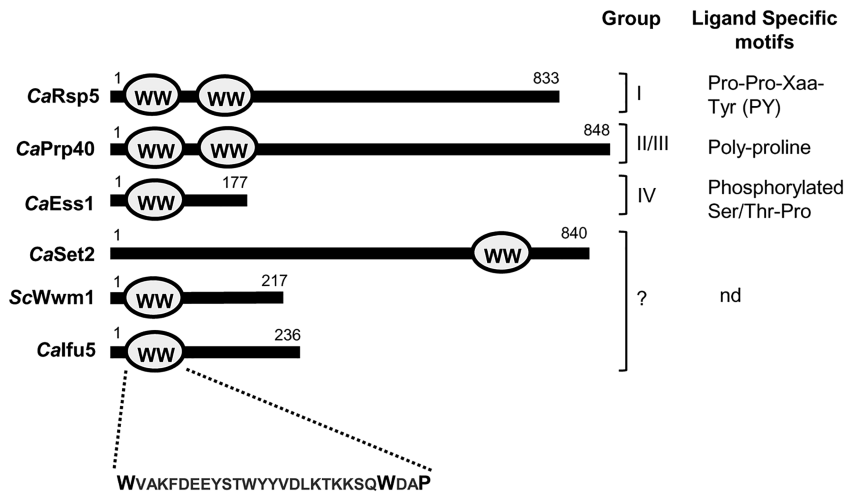


FIGURE 1 Organisation of WW domain in different proteins. WW domain organisation of Calfu5, ScWwm1 and members of different class of WW domain-containing proteins in *Candida albicans*. These proteins are classified into four groups based on their ligand specific motifs. nd, ligand specific motif not determined

fold and four-fold down-regulated, their expression was three-fold and four-fold up-regulated in a *TAC1^{HA}* strain background, respectively (Figure 2a). Treatment of wild-type cells with fluphenazine resulted in an increase in expression of *IFU5* and *CDR1* by 2.5- and 2.6-fold, respectively (Figure 2b). On the contrary, *tac1Δ/Δ* cells failed to enhance the expression of *IFU5* and *CDR1*, upon fluphenazine treatment (Figure 2 b). This set of data suggest that functional Tac1 is requisite for transcriptional regulation of *IFU5* in both unstressed and stressed conditions, affirming that *IFU5* is a target of Tac1.

To determine the function of *lfu5* in *C. albicans*, *ifu5Δ/Δ* and *IFU5* reconstituted strains were constructed using the *SAT1* flipper strategy and confirmed by Southern blot analysis (Figure S2). In an attempt to understand the importance of the WW domain in the function of *lfu5*, we also mutagenised tryptophan and proline of this domain as these amino acids in other proteins are important for ligand (PPXY or PPLP motif) interactions (Figure 1; Hesselberth et al., 2006). We first examined *ifu5Δ/Δ* cells and *mutlfu5* for their ability to grow in presence of various antifungal compounds. Both the mutant strains displayed wild-type susceptibility to azole antifungals, suggesting that *lfu5* does not contribute to azole tolerance in the laboratory strain, SC5314 (Figure S3). These mutants were then tested for their ability to grow in the presence of agents that target the membrane or the cell wall assembly such as caspofungin, calcofluor white, sodium dodecyl sulfate, and tunicamycin. Interestingly, *ifu5Δ/Δ* cells, but not *mutlfu5*, exhibited a growth defect in the presence of these drugs (Figure 2c). The *IFU5*-reconstituted strain restored the growth defect of the *ifu5Δ/Δ* cells to wild-type levels (Figure 2c).

Previous studies have correlated increased susceptibility to cell wall-damaging agents with alterations in cell wall composition and architecture (Lee et al., 2012). In order to assess for alterations in cell wall integrity, *ifu5Δ/Δ* cells were subjected to transmission electron microscopy and cell wall composition analysis. Transmission electron microscopy revealed the presence of compromised fibrillar mannoprotein layer in the *ifu5Δ/Δ* cells with no alteration in cell wall thickness compared with wild type (Figure 2d). Cell wall composition analysis showed significant changes in cell wall constituents in the mutant compared with wild type. Glucan constituted 66% of the total

cell wall polysaccharide in *ifu5Δ/Δ* cells, compared with 53% in the wild type. Consistent with the compromised fibrillar mannoprotein layer, there was a significant reduction in the mannan content in the *ifu5Δ/Δ* cells (28% of total cell wall polysaccharide in mutant vs. 43% in wild type). This data also indicated a two-fold increase in the chitin content as determined by measuring the glucosamine content (6% vs. 3% in the wild type) in the *ifu5Δ/Δ* cells (Figure 2e). Cell wall damage causes changes in cell surface hydrophobicity thus affecting cell-cell and cell-to-surface adhesion properties (Masuoka & Hazen, 1997). Hence, to investigate the effect of altered cell wall integrity on cell-cell adhesion, we performed flocculation assay with the mutant. The *ifu5Δ/Δ* cells flocculated extensively and aggregated at the bottom of the tube as indicated by a sharp decline in OD₆₀₀ (>50% decline) within 15 min after the shaking was stopped in contrast to the wild type and the reconstituted strain (Figure 2f).

The cell wall integrity (CWI) pathway involving the Cek1 and Mkc1 mitogen-activated protein kinases (MAPKs) and the unfolded protein response pathway are requisite for cellular adaptation to cell wall stress (Román, Alonso-Monge, Miranda, & Pla, 2015). Given the strong cell wall phenotypes in *ifu5Δ/Δ*, we sought to analyse the impact of *lfu5* on the aforesaid adaptation processes and show that *ifu5Δ/Δ* cells exhibit constitutive phosphorylation of Mkc1 and Cek1 (1.4- and 1.5-fold induction for Mkc1 and Cek1, respectively in mutant vs. wild type) under basal conditions (Figures 2g and S4). As activated Cek1 signalling pathway is equated to glycostress in *C. albicans* (van Wijlick, Swidergall, Brandt, & Ernst, 2016), we propose that absence of *lfu5* results in glycostress. The increased sensitivity of *ifu5Δ/Δ* to tunicamycin (*N*-glycosylation inhibitor) and altered cell wall composition is consistent with this notion (Figure 2c,d). Cek1 pathway compensates for glycostress-induced cell wall damage by regulating the activity of *O*-mannosyltransferases (Pmt proteins), especially *PMT1* (van Wijlick et al., 2016). *PMT1* expression is repressed in cells with intact *N*-glycosylation, whereas the repression on *PMT1* is relieved in cells with defective *N*-glycosylation via the Cek1 pathway (Cantero & Ernst, 2011). The *ifu5Δ/Δ* mutant exhibited eightfold up-regulation in the transcript levels of *PMT1* (Figure 2h), concordant with glycostress-induced Cek1 phosphorylation. These findings suggest

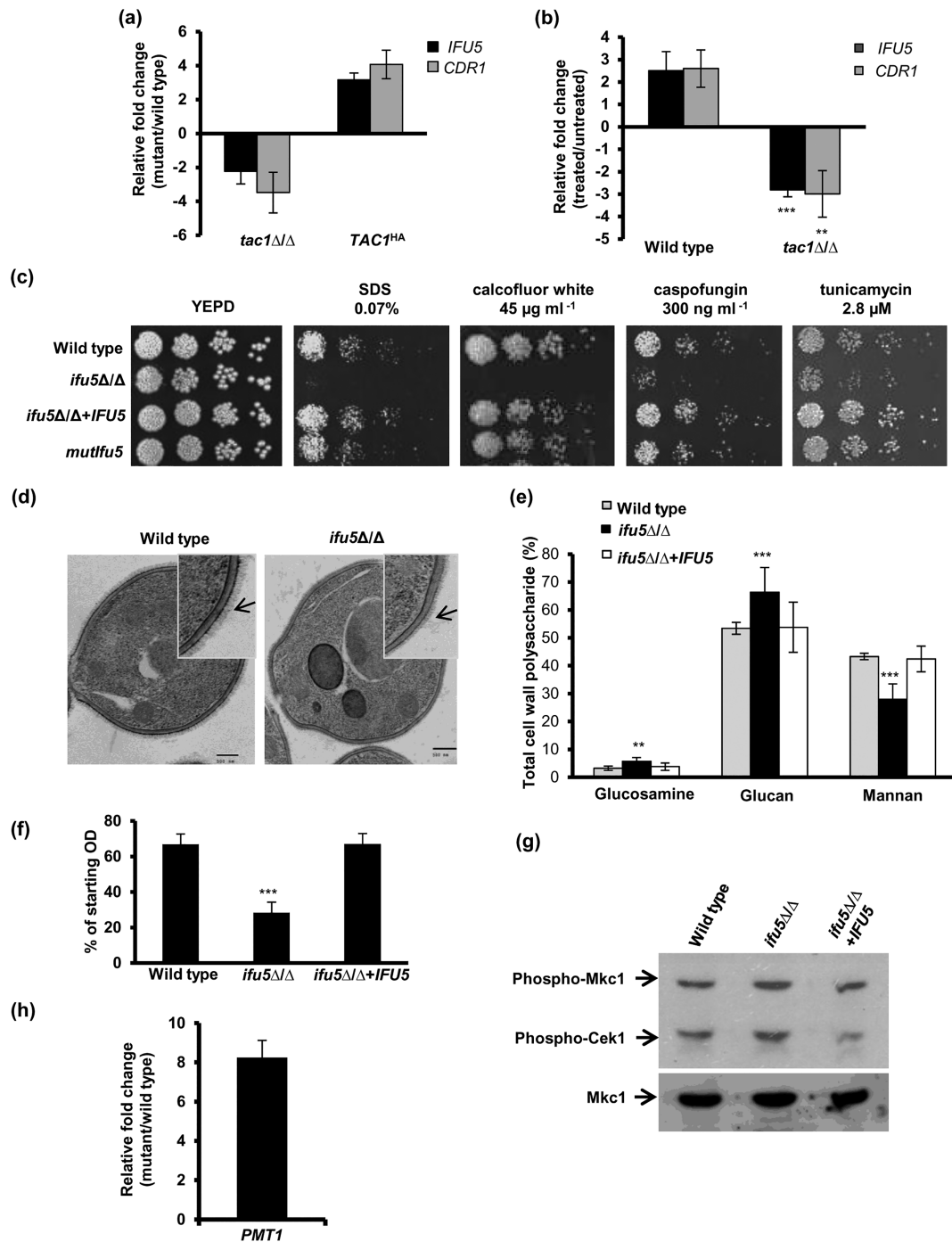


FIGURE 2 Tac1-regulated Ifu5 is required for cell wall integrity. (a) Expression analysis of *IFU5* and *CDR1* in *tac1Δ/Δ* and *TAC1^{HA}* cells. (b) Expression analysis of *IFU5* and *CDR1* upon fluphenazine (20- $\mu\text{g}\cdot\text{ml}^{-1}$, 30 min) treatment in indicated strains. (c) Fivefold serial dilution of cell suspensions was spotted onto YEPD plates supplemented with indicated concentrations of drugs and incubated at 30°C for 48 hr. (d) Representative images of transmission electron microscopy analysis for the cell walls of wild type strain SC5314 and *ifu5Δ/Δ*. Arrow indicates the mannofibril layer. (e) Analysis of carbohydrate content of cell wall. Cell walls of the wild type, *ifu5Δ/Δ*, and the reconstituted strain were acid hydrolysed, and released monosaccharide was detected by HPAEC-PAD using a CarboPac PA10 analytical column. Results are expressed as a percentage of dried cell wall ($\mu\text{g}\cdot\text{mg}^{-1}$). Shown is the mole percentage average from four or five replicates analysed over two experiments and two-tailed, unpaired *t* test was used to determine the statistical relevance. ***p* < .01, ****p* < .001. (f) Flocculation assay was done by measuring optical density of the cultures directly after vortex mixing followed by a resting period of 15 min. Values shown represent the ratio of the $\text{OD}_{\text{final}}/\text{OD}_{\text{initial}}$. Values are means \pm SD and are derived from three independent cultures. (g) Mitogen-activated protein kinase activation in indicated strains grown in YEPD medium at 37°C was performed. Anti-phospho-p44/p42 MAPK (Thr202/Tyr204) antibody was used to detect dually phosphorylated Mkc1 and Cek1 MAPKs. (h) Expression of *PMT1* in *ifu5Δ/Δ*. Fold change in (a), (b), and (h; mutant/wild type or treated/untreated) is calculated by $2^{-\Delta\Delta\text{C}_T}$, normalised to *ACT1* (endogenous control), with untreated strain as calibrator. Values are means \pm SD and derived from three independent RNA preparations. Two-tailed, unpaired *t* test was used to determine the statistical relevance. ***p* < .01, ****p* < .001

that *Ifu5* impacts cell wall regulation by influencing glycosylation homeostasis in *C. albicans*.

2.2 | *EFG1* and biofilm-specific class of genes are differentially regulated in the absence of *IFU5*

In order to obtain an insight into the genome-wide role of *IFU5* in *C. albicans*, we compared the transcript profiles of wild-type and *ifu5Δ/Δ* cells. After filtering, the entire data set resulted in a total of 106 statistically significant differentially regulated genes ($p < .05$, >1.5 -fold up-regulated or down-regulated; Table S5). A total of 75 genes that were down-regulated were enriched for the GO annotation filamentous growth (*FGR12*, *FGR18*, *NRG2*, and *HSP21*), mitochondria (*NAD1*, *COX2*, *CRD1*, and *COQ10*), cell surface (*PGA13*, *PGA16*, and *PGA46*), and protein modification and transport (Figure 3a). The up-regulated genes (total of 30) were significantly enriched for the GO annotation protein modification and transport (*PEX14*, *BMT4*, *ARC18*, and *RPT2*), adhesion and filamentation (*EFG1*, *ALS4*, *SSY1*, and *MHP1*), oxidation–reduction (*SOD3* and *orf19.225*), and cell surface (*PGA39* and *PGA22*; Figure 2a). *PEX14* (3.73-fold) and *BMT4* (3.24-fold) were the highest up-regulated genes, whereas *orf19.1557* (6.58-fold) was the highest down-regulated gene (Table 1). Out of the 106 differentially regulated genes, 24 genes were described as genes that are induced or repressed during biofilm formation (Figure 3a).

Interestingly, our data set shows two-fold transcriptional up-regulation of *EFG1* in *ifu5Δ/Δ* cells (Table 1). Previous transcriptional analysis shows that induced production of *Efg1* under normoxia coincides the expression of a subset of genes such as genes coding for cell wall proteins, superoxide dismutase, Fe^{3+} reductases, copper transport protein, and an *O*-mannosyltransferase (Stichternoth & Ernst, 2009). In accord with this, absence of *IFU5* also results in a significant increase in expression of these aforesaid normoxia-dependent genes (Table 1). Genes such as *ALS3*, *ALS4*, *PGA39*, and *PGA22* (cell wall proteins), *BMT4* (beta-mannosyltransferase), *FRE30*, and *SOD3* (redox homeostasis) are coincued with *EFG1* in *ifu5Δ/Δ* cells. Furthermore, induced production of *Efg1* also represses genes involved in oxidative metabolism (Doedt et al., 2004) in line with the reduced expression of genes such as *NAD1*, *COX2*, *CRD1*, and *COQ10* observed in *ifu5Δ/Δ* cells (Table 1). The expression of *EFG1* and coincued genes was validated by quantitative polymerase chain reaction (qPCR) analysis (Figure 3b). Coupled together, our data show that deletion of *IFU5* results in altered expression of (a) biofilm associated genes and (b) genes that are induced in an *Efg1*-dependent manner under normoxia.

2.3 | *Ifu5* affects normoxic and hypoxic expression of *EFG1*

WW domains, present in structural and signalling proteins mediate protein–protein interactions by binding to specific motifs within their

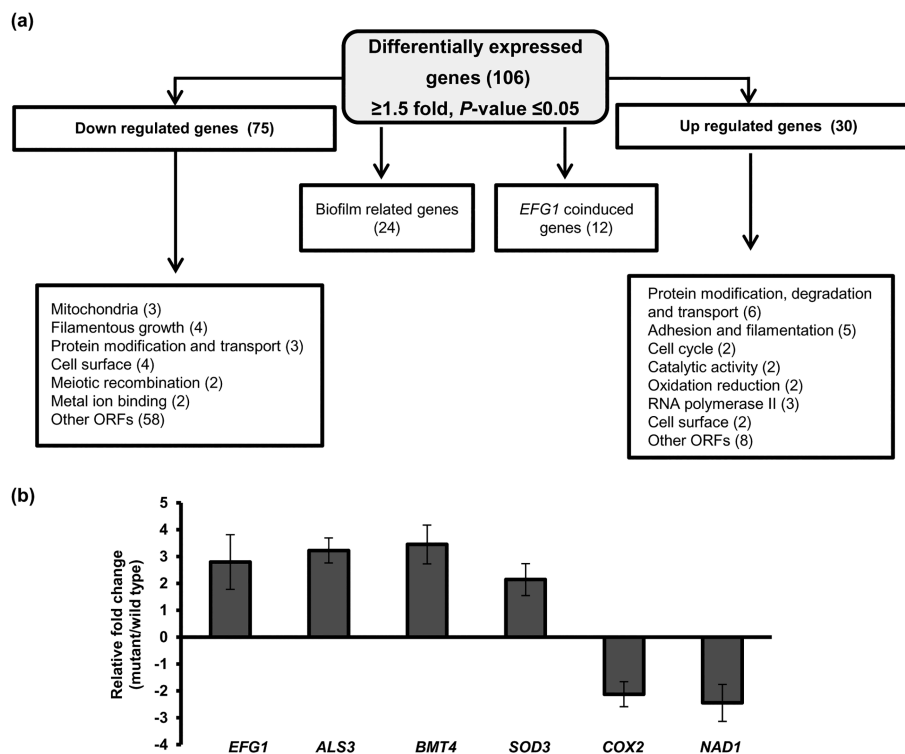


FIGURE 3 Transcriptional profiling of *ifu5Δ/Δ* cells. (a) Flow chart indicating differential expression of genes in *ifu5Δ/Δ*. Boxes indicate list of functional categories according to GO annotation. Number of differentially expressed genes is indicated in brackets. (b) Quantitative polymerase chain reaction-based transcript analysis of *Efg1* and its coregulated genes in *ifu5Δ/Δ*. Fold change (mutant/wild type) is calculated by $2^{-\Delta\Delta C_T}$, normalised to *ACT1* (endogenous control) with untreated strain as calibrator. Values are means \pm SD and are derived from three independent RNA preparations. A two-tailed, unpaired *t* test was used to determine the statistical relevance: *** $p < .001$

TABLE 1 Functional category of *C. albicans* genes whose transcript levels in the *ifu5Δ/Δ* strain are 1.5-fold up- and down-regulated ($P \leq 0.05$)

Category and System Name	Gene	Function	Fold Change
Protein modification degradation and transport			
orf19.1557	<i>RKM5</i>	S-adenosylmethionine-dependent methyltransferase activity	-7.34
orf19.1805	<i>PEX14</i>	role in protein import into peroxisome matrix	3.73
orf19.5612	<i>BMT4</i> ^{a,b,c}	Beta-mannosyltransferase	3.24
orf19.5440	<i>RPT2</i> ^b	Putative ATPase of the 19S regulatory particle of the 26S proteasome	1.96
orf19.7106	<i>VPS70</i>	Ortholog(s) have role in protein targeting to vacuole	1.76
Cell Surface			
orf19.3638	<i>PGA46</i>	GPI-anchored cell wall protein involved in cell wall synthesis	-2.62
orf19.6420	<i>PGA13</i> ^b	GPI-anchored cell wall protein involved in cell wall synthesis	-1.88
orf19.848	<i>PGA16</i> ^b	Putative GPI-anchored protein	-1.86
orf19.6302	<i>PGA39</i>	GPI-anchored protein	1.85
orf19.3738	<i>PGA22</i>	Putative GPI-anchored protein	1.54
orf19.4555	<i>ALS4</i> ^b	GPI-anchored adhesion, Role in adhesion	1.64
orf19.1816	<i>ALS3</i> ^{b,c}	Cell wall adhesion, Promotes biofilm formation	1.63
Hypha formation and Virulence			
orf19.5454	<i>FGR12</i> ^b	Filamentous growth	-5.17
orf19.6339	<i>NRG2</i>	Transcription factor involved in biofilm	-3.60
orf19.4067	<i>FGR18</i>	Filamentous growth	-2.61
orf19.935	<i>AGA1</i> ^b	Spider biofilm induced	-2.47
orf19.610	<i>EFG1</i> ^{a,b}	Transcription factor involved in biofilm	2.73
orf19.822	<i>HSP21</i> ^b	Small heat shock protein	-3.01
Iron assimilation			
orf19.1673	<i>PPT1</i>	Induced in high iron	-2.24
orf19.6140	<i>FRE30</i> ^c	Protein with similarity to ferric reductases	3.19
Mitochondrial Function and Oxidation-Reduction Processes			
CaalfMp01	<i>COX2</i> ^a	Subunit II of cytochrome c oxidase	-2.05
orf19.6100	<i>CRD1</i> ^b	Cardiolipin synthase	-1.70
orf19.6662	<i>COQ10</i>	Putative coenzyme Q (ubiquinone) binding protein	-1.50
CaalfMp03	<i>NAD1</i> ^c	Subunit 6 of NADH:ubiquinone oxidoreductase (NADH:ubiquinone dehydrogenase)	-2.59
orf19.7111.1	<i>SOD3</i> ^{a,b,c}	Cytosolic manganese-containing superoxide dismutase	2.9

^aGenes that were validated by qPCR, ^bGenes that are annotated as flow model/RPMI/Spider/rat catheter biofilm induced or repressed in CGD. ^cGenes that are Efg1 regulated.

partners to coordinate cellular processes such as transcription, differentiation, and ubiquitination (Hesselberth et al., 2006). Considering that Ifu5 contains a WW domain and given the up-regulation of *EFG1* in *ifu5Δ/Δ* cells (Figure 3b), we predicted that Ifu5 could be negatively influencing the expression of Efg1 under normoxia, which may be due to direct interaction between these two proteins. Hypoxic conditions may relieve this repression resulting in disrupting the interaction between Ifu5 and Efg1; basis for the increased expression of Efg1 under hypoxia (Stichternoth & Ernst, 2009). Therefore, to assess for the interaction, strains producing hemagglutinin (HA)-tagged Efg1, tandem affinity purification (TAP)-tagged Ifu5 and mutIfu5 and a strain expressing both Ifu5-TAP and Efg1-HA were grown in yeast extract peptone dextrose (YEPD) at 30°C for 4 hr, under normoxia and hypoxia followed by cross-linking with formaldehyde to stabilise

protein complexes. Thereafter, the total protein extracts were incubated with IgG-coated beads for immunoprecipitation of the Ifu5-TAP protein in the corresponding strain backgrounds. The Ifu5-TAP signal in beads incubated with extract from the strains carrying Ifu5-TAP allele was confirmed by immunoblotting with anti-TAP antibody, under both normoxia and hypoxia (Figure 4a, Anti-TAP panel). Interestingly, immunoblotting of the bound fractions with an anti-HA antibody (Co-IP, Anti-HA panel) allowed to detect Efg1-HA co-immunoprecipitation with Ifu5-TAP exclusively in normoxic conditions (Figure 4a). The Ifu5-Efg1 interaction was not detected with mutIfu5-TAP (Co-IP, Anti-HA panel), pointing to the essentiality of the WW domain in interacting with Efg1 (Figure 4a). Our result therefore shows that Ifu5 protein via its WW domain physically associates with Efg1 protein solely during normoxia.

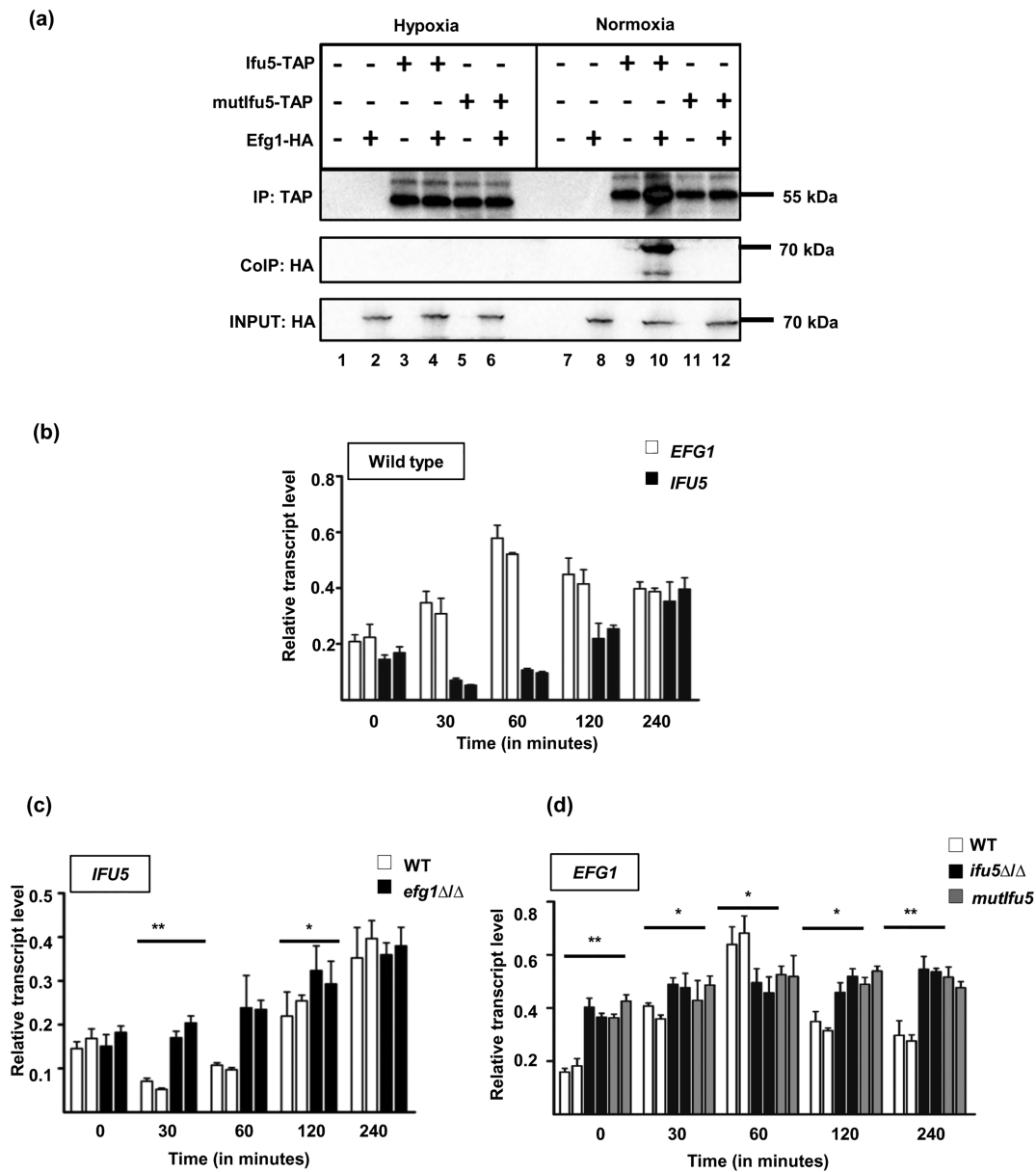


FIGURE 4 Role of Ifu5 in hypoxic adaptation. (a) Strains expressing HA-Efg1 (AVL12, lanes 2 and 8), Ifu5-TAP (CLvW997, lanes 3 and 9), both HA-Efg1 and Ifu5-TAP (CLvW998, lanes 4 and 10), mutIfu5-TAP (CLvW990, lanes 5 and 11), HA-Efg1 and mutIfu5-TAP (CLvW989, lanes 6 and 12), and the control strain BWP17 (lanes 1 and 7) were grown in yeast extract peptone dextrose medium at 30°C in either hypoxic or normoxic conditions for 4 hr. The samples were immunoblotted and developed using anti-TAP (IP) or anti-HA (CoIP) antibodies (\pm). To verify presence of Efg1-HA, 1% of the total protein extracts was blotted and investigated with anti-HA. (b) Relative transcript levels of *IFU5* and *EFG1* were determined by quantitative polymerase chain reaction (qPCR). The indicated strains grown under normoxic conditions in yeast extract peptone dextrose medium for 4 hr at 30°C, were shifted under hypoxia (0.2% O₂) and grown for additional 4 hr at 30°C, and 0.2% O₂. RNA was isolated from cells at indicated time points. Time point 0 corresponds to 4-hr growth under normoxic conditions before shifting cells to hypoxic conditions. At each time point, two biological replicates and three technical replicates were assayed by qPCR. The *ACT1* transcript was used as a calibrator to normalise *IFU5* and *EFG1* transcript levels. A two-tailed, unpaired *t* test was used to determine the statistical relevance: **p* < .05, ***p* < .01. Relative transcript levels of (c) *IFU5* transcript in wild type and *efg1Δ/Δ* and (d) *EFG1* transcript in wild type, *ifu5Δ/Δ*, and *mutIfu5* was analysed upon shifting normoxia grown cells to hypoxic conditions. At each time point, two biological replicates and three technical replicates were assayed by qPCR. The *ACT1* transcript was used as a calibrator to normalise *IFU5* and *EFG1* transcript levels, respectively. A two-tailed, unpaired *t* test was used to determine the statistical relevance: **p* < .05; ***p* < .01

Thereafter, based on the role of Efg1 in hypoxic adaptation in *C. albicans*, we were prompted to analyse the relevance of Ifu5–Efg1 interaction under hypoxia. First, we show that absence of Ifu5 does not affect growth under hypoxia suggesting that Ifu5 is not a

determinant of hypoxic growth in *C. albicans* (data not shown). Second, we monitored transcript levels of *EFG1* and *IFU5* during the shift from normoxia to hypoxia in wild-type, *efg1Δ/Δ*, *ifu5Δ/Δ*, and *mutIfu5* cells. We observed a decrease in the transcript levels of *IFU5* after

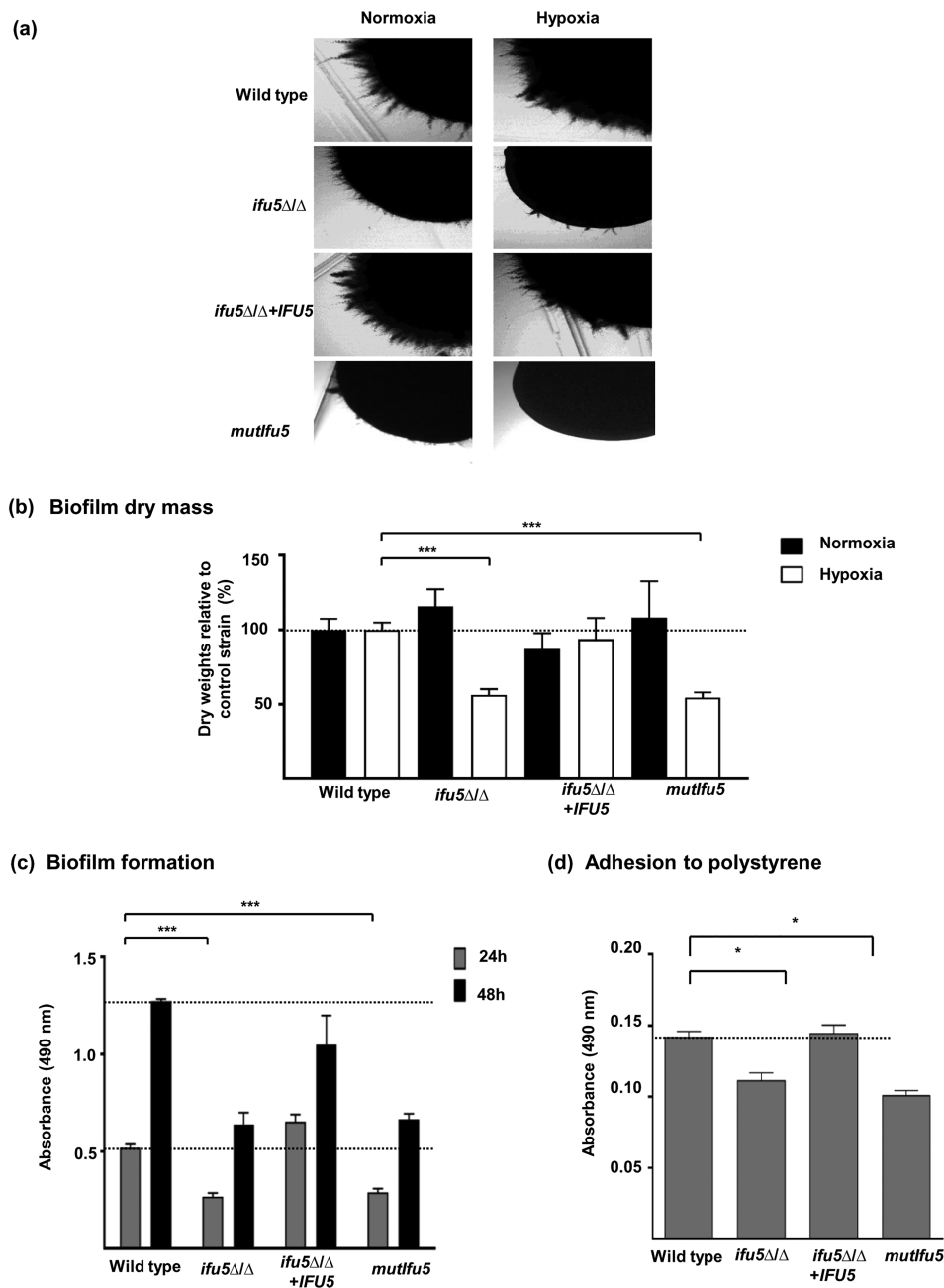


FIGURE 5 *Ifu5* influences filamentation and biofilm formation. (a) Indicated strains were grown under hypoxia (0.2% O₂) and normoxia (21% O₂) on the surface of spider agar at 37°C for 3 days and photographed. (b) Biofilm mass (dry weight) after growth at 37°C under normoxia (21% O₂, 6% CO₂) and hypoxia (0.2% O₂, 6% CO₂) was estimated. Polystyrene wells were inoculated with 10⁵ cells·ml⁻¹ of the indicated strains and supplemented with Roswell Park Memorial Institute 1640 medium and incubated for 48 hr at 37°C under normoxia and hypoxia. Biofilms were washed twice with phosphate-buffered saline (PBS), and dry biomass of the biofilms were quantified and expressed as ratio of the indicated strain versus control strain (wild type). Means and standard deviations were determined from the results of three independent experiments. A t test was used to calculate the statistical relevance: ****p* < .001. The dashed line indicates the relative mass of the control strain which was set to 100%. (c) *Candida albicans* wild type, *ifu5*ΔΔ, *IFU5* reconstituted, and *mutfu5* strains were allowed to form biofilm under earlier performed gaseous conditions. Indicated strains were allowed to adhere to the surface of a polystyrene plate for 90 min in PBS at 37°C under hypoxic (0.2% O₂) conditions. The wells were supplemented with Roswell Park Memorial Institute 1640 medium and incubated for 24 and 48 hr at 37°C under hypoxia. Biofilms were washed with PBS after the indicated time points and supplemented with XTT-menadione solution. After incubation in the dark for 30 min at 37°C, the supernatant was transferred to a new 96-well microtiter plate, and the colour change was measured at 490 nm. Dashed lines indicate absorbance of the control strain after 24 and 48 hr, respectively. A t test was used to calculate the statistical relevance: ****p* < .001. Dashed lines indicate absorbance of the control strain after 24 and 48 hr, respectively. (d) Adhesion of *C. albicans* indicated strains to polystyrene wells was observed using XTT reduction assay. Strains were inoculated into polystyrene wells as they were for biofilm experiments. Following 90 min of incubation, non-adherent cells were removed by washing, and the numbers of cells were assessed by using an XTT reduction assay. A t test was used to calculate the statistical relevance: **p* < .05. Dashed lines indicate absorbance of the control strain

the shift to hypoxia with a simultaneous increase in the *EFG1* transcript levels at the 30 and 60-min time points, compared with their transcript levels at the 0 time point in the wild type (Figure 4b). At the later time points of 120 and 240 min, there was an increase in the transcript level of *IFU5* with a commensurate decrease in *EFG1* transcript level, suggesting hypoxic repression of *IFU5* during the early stages of hypoxia (Figure 4b). Additionally, transcript levels of *IFU5* in *efg1 Δ* cells and of *EFG1* in *ifu5 Δ* and *mutIfu5* increased with time, pointing to the existence of reciprocal negative regulation between *IFU5* and *EFG1* (Figure 4c,d). Thus, the result indicates that one of the functions of Ifu5 may be to effectively negatively regulate Efg1 expression by virtue of its WW domain under normoxia by physically interacting with this hypoxic regulator. Hypoxic growth conditions may result in the loss of this interaction, and negative reciprocal regulation coordinates the expression of *IFU5* and *EFG1* during various stages of hypoxia. Collectively, we surmise that Ifu5 is tied to regulating Efg1 expression and thus to hypoxic adaptation by means of its WW domain in *C. albicans*.

2.4 | Ifu5 regulates filamentation and affects biofilm formation under hypoxia

Hyphal morphogenesis is one of the process that is required by *C. albicans* to adapt to hypoxia, especially during its growth on agar surface (Setiadi et al., 2006). Therefore, given the role of Ifu5 in hypoxic adaptation, we were prompted to analyse the influence of Ifu5 on hyphal morphogenesis. Absence of *IFU5* did not affect hyphal induction in liquid hyphal-inducing conditions such as Spider and serum-containing media. On the contrary, both *ifu5 Δ* and *mutIfu5* exhibited filamentation (surface growth) defects on all the examined media in both normoxia and hypoxia, with the effect being more pronounced under hypoxia (Figure 5a).

Next, as cells in *C. albicans* biofilms go through Efg1-dependent hypoxic adaptation (Stichternoth & Ernst, 2009), we sought to assess the link between Ifu5 and this cellular process. As the ability of microbial cells to adhere to the substrate is central to the formation of fungal biofilms, we tested the strains of interest for their ability to adhere and form biofilm on 24-well polystyrene plate grown under normoxia and hypoxia. The dry mass of the biofilms formed by *ifu5 Δ* and *mutIfu5* was similar to the wild type during normoxic growth (Figure 5b). Strikingly, although *ifu5 Δ* was able to form biofilm under hypoxia, the dry mass of the biofilm was two-fold less than that of the wild type, indicating that absence of Ifu5 impacts biofilm formation solely under hypoxia (Figure 5b). The difference in the extent of biofilm growth between the wild type, *ifu5 Δ* cells, *mutIfu5*, and the reconstituted strains in hypoxic condition was further assessed by the Cell Proliferation Kit II (XTT) reduction assay. In line with the decreased dry mass of biofilms, the mutants displayed a 50% reduction in the metabolic activity after 24 and 48 hr, compared with the wild type (Figure 5c). These data revealed that *ifu5 Δ* cells and *mutIfu5* display a delay in mature biofilm formation. We then monitored the adherence ability of the mutant onto polystyrene plates

under hypoxia. The adherence assay further confirmed the results of our metabolic assay as *ifu5 Δ* and *mutIfu5* cells showed a significant 66% reduction in cells that had grown on the polystyrene surface compared with the wild type (Figure 5d). The extent of biofilm growth and adherence in the reconstituted strain was similar to wild type (Figure 5b–d). This set of data points to the role of Ifu5 in biofilm formation, specifically in oxygen-limiting conditions. Coupled together, we conclude that Ifu5 serves as a positive regulator of filamentation and hypoxic biofilm formation in *C. albicans* and that these processes are facilitated by the WW domain of Ifu5.

3 | DISCUSSION

In this study, we spotlight Ifu5, a Tac1-regulated WW domain-containing protein (Figure 1) that serves a role in hypoxic signalling and influences virulence related traits of *C. albicans* in oxygen-surfeit and oxygen-limiting niches. Despite being coregulated with the drug efflux pumps (Figure 2a,b), Ifu5 does not contribute to azole susceptibility in wild-type *C. albicans* (Figure S3). Through this study, we also demonstrate the significance of Ifu5 in maintaining cell wall integrity, one of the functions of this protein under normoxia (Figures 2–6). We propose that compromised Ifu5 function causes glycostress in unstressed cells, leading to constitutive high levels of phospho-Cek1 and consequentially up-regulated *PMT1* (Figure 2g,h). Thus, the ability of Ifu5 to contribute to cell wall regulation can be attributed to its role in maintaining glycosylation homeostasis in *C. albicans*. WW domain is a well-characterised, highly conserved protein domain implicated in variety of cellular processes. However, protein interaction partners of many WW domain-containing proteins are largely unknown (Figure 1). In this context, this study identifies the hypoxic regulator Efg1 as the interaction partner of Ifu5 and brings forward a relationship between Ifu5 and Efg1 that may be one of the underlying mechanisms for hypoxic adaptation in *C. albicans* (Figure 6).

Transcriptome analysis of *ifu5 Δ* showed up-regulation of the hypoxic regulator *EFG1*, its normoxia-dependent target genes and biofilm-specific set of genes (Figure 3). We infer that Ifu5 not only regulates *EFG1* expression but also Efg1 allied pathways involved in hypoxic adaptation. We propose that there is a complex molecular interaction between Ifu5 and Efg1 wherein Ifu5 regulates both normoxic and hypoxic expression of *EFG1* transcript (Figure 4b–d) and coordinates with Efg1 to influence hypoxic responses in *C. albicans*. The repressive effect of Ifu5 on normoxic *EFG1* expression and Efg1 activity is evident from transcriptional induction of *EFG1* and its dependent genes in *ifu5 Δ* cells (Figure 3b). This repression could be facilitated by WW domain-mediated direct interaction between Ifu5 and Efg1 under normoxia (Figure 4a). Considering that *EFG1* negatively regulates its own transcription (Tebarth et al., 2003), we propose the possibility that Ifu5, by functioning as a corepressor of Efg1, may presumably allow this regulator to efficiently down-regulate its own expression. Thus, in *ifu5 Δ* cells, the ability of Efg1 to autoregulate itself is compromised leading to its constitutive up-regulation (Figure 4d). This plausible explanation is justified by

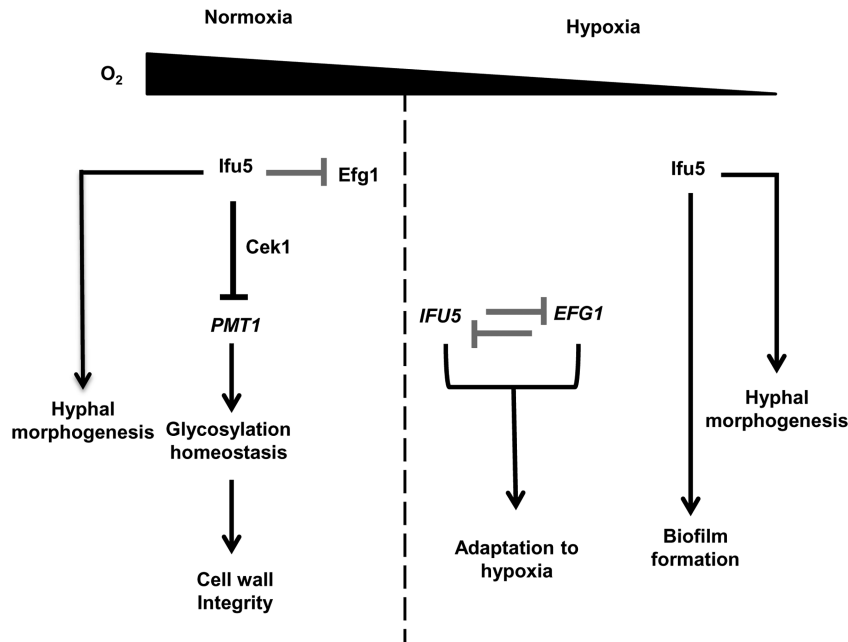


FIGURE 6 Model depicting Ifu5 functions in *Candida albicans*. Ifu5 influences normoxic and hypoxic responses in *C. albicans*. Ifu5 represses *PMT1* expression via the Cek1 MAP kinase pathway to maintain glycosylation homeostasis and thus cell wall integrity under normoxia. Direct binding of Ifu5 to Efg1 (grey blunt arrow) represses the function of this regulator. Hypoxia relieves this repression, and a negative reciprocal loop (grey blunt arrows) of regulation between *IFU5* and *EFG1* allows rapid hypoxic adaptation. Ifu5 positively regulates hypoxic biofilm formation and hyphal morphogenesis in both normoxic and hypoxic conditions

the established role of WW domain-containing proteins in binding to proline-rich sequences of transcription factors such as human *PEBP2* (polyoma enhancer binding protein), *NF-E2* (nuclear factor, erythroid 2) and *BRN-2/POU3F2* (POU domain, class 3, transcription factor 2). The C-terminus of Efg1 contains a stretch of prolines (residues 332 to 338), located C-terminal to its APSES domain (Noffz, Liedschulte, Lengeler, & Ernst, 2008), which may serve as a putative binding site for Ifu5. The significance of the proline-rich stretch in mediating Ifu5–Efg1 interaction needs further investigations. During early hypoxic stress, it is likely that the repressive effect of Ifu5 on Efg1 is relieved, resulting in Efg1-mediated transcriptional repression of *IFU5* (Figure 4c). Increased *IFU5* transcripts at later stages of hypoxic stress may be facilitated by low Efg1 levels, owing to the autoregulation of Efg1 that eventually causes a reduction in Efg1 protein levels (Lassak et al., 2011; Tebarth et al., 2003). Coupled together, these data suggest that Ifu5 in concert with Efg1 and unknown hypoxic regulators may ensure rapid adaptation to hypoxic environments and that Ifu5 and Efg1 may act as major points of integration for hypoxic adaptation in *C. albicans* (Figure 6).

Ifu5 also functions as a positive regulator of both filamentation and biofilm formation: two distinct hypoxia-dependent adaptation processes (Figure 6). Hyphal morphogenesis and hypoxic biofilm formation was blocked in *ifu5Δ/Δ* cells despite the up-regulation of Efg1 (Figure 5), suggesting that the requirement for Ifu5 during these processes cannot be bypassed by increased *EFG1* expression in the mutant. This is in contrast to the established role of Efg1 as an inducer of morphogenesis and biofilm formation in both gas conditions (Desai et al., 2015; Setiadi et al., 2006). Our results thus argue that both Ifu5 and Efg1 induce filamentation and hypoxic biofilm development via similar factors and that the expression of these factors is largely dependent on functional Ifu5. It is likely that Efg1-dependent activation of biofilm-specific genes, especially under hypoxia, requires Ifu5-dependent expression of additional hypoxic regulators/factors that link to the

Ifu5–Efg1 regulatory loop. Thus, the absence of Ifu5-dependent unknown hypoxic regulators may not allow Efg1 to fully exert its inducing effect on filamentation and biofilm formation in the mutant. The lack of normoxic biofilm phenotype (Figure 5b–d) for *ifu5Δ/Δ* is surprising as the mutant shows reduced filamentation on agar surface. Likewise, mutants of *ace2* and *czf1* that are considered crucial for hypoxic filamentation are dispensable for hypoxic biofilm formation (Giusani, Vincens, & Kumamoto, 2002; Kelly et al., 2004). This indicates that regulators (factors) required for filamentation under specific environments may not have a role in biofilm development in similar environments. Collectively, our data reveal synergistic function for Ifu5 and Efg1 in promoting filamentation and hypoxic biofilm formation in *C. albicans*.

WW domain is the predominant interacting module within Ifu5 as mutagenising this domain resulted in not only loss of Ifu5–Efg1 interaction under normoxia but also filamentation and hypoxic biofilm formation (Figures 4a and 5). We posit that the WW domain of Ifu5 may serve as a platform linking Ifu5 with distinct proteins affiliated with multiple physiological networks. Although protein–protein interactions through WW domain may be crucial for Ifu5 to regulate Efg1 activity, its involvement in cell wall regulation could be a separate function independent of the WW domain (Figure 2c). The link between Ifu5 and cell wall regulation is reminiscent of the role of *Sordaria macrospora* protein PRO40 (protoperithecia) in modulating the CWI pathway (Teichert et al., 2014). PRO40 serves as a scaffold for the proteins of the CWI MAPK module, independent of the WW domain, linking them to the upstream activator Pkc1 (Teichert et al., 2014). It is plausible that similar to PRO40, Ifu5 may serve as the scaffold protein to regulate the activity of the *C. albicans* CWI pathway in a WW domain-independent manner, an area that ought to be explored. The mammalian tumor suppressor gene *WWOX* (WW domain-containing oxidoreductase) and the SO (SOFT) protein involved in hyphal fusion in *Neurospora crassa* are few additional examples that mediate certain

functions in a WW domain-independent manner (Fleißner & Glass, 2007; Jamous & Salah, 2018). It seems likely that *Ifu5* may mediate its functions in *C. albicans* by interacting with and influencing the activities of different proteins in WW domain-dependent as well as WW domain-independent manner. Fungal hypoxic adaptation pathways are critical for virulence and exploiting them for antifungal therapy may improve the outcome of treating fungal infections. In vivo relevance of interfering with molecules involved in hypoxic adaptation may offer opportunities for prevention of fungal infections and prove to be favourable targets for drug development. We propose that *Ifu5* is a promising component for potential therapeutic targeting of *C. albicans* associated infections under varying oxygen niches.

4 | EXPERIMENTAL PROCEDURES

4.1 | Strains, chemicals, and growth conditions

Strains were maintained and propagated on YEPD medium (1% yeast extract, 2% Bacto peptone, 2% glucose, and 2% agar for solidification). YEPD medium supplemented with 200- $\mu\text{g}\cdot\text{ml}^{-1}$ of nourseothricin (Werner Bioagents, Jena, Germany) was used for selection of deletion mutants. To obtain nourseothricin-sensitive derivatives of transformants, strains were grown in yeast extract-peptone-maltose (1% yeast extract, 2% peptone, 2% maltose) for 8 hr and plated on 10- $\mu\text{g}\cdot\text{ml}^{-1}$ nourseothricin. For hyphal morphogenesis on solid media, cells were plated on Spider (1% nutrient broth, 1% D-mannitol and 0.2% K_2HPO_4) agar plate, kept under hypoxia (0.2% O_2) and normoxia at 37°C for 3 days, and photographed. Cell surface stress was imposed with sodium dodecyl sulphate (Biobasic), caspofungin (Merck), Calcofluor White (Sigma Aldrich), and tunicamycin (Sigma Aldrich) at the concentrations specified in the Figure 2. For stress sensitivity assay strains grown overnight in YEPD media were diluted in 0.9% saline solution. Thereafter, 5- μl portions of four dilutions (5×10^3 to 5×10^5 cells) were spotted onto YEPD agar plates containing indicated drugs. Plates were photographed after incubation for 48 hr at 30°C.

4.1.1 | Strain construction

Construction of deletion cassettes for *IFU5*

IFU5 was deleted by standard two-step disruptions using *SAT1* flipper using the plasmid pSFS2B (Reuss, Vik, Kolter, & Morschhäuser, 2004). The generated strains, plasmids, and primers used for strain construction are listed in Tables S1, S2, and S3, respectively. Two different disruption cassettes were constructed for the two alleles of *IFU5* in the disruption vector pSFS2B. For the *IFU5* deletion construct, a 300-bp 5' upstream noncoding region (NCR) of *IFU5* (5' *IFU5*^{NCR}) was amplified from SC5314 genomic DNA with primers FP 1 and FP 2 (Table S3), which introduced KpnI and XhoI restriction sites and cloned into 5' end of the *SAT1*-FLP cassette in pSFS2B using the same enzymes. A 300-bp region of 3' *IFU5*^{NCR} was amplified with primers FP 3 and FP 4, which introduced SacII and SacI sites and was cloned in the 3' end of the *SAT1*-FLP cassette (which already contains 5' *IFU5*^{NCR}). The

plasmid thus constructed containing the disruption cassette for deletion of the first allele of *IFU5* is referred to as pSR1 (Table S2). For deleting the second allele, 5' end of pSR1 was replaced by 300 bp of the *IFU5*^{NCR} (amplified by primers FP 5 and FP 6) with KpnI and XhoI restriction sites, generating pSR2 (Table S2). The *IFU5* reconstitution construct was made by amplifying a 1.7-kb fragment containing the *IFU5* ORF (0.7 kb) and the 5' NCR (1.0 kb) by using primers FP 7 and FP 8 that introduced KpnI and XhoI sites. The fragment was then ligated into the KpnI and XhoI digested pSR1, which already contained the 3' *IFU5*^{NCR}. This procedure resulted in the *IFU5* reconstitution plasmid (pSR3). The wild-type strain, SC5314, was electroporated with the first round disruption cassette, and deletion mutants were selected on 200- $\mu\text{g}\cdot\text{ml}^{-1}$ nourseothricin (SR11). To obtain nourseothricin-sensitive derivatives of transformants, strains were grown in yeast extract-peptone-maltose (1% yeast extract, 2% peptone, 2% maltose) and plated on 10- $\mu\text{g}\cdot\text{ml}^{-1}$ nourseothricin. These nourseothricin-sensitive heterozygous mutants (SR12) were then used for the second round of transformation generating the homozygous null mutant strain SR13. The *CaSAT1* construct was flipped out from SR13, resulting in SR14. For reconstituted strain, 5.8-kb fragment from pSR3 digested with KpnI and SacI and was transformed in SR14 to yield, SR15. Proper integration at each step was confirmed by Southern hybridisation.

C-terminal Myc tagging

For constructing C-terminal 13X Myc-tagged *IFU5*, the vector pADH34 was used as described previously (Nobile et al., 2009), which introduces 13X Myc epitope upstream from stop codon of *IFU5*. Cassette carrying *SAT1* marker, homology region of *IFU5* and 13X Myc epitope was transformed in SC5314 and positive transformants were screened by polymerase chain reaction (PCR). *SAT1* marker was recycled, and PCR product from nourseothricin sensitive colonies was sequenced to confirm proper integration of the cassette. Primers used for amplification of cassette and detection for integration are listed in Table S3.

Site-directed mutagenesis of the WW domain

For the construction of *mutIfu5* strain, plasmid containing the gene *IFU5* (pSR3) was used as template and tryptophan and proline substitution was performed by PCR (initial denaturation at 95°C for 5 min, annealing at 61°C for 1 min, extension at 68°C for 9 min, and final extension of 9 min) using primers listed in Table S3. The plasmid amplification products were then digested with DpnI at 37°C for 1 hr and then transformed in *Escherichia coli*. The mutations were confirmed by sequencing and the integration cassette was electroporated into SR16. Effective integration was confirmed by Southern blotting.

Construction of TAP modified *Ifu5* and HA modified *Efg1*

For strains used for co-immunoprecipitation assay, hemagglutinin-epitope modified *Efg1* (HA-*Efg1*) and TAP-epitope modified *Ifu5* (*Ifu5*-TAP) were constructed. For C-terminal tagging of *Ifu5*, plasmid pFA-TAP-HIS (Lavoie, Sellam, Askew, Nantel, & Whiteway, 2008) was used

to amplify sequences encoding the TAP and *HIS1* cassette. The cassette was transformed in strain AVL12 that expresses HA-Efg1 from its native promoter (Noffz et al., 2008) and in BWP17 resulting in strains CLvW998 (HA-Efg1, Ifu5-TAP) and CLvW997 (Ifu5-TAP), respectively. Similarly, strains producing *mutifu5*-TAP were constructed by first replacing both *IFU5* alleles with the mutated version encoded on plasmid pSR4 and subsequent transformation with the TAP-HIS cassette amplified with homologous-overhangs from plasmid pFA-TAP-HIS. The resulting strain CLvW990 (BWP17) produces *mutifu5*-TAP and strain CLvW989 produces (AVL12) HA-Efg1 and *mutifu5*-TAP. Chromosomal integration of the TAP-*HIS1* cassette was confirmed by PCR using oligonucleotides *colo-IFU5*-for and *colo-IFU5*-rev.

Cell wall analysis

Transmission electron microscopy. Exponentially growing *C. albicans* yeast cells were snap-frozen in liquid nitrogen at high pressure using a Leica Empact high-pressure freezer (Leica, Milton Keynes, United Kingdom). The frozen samples were then fixed, warmed to -30°C , processed, and embedded in TAAB812 (TAAB Laboratories, Aldermaston, United Kingdom) epoxy resin as described previously (Walker et al., 2018). Ultrathin sections of 100 nm were cut on a Leica Ultracut E microtome and stained with uranyl acetate and lead citrate. Philips CM10 transmission microscope (FEI UK Ltd., Cambridge, United Kingdom) was used for viewing the samples, and a Gatan BioScan 792 camera system (Gatan UK, Abingdon, United Kingdom) was used for capturing the images.

Cell wall carbohydrate analysis. Yeast cells were grown in YEPD medium at 30°C , broken, and hydrolysed as described previously (Lee et al., 2012). Hydrolyzed samples were analysed by high-performance anion-exchange chromatography with pulsed amperometric detection (HPAEC-PAD) in a carbohydrate analyser system from Dionex. The total concentration of each cell wall component was expressed as microgram per milligram of dried cell wall, determined by calibration from the standard curves of glucosamine, glucose, and mannose monomers, and converted to a percentage of the total cell wall.

Flocculation assay. Overnight YEPD grown cells were harvested and resuspended in Roswell Park Memorial Institute (RPMI) medium with a starting OD_{600} of 0.3 and grown for additional 3 hr at 37°C with shaking at 220 r.p.m. Cells were then transferred to glass tubes and vortexed for 30 s. OD_{600} measured and cells were allowed to settle for 15 min; after which, OD_{600} was measured and an aliquot of cells were photographed. Experiment was done in triplicate and change in absorbance against each time point was plotted.

Microarray analysis

For transcriptional profiling, wild type and mutant cells were grown overnight in YEPD, subcultured from a starting OD_{600} of 0.3 in fresh YEPD and incubated at 30°C till OD_{600} reached 1.0. Thereafter, RNA was extracted from three biological replicates of both strains using an RNeasy minikit (Qiagen) and was used to perform the microarray experiments. The samples for gene expression were labelled

using Agilent Quick-Amp labelling Kit (p/n5190-0442). The cDNA synthesis, *in vitro* transcription steps, and subsequent hybridisation on to genotypic-designed *C. albicans*_GXP_8X15k (AMADID No: 26377) array was carried out as described previously (Thomas et al., 2015). Data extraction from images was done using Feature Extraction software Version 11.5 of Agilent. The microarray data can be accessed under GEO accession number GSE110650.

Quantitative real-time PCR

The levels of specific transcripts were measured by qPCR in triplicate using independent biological replicates. RNA isolation was performed as described above and cDNA synthesis (Thermo scientific) carried out subsequently following manufacturer's protocol. qPCR reactions were performed in a volume of 25 μl using Thermo Scientific Maxima SYBR Green mix in a 96-well plate. For measuring relative transcript levels of *IFU5* and *EFG1* under hypoxia, the indicated strains were first grown under normoxic conditions in YEPD medium for 4 hr at 30°C . Thereafter, a fraction of the cells was used to inoculate fresh YEPD medium (preincubated under hypoxia (0.2% O_2), and cells were allowed to grow under hypoxic conditions for additional 4 hr at 30°C . After 30, 60, 120 and 240 min, a fraction of the cells was harvested, and total RNA was isolated. Time point 0 corresponds to 4hr growth under normoxic conditions before shifting cells to hypoxic conditions. At each time point, two biological replicates and three technical replicates were assayed by qPCR. *ACT1* was used as the internal control and transcript level of the gene of interest was normalised to *ACT1* levels. Results were statistically analysed using Student's *t* test. The qPCR primers used in this study were designed by Primer Express 3.0 and are listed in Table S4.

Immunoblotting

To examine Mkc1 and Cek1 phosphorylation, protein extracts were prepared from exponentially grown *C. albicans* strains and these extracts were subjected to western blotting using previously described protocols (Martín, Arroyo, Sánchez, Molina, & Nombela, 1993). Anti-phospho-p44/p42 MAPK (Thr202/Tyr204) antibody (New England Biolabs) was used to detect dually phosphorylated Mkc1 and Cek1 MAPKs (indicated as Mkc1-P and Cek1-P in Figure 2g); anti-Mkc1 (Román, Nombela, & Pla, 2005) antibodies were used to detect total Mkc1 (loading control) as indicated in the Figure 2g. Blot imaging was done by using an Odyssey fluorescence imager (LI-COR) and quantified using Image Studio Lite (LI-COR).

Co-immunoprecipitation assay

Strains producing HA modified Efg1 (AVL12, lanes 2 and 8), TAP modified Ifu5 (CLvW997, lanes 3 and 9), both, HA modified Efg1 and TAP modified Ifu5 (CLvW998, lanes 4 and 10), *mutifu5* TAP modified (CLvW990, lanes 5 and 11), and a strain producing both HA modified Efg1 and TAP modified *mutifu5* (CLvW989, lanes 6 and 12) were grown in YEPD medium at 30°C in either hypoxic or normoxic (0.2% O_2) conditions for 4 hr. A control strain BWP17 was used, expressing unmodified Efg1 and Ifu5 proteins (lanes 1

and 7). For cross-linking, cultures were treated with formaldehyde (1% v/v). Total protein extracts were incubated with Dynabeads, Mouse IgG (Invitrogen, Cat No: 11041) for immunoprecipitation of TAP modified Irf5. The samples were immunoblotted and developed using anti-TAP (IP; Invitrogen, CAB1001, 1:1000) or anti-HA (ColP; Santa Cruz Biotech, sc-7392, 1:1000) antibodies. To verify presence of HA-Efg1 1% of the total protein extracts was blotted and investigated with anti-HA.

Biofilm formation in polystyrene wells

Quantification of biofilm by dry weight of wells. To quantify the biofilm formation, dry weights of wells were used. Seven hundred microlitre of 10^5 cells ml^{-1} of the indicated strains were allowed to adhere to the surface of a polystyrene flat bottom 24-well plate (Corning Costar) for 90 min in phosphate-buffered saline (PBS) at 37°C under normoxic and hypoxic (0.2% O_2) conditions. The medium and PBS used for hypoxic growth conditions were preincubated under hypoxia for 12 hr. Each well was washed twice with PBS to remove nonadherent cells. The wells were supplemented with RPMI 1640 medium and incubated for 48 hr at 37°C under normoxia and hypoxia. Biofilms were washed twice with PBS, and dry biomass of the biofilms were quantified and expressed as ratio of the indicated strain versus control strain (wild type). The experiment was performed twice, with two independent biological replicates, each assayed with three technical replicates.

Quantification of biofilm by XTT reduction assay. To determine the number of cells in the different biofilm stages, XTT reduction assay was performed. One hundred microlitre of 10^5 cells ml^{-1} of the indicated strains were allowed to adhere to the surface of a polystyrene flat bottom 96-well microtiter plate (Corning Costar) for 90 min in PBS at 37°C under hypoxic (0.2% O_2) conditions. The medium and PBS buffer used was preincubated under hypoxic conditions for 12 hr. Each well was washed twice with PBS to remove nonadherent cells. The wells were supplemented with RPMI 1640 medium and incubated for 24 and 48 hr at 37°C under hypoxia. Biofilms were washed with PBS after the indicated time points and supplemented with XTT-menadione solution (1.5-mM XTT (2, 3-bis (2-methoxy-4-nitro-5-sulfophenyl)-5-[(phenylamino)carbonyl]-2H-tetrazolium hydroxide); 0.4-M menadione). After incubation in the dark for 30 min at 37°C, the supernatant was transferred to a new 96-well microtiter plate, and the colour change was measured at 490 nm. The experiment was performed twice, with two independent biological replicates, each assayed with three technical replicates.

Adhesion of *C. albicans* strains to polystyrene. To quantify adherence, XTT reduction assay was performed as described for quantification of biofilm formation except that after washing each well twice with PBS to remove nonadherent cells, XTT-menadione solution was added to the wells and incubated for 30 min at 37°C in dark. The supernatant was transferred to a new 96-well microtiter plate to monitor colour change at 490 nm. The experiment was performed twice, with two independent biological replicates, each assayed with three technical replicates. A *t* test was used to calculate the statistical relevance in all the aforesaid experiments.

ACKNOWLEDGEMENTS

We are grateful to Joachim Morschhauser and Suzanne Noble for providing us with the plasmids used in this study, to Patrick Van Dijck and Neeru Saini for performing initial experiments for this study and the entire lab for insightful discussions. We acknowledge Genotypic Technology Pvt., Ltd., Bangalore, India for microarray experiments. S. K. R., S. R., and P. A acknowledge the Department of Biotechnology, Council for Scientific and Industrial Research and women Scientist award from Department of Science & Technology, respectively for awarding Junior and Senior Research Fellowships. This work was funded by the Department of Biotechnology (BT/PR5347/MED/29/629/2012) to S. L. P. Umbrella grants from Jawaharlal Nehru University in the form of Capacity Build-up, UGC-Resource Networking and DST-PURSE are also acknowledged. Support from ERA-Net PathoGenoMics project OXYstress (www.pathogenomics-era.net/FundedProjects3rdJoint) and the Infect-ERA JTC2 project FunComPath (<http://www.funcompath.eu/>) to JFE, BIO2015-64777-P to JP and Wellcome Trust (101873, 086827, 075470, & 200208) and MRC Centre for Medical Mycology (N006364/1) to NG is acknowledged.

ORCID

Sneh L. Panwar  <https://orcid.org/0000-0003-0848-8306>

REFERENCES

- Askew, C., Sellam, A., Epp, E., Hogues, H., Mullick, A., Nantel, A., & Whiteway, M. (2009). Transcriptional regulation of carbohydrate metabolism in the human pathogen *Candida albicans*. *PLoS Pathogens*, 5(10), e1000612. <https://doi.org/10.1371/journal.ppat.1000612>
- Bonhomme, J., Chauvel, M., Goyard, S., Roux, P., Rossignol, T., & d'Enfert, C. (2011). Contribution of the glycolytic flux and hypoxia adaptation to efficient biofilm formation by *Candida albicans*: Biofilm formation and adaptation to hypoxia in *C. albicans*. *Molecular Microbiology*, 80(4), 995–1013. <https://doi.org/10.1111/j.1365-2958.2011.07626.x>
- Cantero, P. D., & Ernst, J. F. (2011). Damage to the glycoshield activates PMT-directed O-mannosylation via the Msb2-Cek1 pathway in *Candida albicans*. *Molecular Microbiology*, 80(3), 715–725. <https://doi.org/10.1111/j.1365-2958.2011.07604.x>
- Chang, Y. C., Bien, C. M., Lee, H., Espenshade, P. J., & Kwon-Chung, K. J. (2007). Sre1p, a regulator of oxygen sensing and sterol homeostasis, is required for virulence in *Cryptococcus neoformans*. *Molecular Microbiology*, 64(3), 614–629. <https://doi.org/10.1111/j.1365-2958.2007.05676.x>
- Coste, A. T., Karababa, M., Ischer, F., Bille, J., & Sanglard, D. (2004). TAC1, transcriptional activator of CDR genes, is a new transcription factor involved in the regulation of *Candida albicans* ABC transporters CDR1 and CDR2. *Eukaryotic Cell*, 3(6), 1639–1652. <https://doi.org/10.1128/EC.3.6.1639-1652.2004>
- Desai, P. R., van Wijlick, L., Kurtz, D., Juchimiuk, M., & Ernst, J. F. (2015). Hypoxia and temperature regulated morphogenesis in *Candida albicans*. *PLoS Genetics*, 11(8), e1005447. <https://doi.org/10.1371/journal.pgen.1005447>
- Doedt, T., Krishnamurthy, S., Bockmühl, D. P., Tebarth, B., Stempel, C., Russell, C. L., ... Ernst, J. F. (2004). APSES proteins regulate morphogenesis and metabolism in *Candida albicans*. *Molecular Biology of the Cell*, 15(7), 3167–3180. <https://doi.org/10.1091/mbc.e03-11-0782>

- Ernst, J. F., & Tielker, D. (2009). Responses to hypoxia in fungal pathogens. *Cellular Microbiology*, 11(2), 183–190. <https://doi.org/10.1111/j.1462-5822.2008.01259.x>
- Fleißner, A., & Glass, N. L. (2007). SO, a protein involved in hyphal fusion in *Neurospora crassa*, localizes to septal plugs. *Eukaryotic Cell*, 6(1), 84–94. <https://doi.org/10.1128/EC.00268-06>
- Giusani, A. D., Vinces, M., & Kumamoto, C. A. (2002). Invasive filamentous growth of *Candida albicans* is promoted by Czf1p-dependent relief of Efg1p-mediated repression. *Genetics*, 160(4), 1749–1753.
- Grahl, N., Shepardson, K. M., Chung, D., & Cramer, R. A. (2012). Hypoxia and fungal pathogenesis: To air or not to air? *Eukaryotic Cell*, 11(5), 560–570. <https://doi.org/10.1128/EC.00031-12>
- Hesselberth, J. R., Miller, J. P., Golob, A., Stajich, J. E., Michaud, G. A., & Fields, S. (2006). Comparative analysis of *Saccharomyces cerevisiae* WW domains and their interacting proteins. *Genome Biology*, 7(4), R30. <https://doi.org/10.1186/gb-2006-7-4-r30>
- Jamous, A., & Salah, Z. (2018). WW-domain containing protein poles in breast tumorigenesis. *Frontiers in Oncology*, 8. <https://doi.org/10.3389/fonc.2018.00580>
- Kelly, M. T., MacCallum, D. M., Clancy, S. D., Odds, F. C., Brown, A. J. P., & Butler, G. (2004). The *Candida albicans* CaACE2 gene affects morphogenesis, adherence and virulence: *C. albicans* CaAce2 knock-out affects morphogenesis. *Molecular Microbiology*, 53(3), 969–983. <https://doi.org/10.1111/j.1365-2958.2004.04185.x>
- Lassak, T., Schneider, E., Bussmann, M., Kurtz, D., Manak, J. R., Srikantha, T., ... Ernst, J. F. (2011). Target specificity of the *Candida albicans* Efg1 regulator: Efg1 target recognition. *Molecular Microbiology*, 82(3), 602–618. <https://doi.org/10.1111/j.1365-2958.2011.07837.x>
- Lavoie, H., Sellam, A., Askew, C., Nantel, A., & Whiteway, M. (2008). A toolbox for epitope-tagging and genome-wide location analysis in *Candida albicans*. *BMC Genomics*, 9, 578. <https://doi.org/10.1186/1471-2164-9-578>
- Lee, K. K., MacCallum, D. M., Jacobsen, M. D., Walker, L. A., Odds, F. C., Gow, N. A. R., & Munro, C. A. (2012). Elevated cell wall chitin in *Candida albicans* confers echinocandin resistance in vivo. *Antimicrobial Agents and Chemotherapy*, 56(1), 208–217. <https://doi.org/10.1128/AAC.00683-11>
- Lopes, J. P., Stylianou, M., Backman, E., Holmberg, S., Jass, J., Claesson, R., & Urban, C. F. (2018). Evasion of immune surveillance in low oxygen environments enhances *Candida albicans* virulence. *MBio*, 9(6). <https://doi.org/10.1128/mBio.02120-18>
- Martín, H., Arroyo, J., Sánchez, M., Molina, M., & Nombela, C. (1993). Activity of the yeast MAP kinase homologue Slr2 is critically required for cell integrity at 37 degrees C. *Molecular & General Genetics: MGG*, 241(1–2), 177–184. <https://doi.org/10.1007/bf00280215>
- Masuoka, J., & Hazen, K. C. (1997). Cell wall protein mannosylation determines *Candida albicans* cell surface hydrophobicity. *Microbiology (Reading, England)*, 143(Pt 9), 3015–3021. <https://doi.org/10.1099/00221287-143-9-3015>
- Nobile, C. J., & Mitchell, A. P. (2006). Genetics and genomics of *Candida albicans* biofilm formation. *Cellular Microbiology*, 8(9), 1382–1391. <https://doi.org/10.1111/j.1462-5822.2006.00761.x>
- Nobile, C. J., Nett, J. E., Hernday, A. D., Homann, O. R., Deneault, J.-S., Nantel, A., ... Mitchell, A. P. (2009). Biofilm matrix regulation by *Candida albicans* zap1. *PLoS Biology*, 7(6), e1000133. <https://doi.org/10.1371/journal.pbio.1000133>
- Noffz, C. S., Liedschulte, V., Lengeler, K., & Ernst, J. F. (2008). Functional mapping of the *Candida albicans* Efg1 regulator. *Eukaryotic Cell*, 7(5), 881–893. <https://doi.org/10.1128/EC.00033-08>
- Pierce, J. V., & Kumamoto, C. A. (2012). Variation in *Candida albicans* EFG1 expression enables host-dependent changes in colonizing fungal populations. *MBio*, 3(4), e00117–e00112. <https://doi.org/10.1128/mBio.00117-12>
- Pradhan, A., Avelar, G. M., Bain, J. M., Childers, D. S., Larcombe, D. E., Netea, M. G., ... Brown, A. J. P. (2018). Hypoxia promotes immune evasion by triggering β -glucan masking on the *Candida albicans* cell surface via mitochondrial and cAMP-protein kinase A signaling. *MBio*, 9(6). <https://doi.org/10.1128/mBio.01318-18>
- Reuss, O., Vik, A., Kolter, R., & Morschhäuser, J. (2004). The SAT1 flipper, an optimized tool for gene disruption in *Candida albicans*. *Gene*, 341, 119–127. <https://doi.org/10.1016/j.gene.2004.06.021>
- Román, E., Alonso-Monge, R., Miranda, A., & Pla, J. (2015). The Mkk2 MAPKK regulates cell wall biogenesis in cooperation with the Cek1-pathway in *Candida albicans*. *PLoS One*, 10(7), e0133476. <https://doi.org/10.1371/journal.pone.0133476>
- Román, E., Nombela, C., & Pla, J. (2005). The Sho1 adaptor protein links oxidative stress to morphogenesis and cell wall biosynthesis in the fungal pathogen *Candida albicans*. *Molecular and Cellular Biology*, 25(23), 10611–10627. <https://doi.org/10.1128/MCB.25.23.10611-10627.2005>
- Setiadi, E. R., Doedt, T., Cottier, F., Noffz, C., & Ernst, J. F. (2006). Transcriptional response of *Candida albicans* to hypoxia: Linkage of oxygen sensing and Efg1p-regulatory networks. *Journal of Molecular Biology*, 361(3), 399–411. <https://doi.org/10.1016/j.jmb.2006.06.040>
- Srivastava, A., Sircaik, S., Husain, F., Thomas, E., Ror, S., Rastogi, S., ... Panwar, S. L. (2017). Distinct roles of the 7-transmembrane receptor protein Rta3 in regulating the asymmetric distribution of phosphatidylcholine across the plasma membrane and biofilm formation in *Candida albicans*. *Cellular Microbiology*, 19(12). <https://doi.org/10.1111/cmi.12767>
- Stichternoth, C., & Ernst, J. F. (2009). Hypoxic adaptation by Efg1 regulates biofilm formation by *Candida albicans*. *Applied and Environmental Microbiology*, 75(11), 3663–3672. <https://doi.org/10.1128/AEM.00098-09>
- Synnott, J. M., Guida, A., Mulhern-Haughey, S., Higgins, D. G., & Butler, G. (2010). Regulation of the hypoxic response in *Candida albicans*. *Eukaryotic Cell*, 9(11), 1734–1746. <https://doi.org/10.1128/EC.00159-10>
- Szallies, A., Kubata, B. K., & Duszenko, M. (2002). A metacaspase of *Trypanosoma brucei* causes loss of respiration competence and clonal death in the yeast *Saccharomyces cerevisiae*. *FEBS Letters*, 517(1–3), 144–150. [https://doi.org/10.1016/s0014-5793\(02\)02608-x](https://doi.org/10.1016/s0014-5793(02)02608-x)
- Tebarth, B., Doedt, T., Krishnamurthy, S., Weide, M., Monterola, F., Dominguez, A., & Ernst, J. F. (2003). Adaptation of the Efg1p morphogenetic pathway in *Candida albicans* by negative autoregulation and PKA-dependent repression of the EFG1 gene. *Journal of Molecular Biology*, 329(5), 949–962. [https://doi.org/10.1016/s0022-2836\(03\)00505-9](https://doi.org/10.1016/s0022-2836(03)00505-9)
- Teichert, I., Steffens, E. K., Schnaß, N., Fränzel, B., Krisp, C., Wolters, D. A., & Kück, U. (2014). PRO40 is a scaffold protein of the cell wall integrity pathway, linking the MAP kinase module to the upstream activator protein kinase C. *PLoS Genetics*, 10(9), e1004582. <https://doi.org/10.1371/journal.pgen.1004582>
- Thomas, E., Sircaik, S., Roman, E., Brunel, J.-M., Johri, A. K., Pla, J., & Panwar, S. L. (2015). The activity of RTA2, a downstream effector of the calcineurin pathway, is required during tunicamycin-induced ER stress response in *Candida albicans*. *FEMS Yeast Research*, fov095. <https://doi.org/10.1093/femsyr/fov095>
- van Wijlick, L., Swidrigall, M., Brandt, P., & Ernst, J. F. (2016). *Candida albicans* responds to glycostructure damage by Ace2-mediated feedback regulation of Cek1 signaling. *Molecular Microbiology*, 102(5), 827–849. <https://doi.org/10.1111/mmi.13494>

Walker, L., Sood, P., Lenardon, M. D., Milne, G., Olson, J., Jensen, G., ... Gow, N. A. R. (2018). The viscoelastic properties of the fungal cell wall allow traffic of amBisome as intact liposome vesicles. *MBio*, 9(1). <https://doi.org/10.1128/mBio.02383-17>

SUPPORTING INFORMATION

Additional supporting information may be found online in the Supporting Information section at the end of the article.

How to cite this article: Rastogi SK, van Wijlick L, Ror S, et al. Ifu5, a WW domain-containing protein interacts with Efg1 to achieve coordination of normoxic and hypoxic functions to influence pathogenicity traits in *Candida albicans*. *Cellular Microbiology*. 2019;e13140. <https://doi.org/10.1111/cmi.13140>